Monitoring and Predictive Modeling of Water Temperatures in the Laguna Madre

A Report Submitted to Texas Parks & Wildlife and the Coastal Conservation Association

Philippe E. Tissot, Robyn Ball and John S. Adams
Texas A&M University-Corpus Christi
Conrad Blucher Institute
6300 Ocean Drive
Corpus Christi, TX 78412

November 9, 2007

Executive Summary

The study focuses on the measurement and predictability of cold water events in the Laguna Madre. These events have previously resulted in significant fish mortality. This study seeks to better understand the dynamic and forcings of the water column temperatures during these events as well as to develop a predictive model that could help implement possible preventive action ahead and during the cold water events. The objective of the study were to (1) install water temperature profiling stations in and around the 'land cut' area of the Upper Laguna Madre, Texas, (2) test, monitor, maintain, and analyze the data from the water temperature profiling stations, (3) develop a water temperature predictive model particularly for the prediction of cold water events i.e. events resulting in water temperatures at or below 45F and (4) implement the model on the world wide web to make its predictions accessible to decision makers.

Two measuring stations were installed at existing platforms to leverage existing infrastructure of the Texas A&M University-Corpus Christi (TAMUCC) Division of Nearshore Research (DNR) and the Texas Coastal Ocean Observation Network (TCOON). One set of instruments was installed at the TCOON Rincon station and the other set of instruments was installed at the former TCOON El Toro Island station. Water temperatures at approximately 3', 6', 9' and 12' within the water column were measured hourly starting respectively on February 27, 2006 and December 13, 2005. The temperature time series are available on the World Wide Web through the DNR website (http://lighthouse.tamucc.edu).

Data quality was excellent at the Rincon station and is the main data set used for the analysis. Problems were encountered at the Land Cut station. This later data set is discussed in the report and mostly used to complement the data collected at the Rincon station. Several cold water events were monitored during the study including a January 2007 event with water temperatures decreasing from 22.5°C down to 4.6°C in 60 hours. Throughout the study period the water temperatures were found to be mostly homogenous, i.e. temperatures within a 0.5°C range throughout the water column. A small moderating effect at the bottom of the channel, i.e. for the 12' sensor, was observed during sharp temperature rises. Bottom temperatures during these events stayed cooler by 1°C to 2°C up to 5°C but the temperature gradients always rapidly disappeared at the most within 8 hours. This moderating effect at the bottom of the Laguna Madre was however not observed during the sharp temperature decreases associated with frontal passages. The results of this study indicate a homogeneous temperature throughout the water column during cold water events. Further monitoring could attempt to measure temperatures in the muddy bottom of the Laguna Madre to confirm that there is indeed no location within the water column where marine life may seek warmer temperatures during cold water events. Temperatures in shallow waters could also be recorded to investigate if significantly lower temperatures are reached at such locations. Comparing temperature records at both project stations and other DNR stations show a mostly homogeneous temperature distribution throughout the Laguna Madre with variability observed in the deeper waters of Corpus Christi Bay northward the Brownsville ship channel southward and at the Mansfield station which is linked to the Gulf of Mexico by a smaller ship channel.

The water temperature predictive model was designed and implemented using Artificial Neural Network (ANN) methodology. The methodology had been previously used for the modeling of water levels along the Texas Coast and is particularly well suited to model non linear systems

when large data sets are available. The performance of the ANN model was also compared with a multi linear regression approach to confirm the advantage of the selected methodology. The model was developed for the Bird Island Station in the northern portion of the Laguna Madre because of the considerably longer time series and number of cold events available for that station. Small modifications were made to adapt the model to the project stations (described later in this summary). A statistical analysis highlighted that air temperature is by far the main forcing for water temperatures in the Laguna Madre away from ship channels. The statistical analysis also identified the relative importance and time lags for the other forcings to the system. Given the importance of the air temperature forcing, air temperature predictions were included in the model. The model was first designed using measurements as forecasts (perfect prog approach) and then tested with actual predictions provided by the Corpus Christi Weather Forecasting Office (CCWFO). For the present operational model air temperature predictions are being sent 4 times a day as part of a broader collaboration with CCWFO. The predictions are presently extracted from the National Centers for Environmental Prediction (NCEP) Nonhydrostatic Mesoscale Model (NMM) recently integrated within the Weather Research and Forecasting (WRF) framework from the North American Model (NAM-WRF). The NAM-WRF air temperature predictions are adjusted with a linear transformation for air temperatures below 18°C to improve model performance for the project stations (MOS approach).

A short term model was designed for 3 and 12 hour forecasts and a longer term model was constructed for 24 and 48 hour forecasts. The models were designed following a stepwise method, consecutively adding possible inputs and then comparing the average absolute error of the models. Both models included the previous 26 hours of water temperature at Bird Island and air temperature forecasts. The short term model inputs also consisted of the previous 22 hours of air temperature measurements and the past 16 hours of a 24 hour time stamp. Long term model inputs included the previous 16 hours of air temperature measurements along with the most recent available water temperature measurement at the nearby Gulf of Mexico station of Bob Hall Pier.

Performance was analyzed for both the perfect prog approach for several test years and using a historical data base of actual WRF-NAM predictions for a shorter time span. Using the perfect prog approach yearly average absolute error ranged from about 0.3°C for 3 hour predictions to about 0.7°C for 12 hour predictions, to about 1.0°C for 24 hour predictions and 1.7°C for 24 hour predictions. Year to year variability increased from up to 0.2°C for 3 hour predictions to up to 0.6°C, 0.14°C and 0.23°C for respectively 12 hour, 24 hour and 48 hour predictions. Cold water performance was analyzed for four events between 2003 and 2007 during which cold water temperature reached 8°C or below. The performance during these events was computed using past WRF-NAM predictions. During the cold events the mean average absolute error was lower than 1°C for all predictions increasing from 0.1°C for 3 hour predictions to 0.9°C for the longer prediction times. While the number of cold events with WFR-NAM predictions available is still small a mean average absolute error of 1°C is likely a good estimate of the average performance of the model for cold events. The cold event performance was homogeneous across the temperature range with variability and performance dominated by the accuracy of the WRF-NAM atmospheric predictions, i.e. the performance of the model will mostly depend on how well the atmospheric models capture the future dynamic of the cold fronts.

While the model was developed for the Bird Island TCOON station because of the considerably longer time series available, the study shows no significant biases or lags between that station

and the project stations. Consequently the Bird Island model can be considered valid for the Upper Laguna Madre, at least for the Intracoastal Water Way and nearby waters. Water temperatures near the ship channels in the northern and southern ends of the Laguna Madre as well as the Port Mansfield station are affected by the link with the Gulf of Mexico and higher temperature lows are observed. Water temperatures in the very shallow portions of the Laguna Madre are also expected to exhibit differences.

The performance of the model for cold water event was also evaluated based on its accuracy to detect an event. Based on the available data if a cold event is not predicted by the model, the chances of such event taking place are virtually nil. Once an event is predicted, the chances that the event will indeed take place varies depending on the extent of the forecast from 90% for 3 hour predictions to 85%, 83% and 64% for 12, 24 and 40 hour predictions. If an event is not observed the chances that one was predicted are virtually nil and if a cold water event takes place there is a 70% to 80% chance that the event was indeed predicted. The operational model was implemented as part of the DNR/TCOON website (http://lighthouse.tamucc.edu/) Forecasts portion and is presently available at the following link: http://lighthouse.tamucc.edu/Forecasts/WTPTests.

Continuous monitoring of the water temperature gradient at the station locations is highly desirable particularly to capture more cold water events. Additional events, particularly colder events would be helpful to better define the performance of the model during these conditions and confirm the absence of a vertical temperature gradient. Other recommendations for possible other locations south of the present locations, in shallower waters or in the muddy Laguna Madre bottom are included in the report. The use of other machine learning based techniques such as random forest modeling could prove helpful in improving predictions specifically during cold events.

Table of Contents

1. Introduction and Project Objectives

The Laguna Madre is the longest hypersaline lagoon in the United States and extends southward for over 200 miles from Corpus Christi, Texas to the United States-Mexican border. The Laguna Madre is home to fragile young finfish, shrimp, and shellfish as well as redfish, spotted sea trout, a host of birds, and endangered sea turtles (Britton and Morton, 1989). The passage of cold fronts can dramatically lower air temperatures by more than 10°C in less than 24 hours which leads to a considerable decrease in water temperature. Records from the past 20 years reveal that some of these cold water events resulted in massive fish kills. In 1997, more than 94,000 fish died in the Lower Laguna Madre and over 48,000 fish died in the Upper Laguna Madre (TPWD, 1997). To mitigate the impact of these cold events, local agencies and stakeholders are considering interrupting activities such as fishing and boating during these events. To help manage such interruptions accurate predictions of occurrences and length of cold water events are critical. An accurate model would result in significant economical benefits as the water bodies could be closed for an optimum time span .limiting short term economic losses due to the interruption of recreational and commercial activities while helping mitigate the impact of the cold water events. One of the main objectives of this study is to design and assess the performance of a predictive water temperature model for the Upper Laguna Madre

Another goal of the study is to answer the related question of the possible presence of a thermal gradient within the water column. If such a gradient is observed marine life will likely migrate to the warmer section of the water column. If the warmer section of the water column is near the muddy bottom, marine life will likely migrate towards the deepest local water i.e. the bottom of the Intracoastal Waterway. Such behavior could result in added mortality during the passage of deep draft vessels, mainly barges in the ICW. To determine if such gradient takes place and to provide additional data for the design and testing of a water temperature predictive model, two stations were installed at Rincon del San Jose and within the Landcut.

The general project methodology is illustrated in Figure 1. During the initial part of the study a predictive model was developed for an existing station in the Upper Laguna Madre, the Bird Island station (modeling track), while thermistor strings were installed to monitor water temperatures at the two project locations (monitoring track). The installation of the monitoring station, the analysis of the collected data and a discussion of a possible vertical thermal gradient are presented in section 2. The design and performance of a water temperature predictive model for the Bird Island station are detailed in sections 4 and 5. Section 6 discusses the applicability of the model to other locations including the two project station locations. Section 7 presents the model performance during cold events and section 8 presents other performance metrics which should be helpful for future users of the model. Section 9 describes the web implementation of the model.

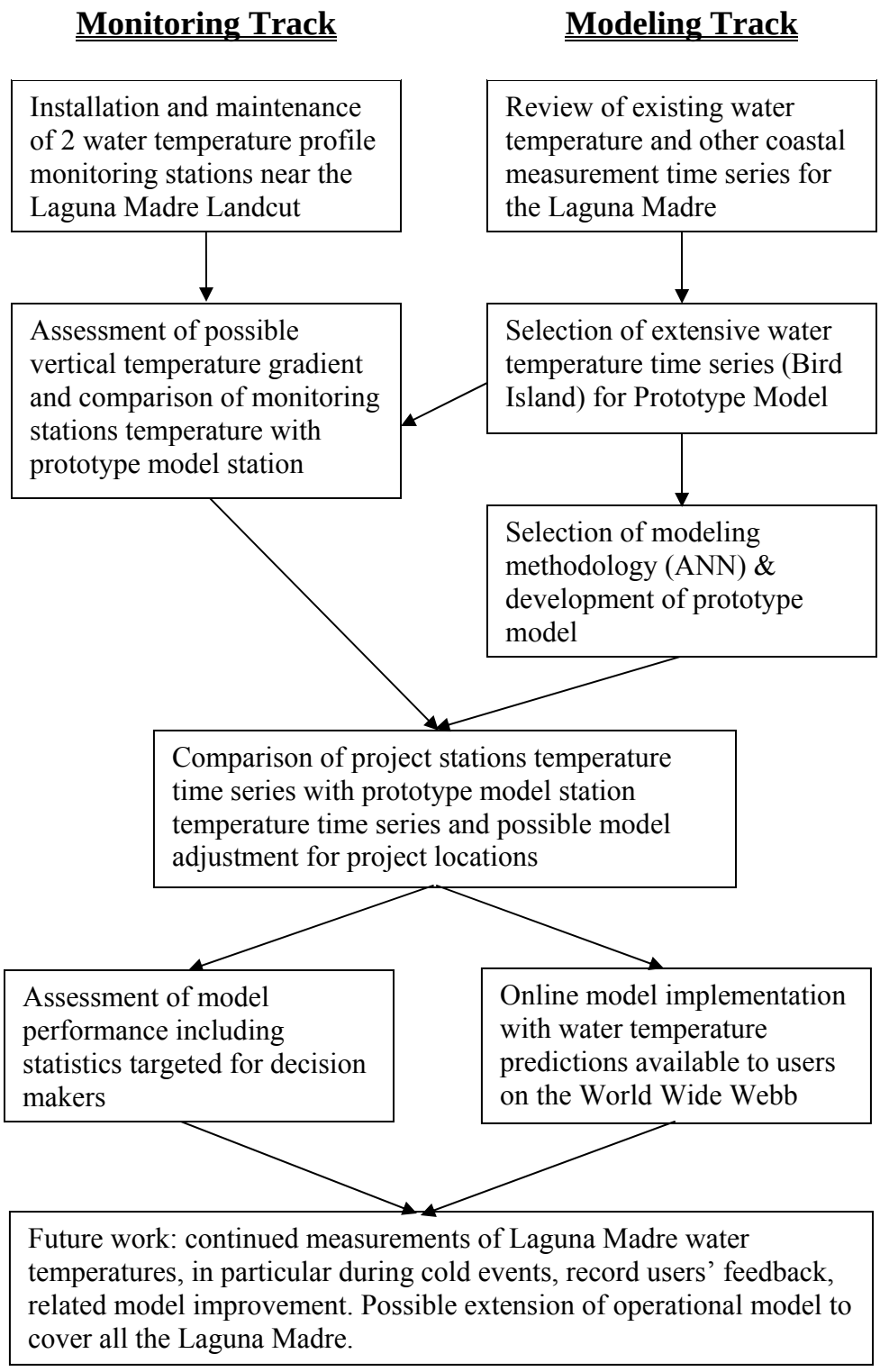

Figure 1. General study plan for monitoring, study and design and implementation of predictive model of water temperatures in the Laguna Madre.

2. Monitoring Platforms: Installation, Equipment & Measurements Analysis

2.1 Stations Locations

Instrumentation to monitor vertical temperature profiles were installed in the central portion of the Laguna Madre near the Land Cut on two platforms operated by DNR. Station locations are illustrated in figure 2 with the abbreviations TPWD (Texas Parks & Wildlife Department) LC for the Land Cut station and RI for the Rincon station. The Land Cut station was installed on the same platform as the Texas Coastal and Ocean Observation Network (TCOON) Rincon station platform (26° 48.090' N, 97° 28.236' W). The concurrent installation provided for a sturdy platform, and the concurrent measurement of other related variables such as wind, air temperature, barometric pressure and water level at the same location. The Land Cut station was installed using the platform of the former El Toro station (26° 55.883' N, 97° 27.388' W). In this later case no other instrumentation is located on the station besides the project sensors. Two other TCOON stations are located near the project station, the Baffin Bay station northward and the Port Mansfield station southward of the project stations.

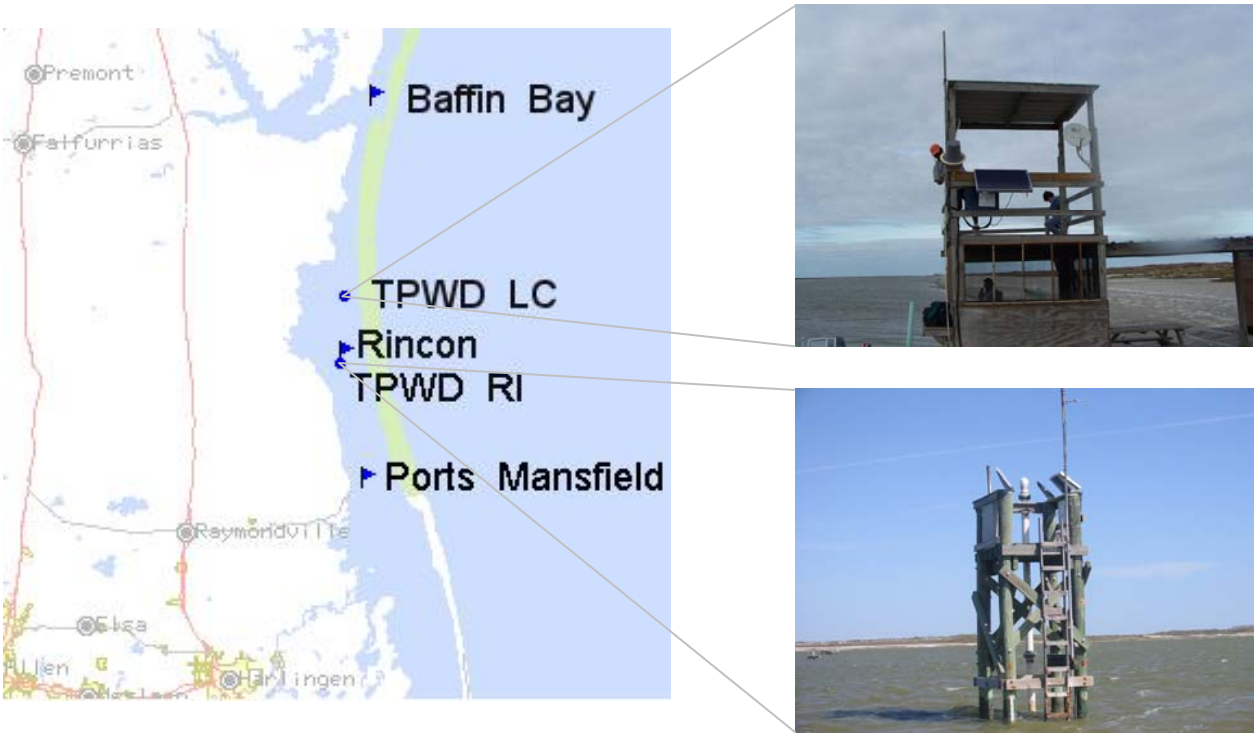

Figure 2. Locations and pictures of of the project stations the Land Cut Station (TPWD LC) & the Rincon Station (TPWD RI) as well as surrounding TCOON stations.

2.2 Stations Instrumentation

Thermistor strings composed of 4 YSI® 44032 (YSI, 2007)] thermistors attached to a steel cable were assembled for the project. The YSI thermistors are purchased in bulk and assembled each with 18-2 gauge copper wires for the electrical connection, and potted into an ECOBOND epoxy matrix (Emerson & Cuming ECCOBOND 45 Black plus ECCOBOND Catalyst 15 Black epoxy). The in-house manufacturing of the thermistor strings gives the flexibility to have strings

of any desired length and spacing. It also brings considerable cost savings to the project. Each thermistor is tested for accuracy prior to field deployment. The test is carried out by submerging the sensors in an ice bath and comparing their readings to a laboratory thermometer. The voltage response of each thermistor is monitored as the ice melts and as the bath reaches room temperature. The temperatures are then computed from the voltage outputs.

Once calibrated the thermistors and the rest of the equipment is transported to the station location. The deployment geometry is illustrated in figure 3. The steel cable is deployed from the platform and along the slope of the dredged Intracoastal Waterway. The platform is in typically 2-3' of water while the nominal dredged depth of the Intracoastal Waterway is 14-15'. The thermistors are attached to the cable at locations selected such that their respective depths are approximately 3', 6', 9' and 12'. The sensor locations, i.e. locations along the steel cable, are established using a Garmin GPS492 depth sounder/GPS unit. The thermistors are zip-tied to the steel cable. The tip of each thermistor is left free to float 8"-10" above the Laguna floor and its muddy bottom with a fishing cork attached to the sensor for flotation. All 4 thermistors are connected to a Sutron Satlink II dataloger (SL2- G312-1) (Sutron, 2007) purchased from Sutron

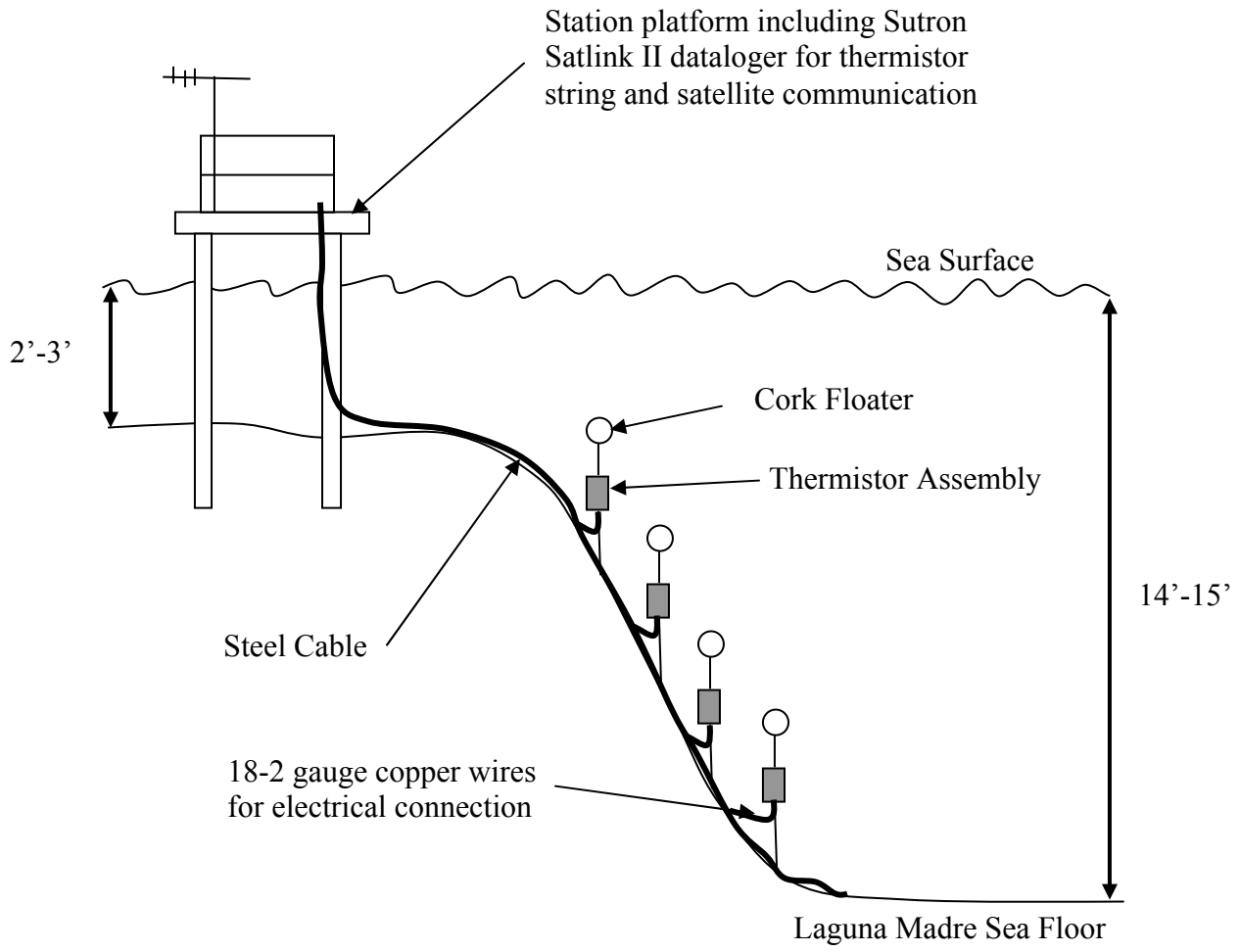

Figure 3. Schematic of the sensor deployment for both project stations.

Corperation (Sutron, 2007). A 30KOhm Resistor is placed in series with each thermistor circuit per Sutron Satlink II instructions which completes the sensor deployment. Transmission of the measurements takes place through satellite communication typically on an hourly basis.

2.3 Stations Abbreviated Information

The main information regarding location, installation, instrumentation and maintenance of the stations is also presented in abbreviated format in Table 1.

Table 1. Detailed information for the two project stations and the collected time series

Station Name:	Texas Parks & WIldlife Department, Rincon Station	Texas Parks & WIldlife Department, Land Cut Station
DNR ID:	140	141
Abbreviation:	TPWDRI	TPWDLC
Location:	26° 48.090' N, 97° 28.236' W	26° 55.883' N, 97° 27.388' W
	26.8015000 / -97.4706000	26.9313900 / -97.4564700
url:	http://lighthouse.tamucc.edu/overview/140	http://lighthouse.tamucc.edu/overview/141
Information collected:	water temperatures at 4 depth within the water column	water temperatures at 4 depth within the water column
Data collection Start:	February 27, 2006	December 13, 2005
Communication:	Satellite transmission, measurements available on the web typically within 1 hr.	Satellite transmission, measurements available on the web typically within 1 hr.
Check / Maintenance:	July 24, 2007: Station inspection – No replacement	July 24, 2007: Replacement of thermistor string
Other information:		Added correction record for wtp1, wtp3, wtp4 to remove data from 2007178+1130 to 2007198+0000 as per John Adams.

2.4 Temperature Profiles History

2.4.1 TPWD Rincon Station

Temperature histories for the duration of the project are presented in Figure 4 for the 4 water temperature sensors of the Rincon station. More detailed monthly graphs of the measured temperature profiles are presented in tables 2 & 3 for both the Rincon and the Land Cut stations. The Overall temperature measurements for both stations show higher temperatures in the summers in the 25°C to 34°C range from about mid May to mid October. During the rest of the year the temperature profiles are dominated by sharp and large temperature decreases created by the passage of cold fronts followed by more progressive temperature increases between frontal passages. The general tendency is for the low water temperatures reached to progressively

Table 2. Temperature profiles for selected time periods for the TPWD Rincon Station (full records in Appendix I)

March 2006 Temperature records for the TPWD Rincon Station

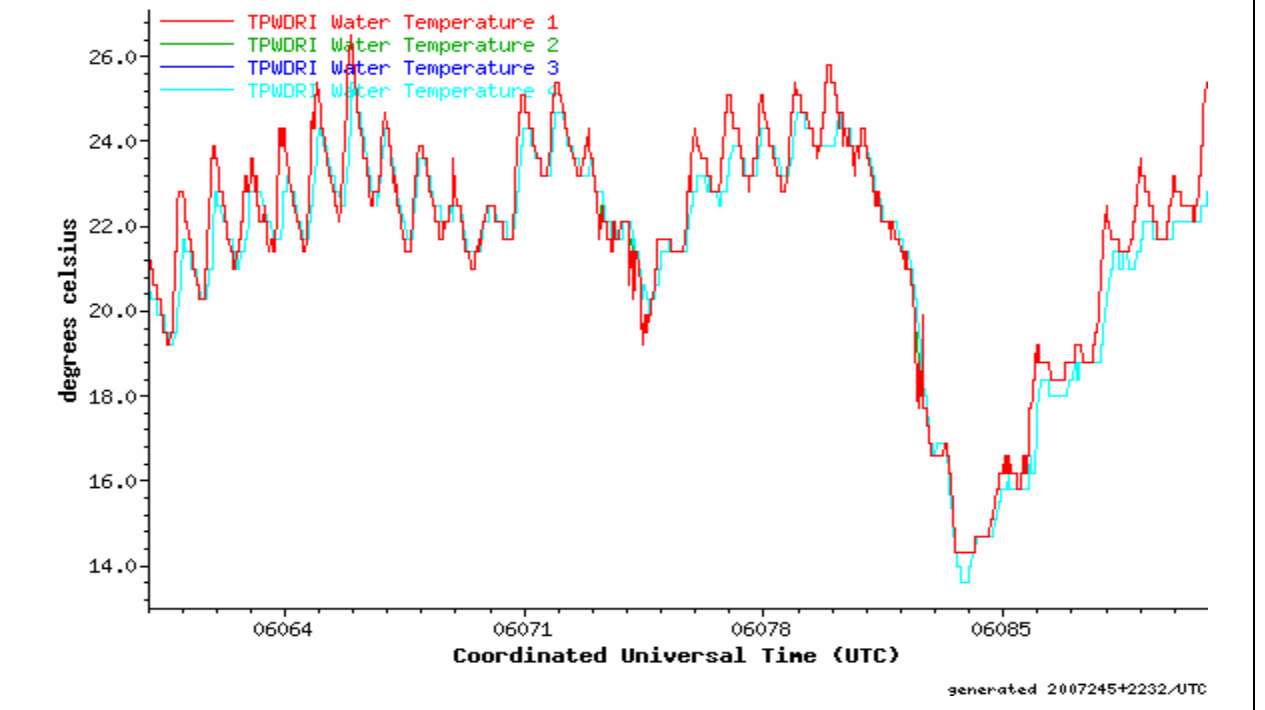

May 2006 Temperature records for the TPWD Rincon Station

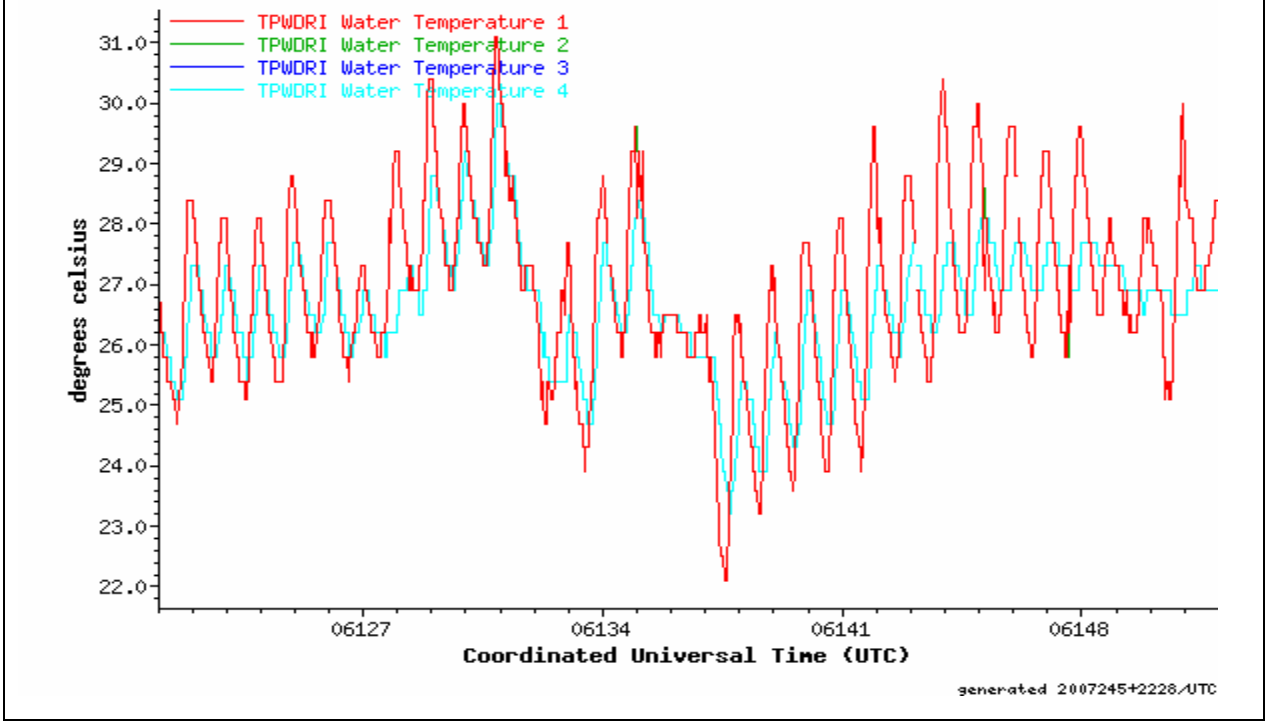

Table 2 cont. (full records in Appendix I).

July 2006 Temperature records for the TPWD Rincon Station

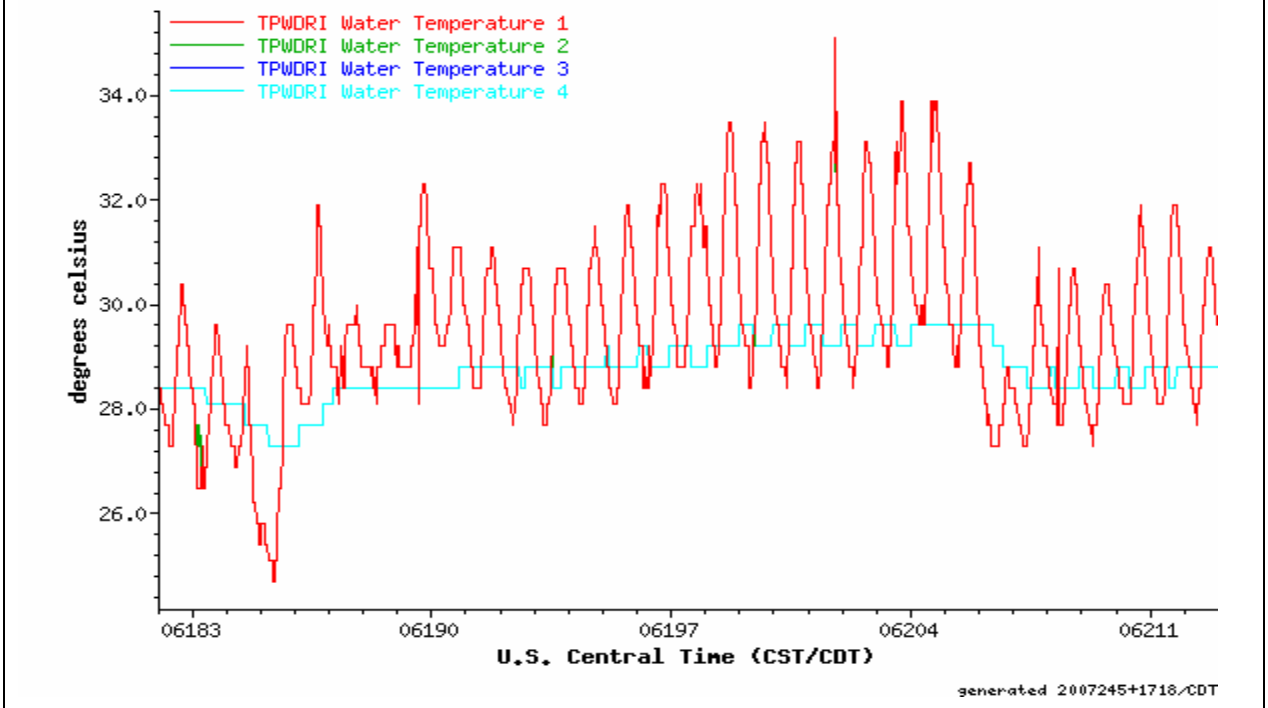

October 2006 Temperature records for the TPWD Rincon Station

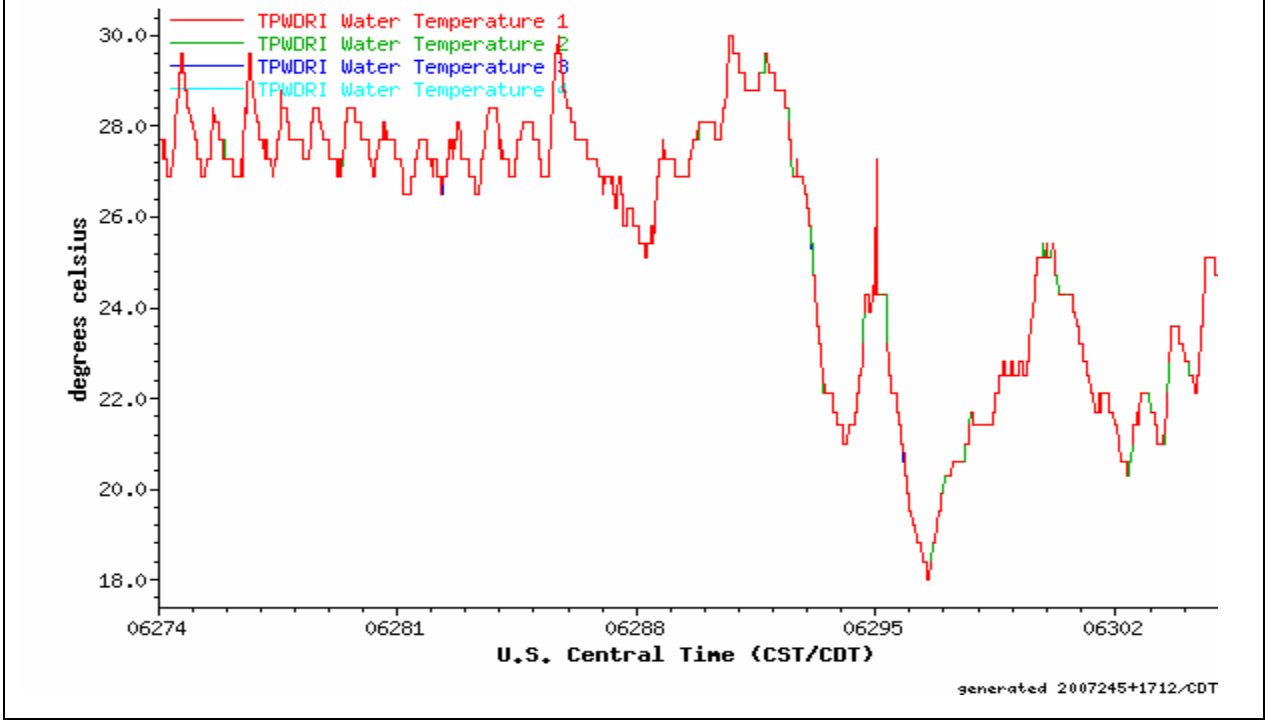

Table 2 cont. (full records in Appendix I).

January 2007 Temperature records for the TPWD Rincon Station

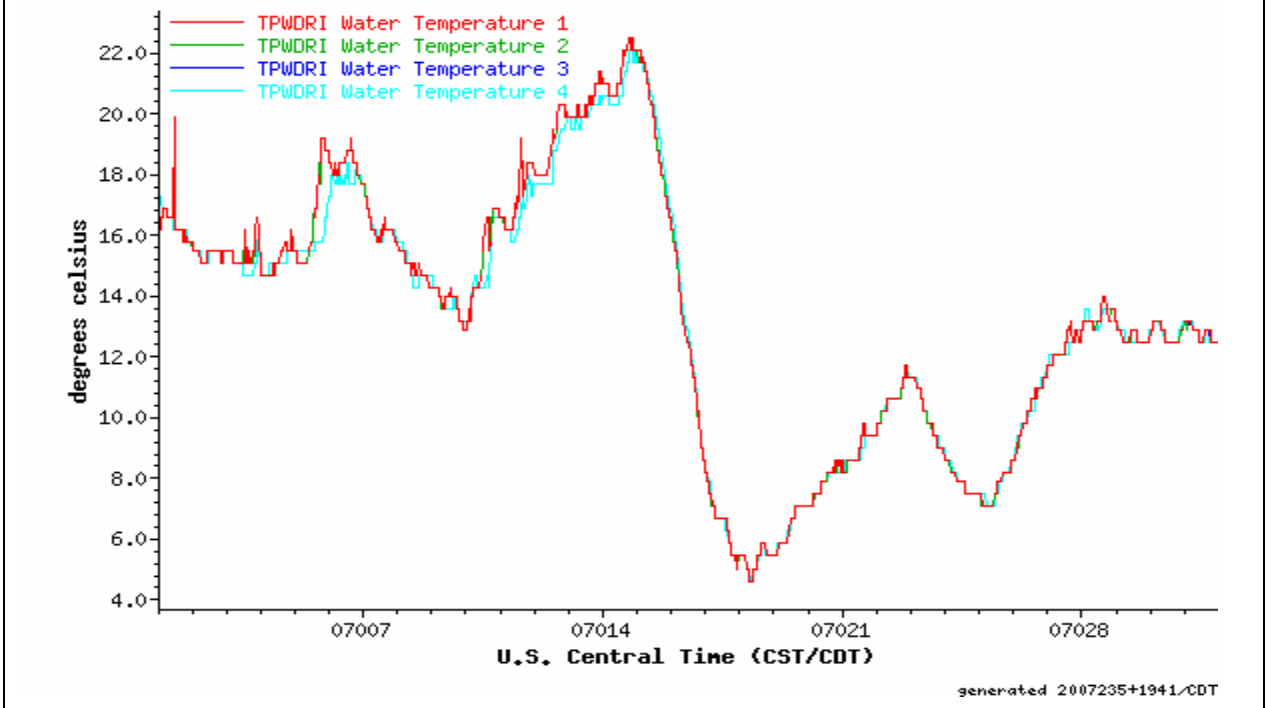

April 2007 Temperature records for the TPWD Rincon Station

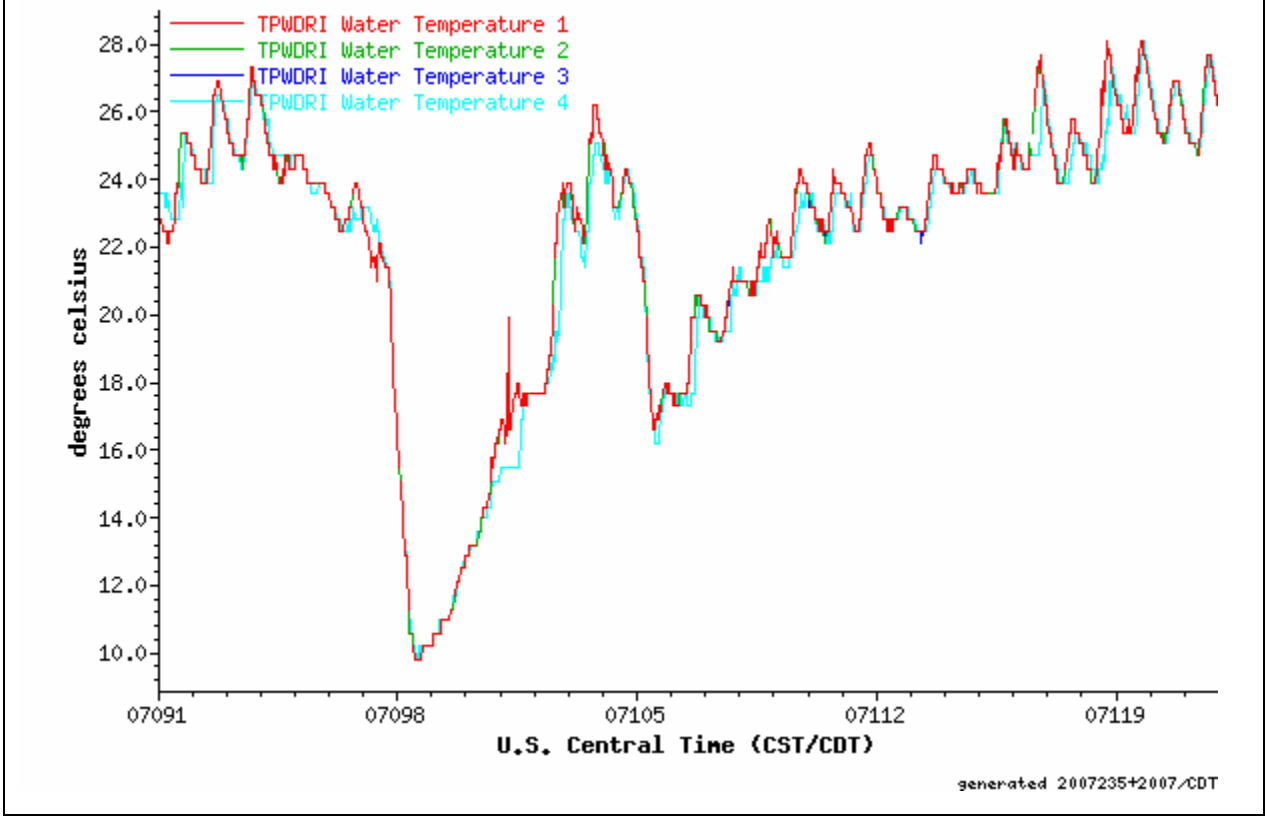

Table 2 cont. (full records in Appendix I).

July 2007 Temperature records for the TPWD Rincon Station

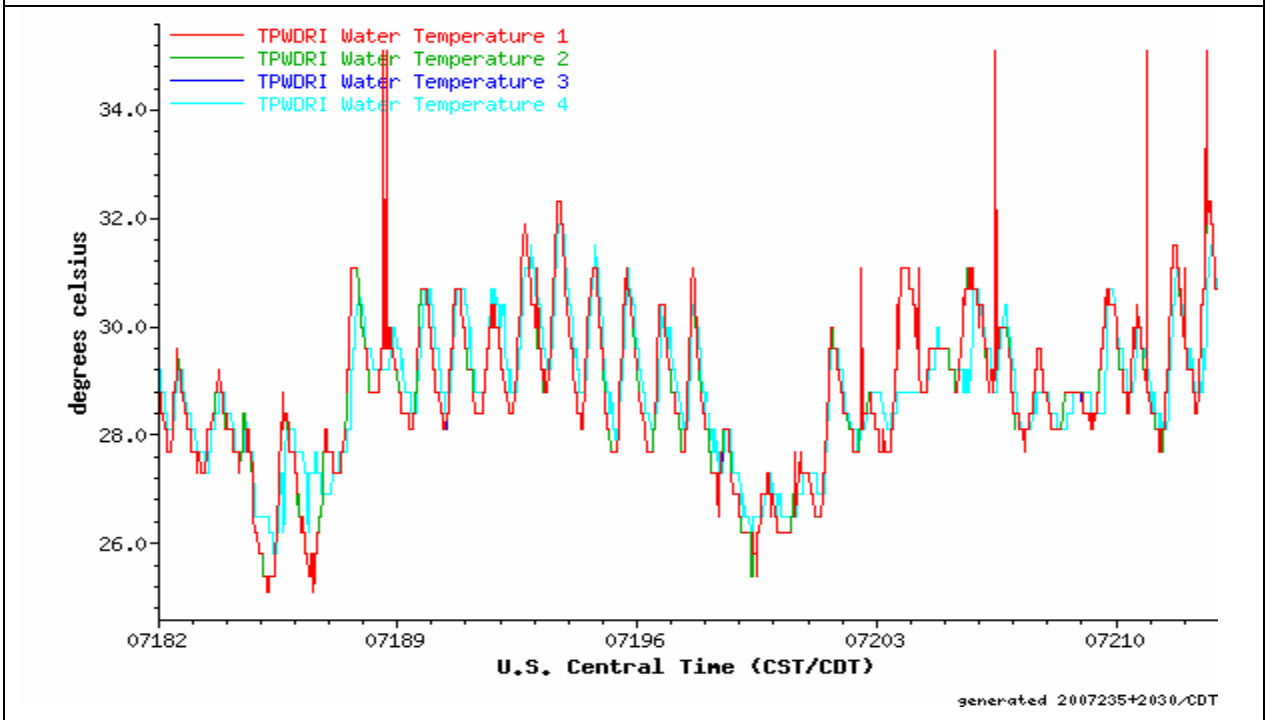

August 2007 Temperature records for the TPWD Rincon Station

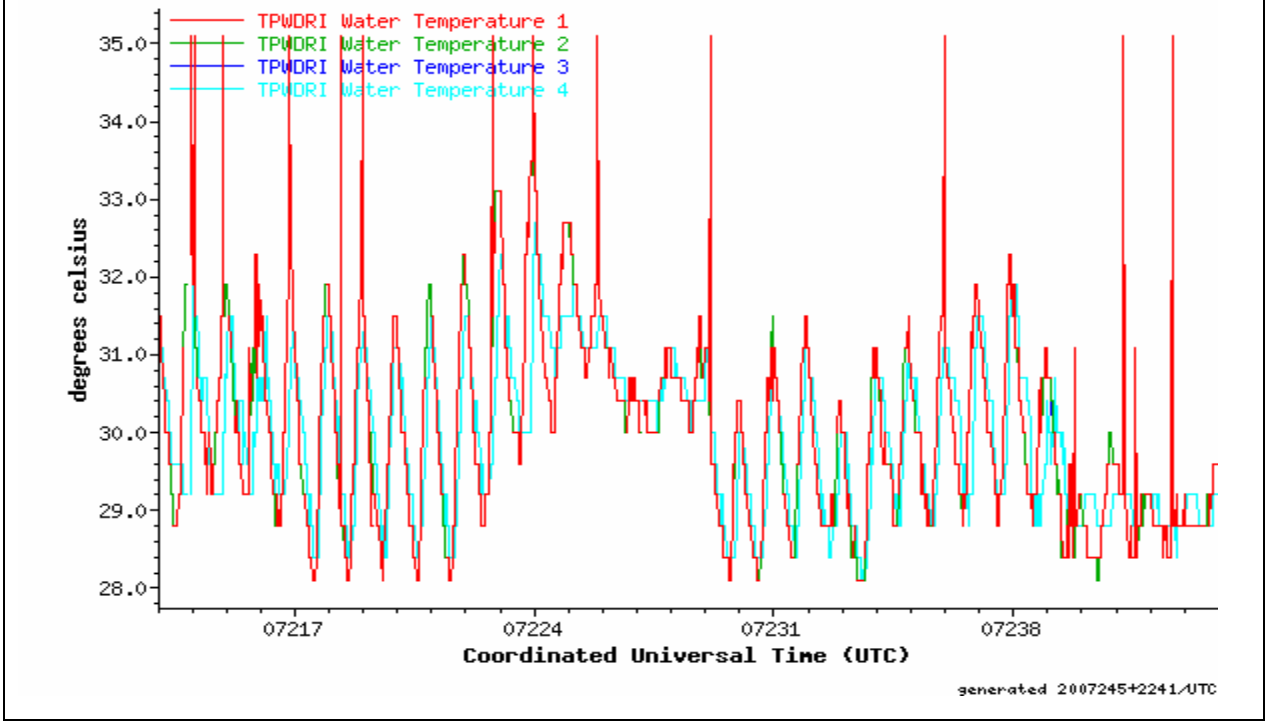

Table 3. Temperature profiles for selected time periods for the TPWD Land Cut Station (full records in Appendix)

December 2005 Temperature records for the TPWD Land Cut Station

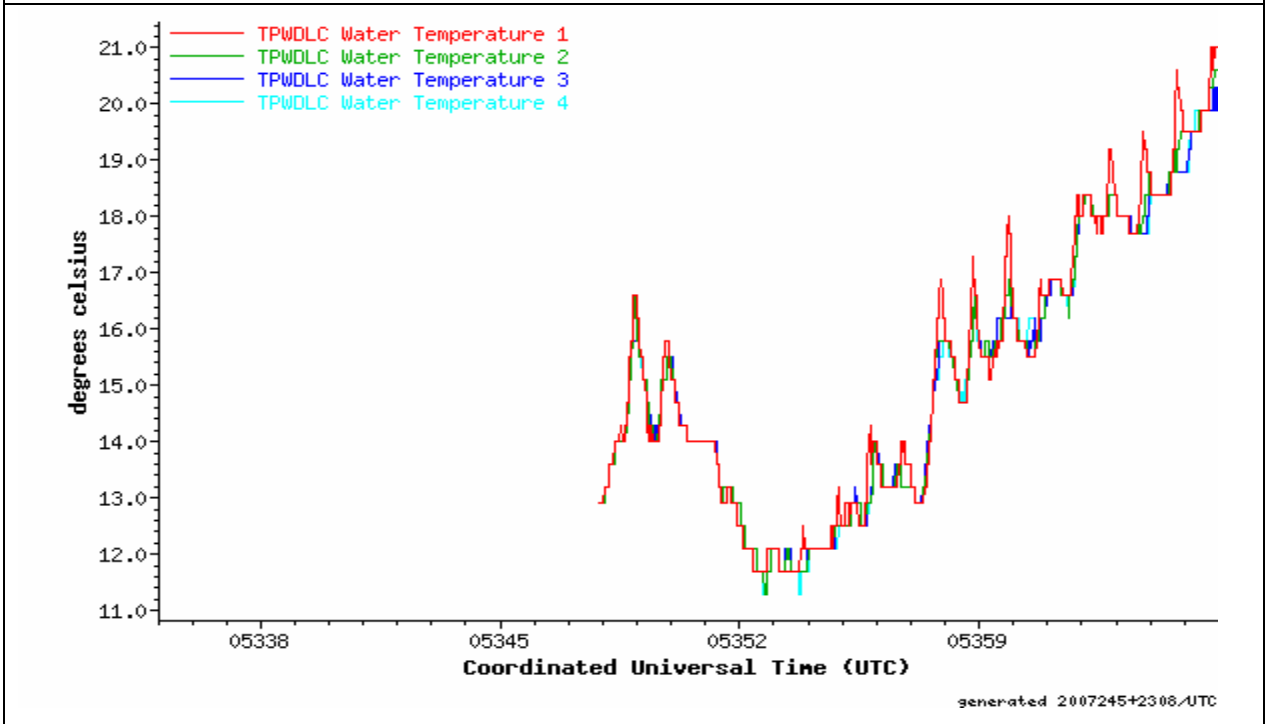

January 2006 Temperature records for the TPWD Land Cut Station

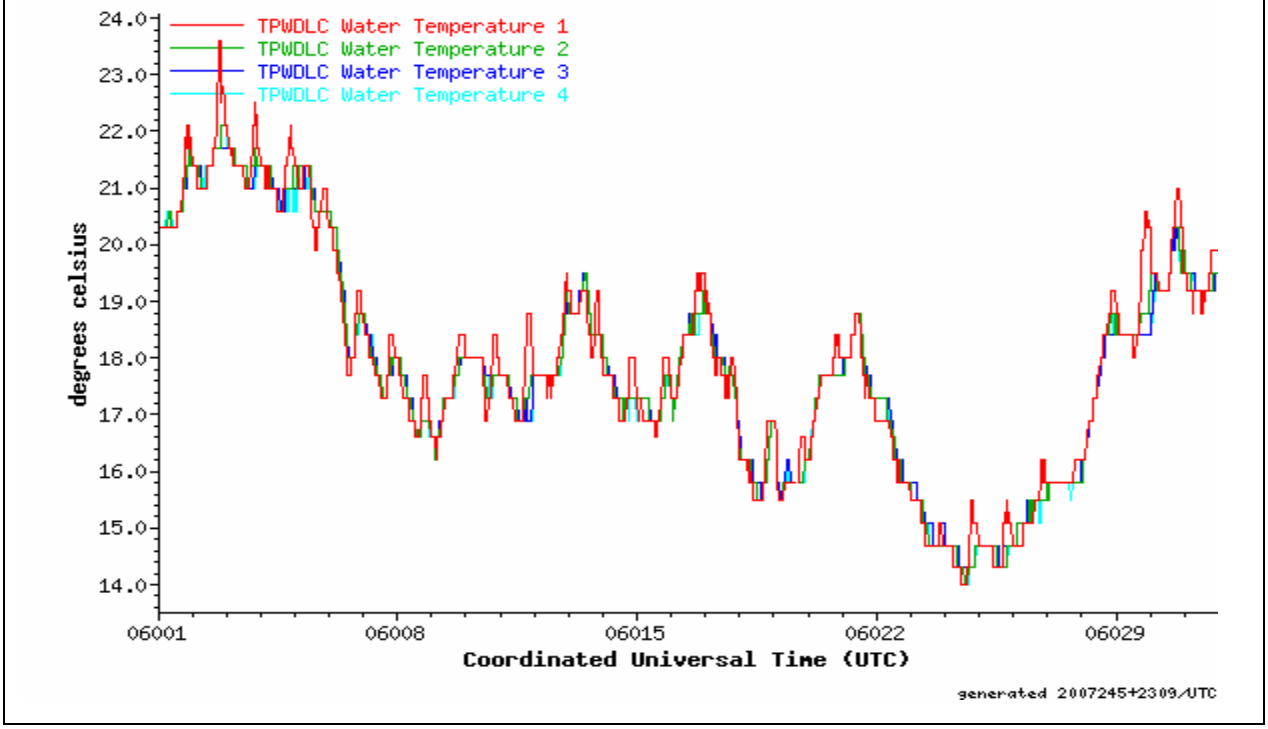

Table 3 cont. (full records in Appendix II).

February 2006 Temperature records for the TPWD Land Cut Station

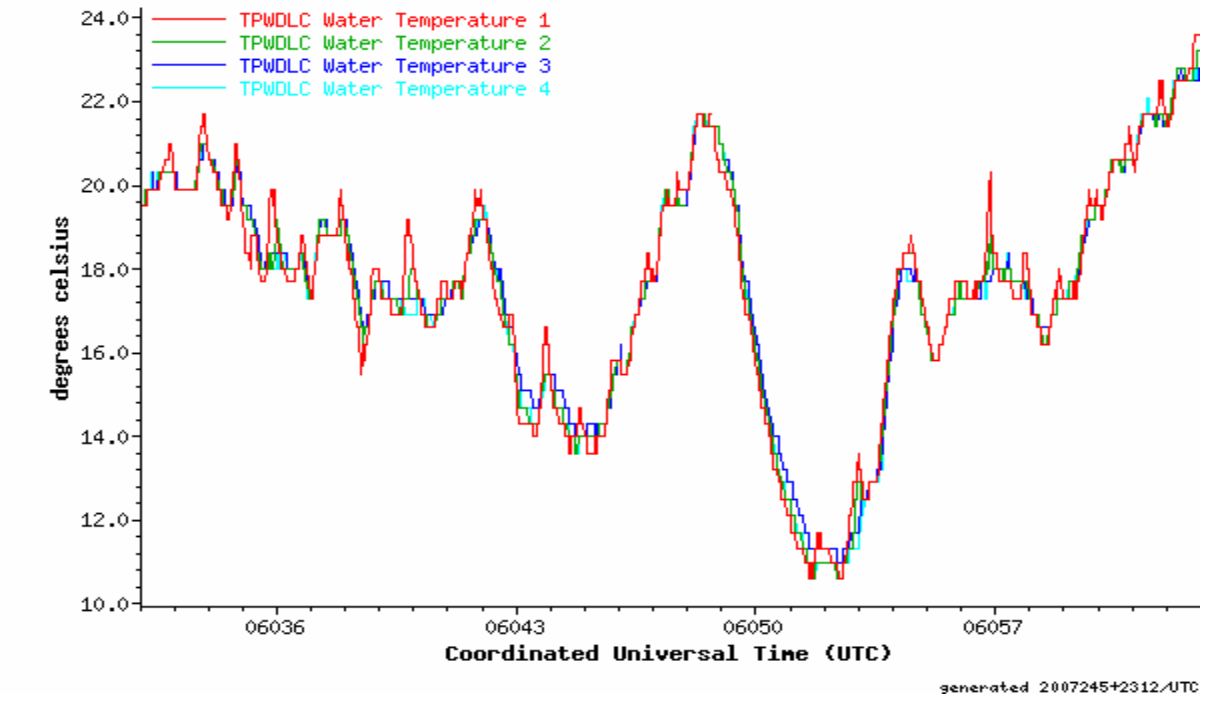

May 2006 Temperature records for the TPWD Land Cut Station

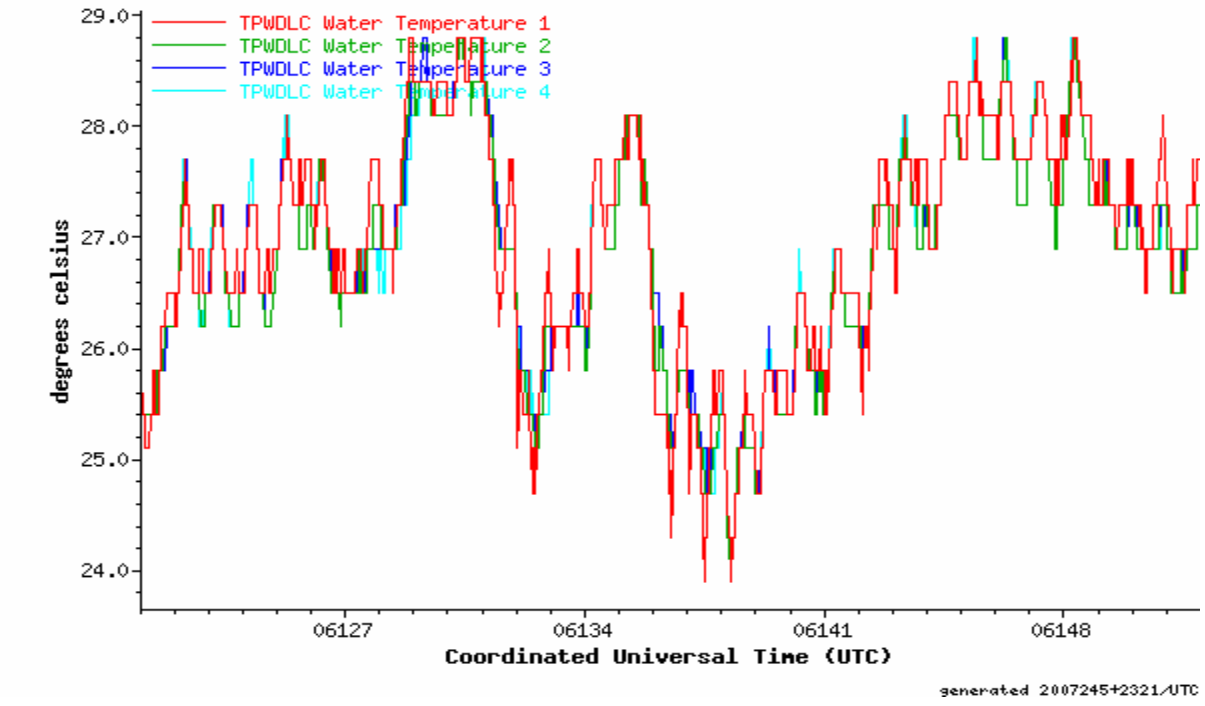

Table 3 cont. (full records in Appendix II).

July 2006 Temperature records for the TPWD Land Cut Station

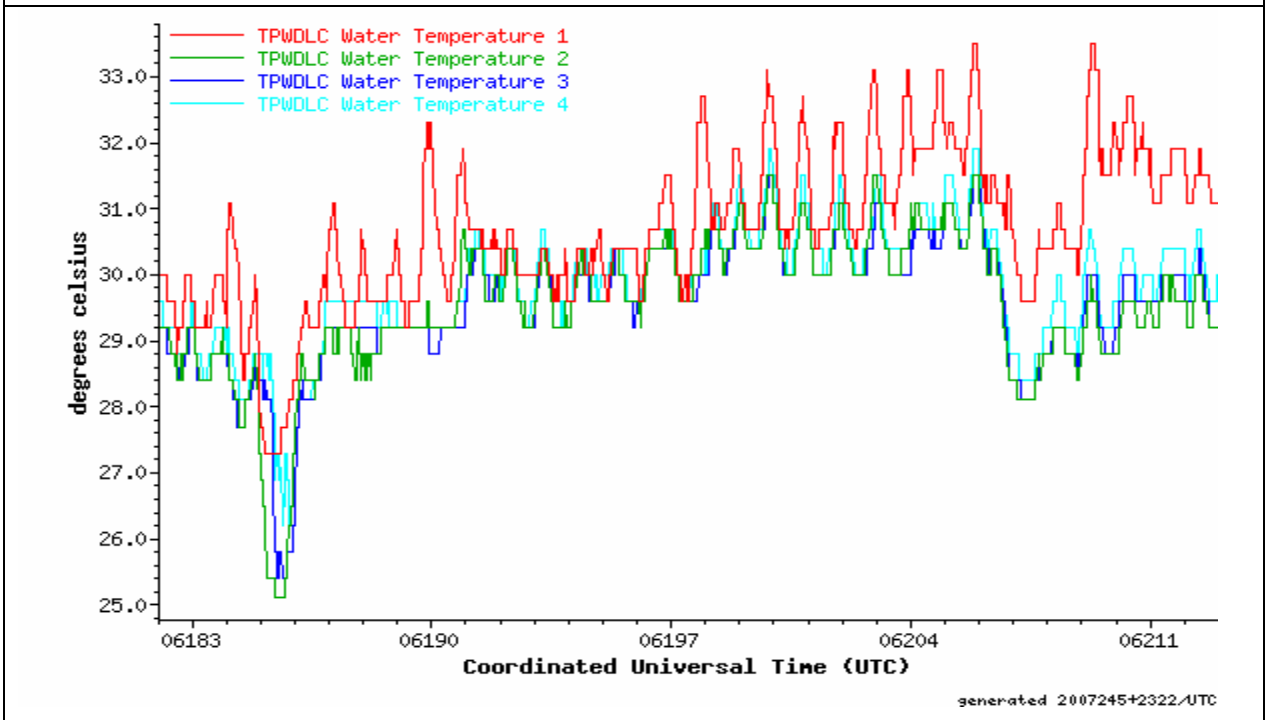

October 2006 Temperature records for the TPWD Land Cut Station

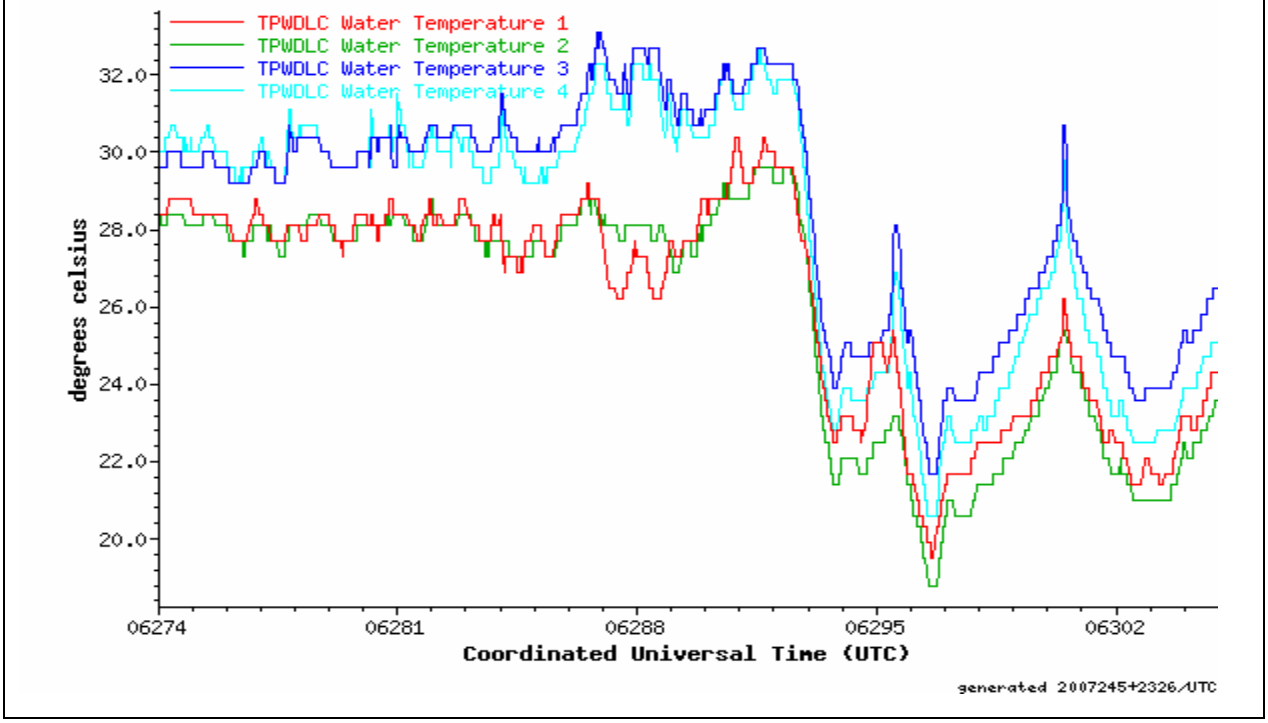

Table 3 cont. (full records in Appendix II).

January 2007 Temperature records for the TPWD Land Cut Station

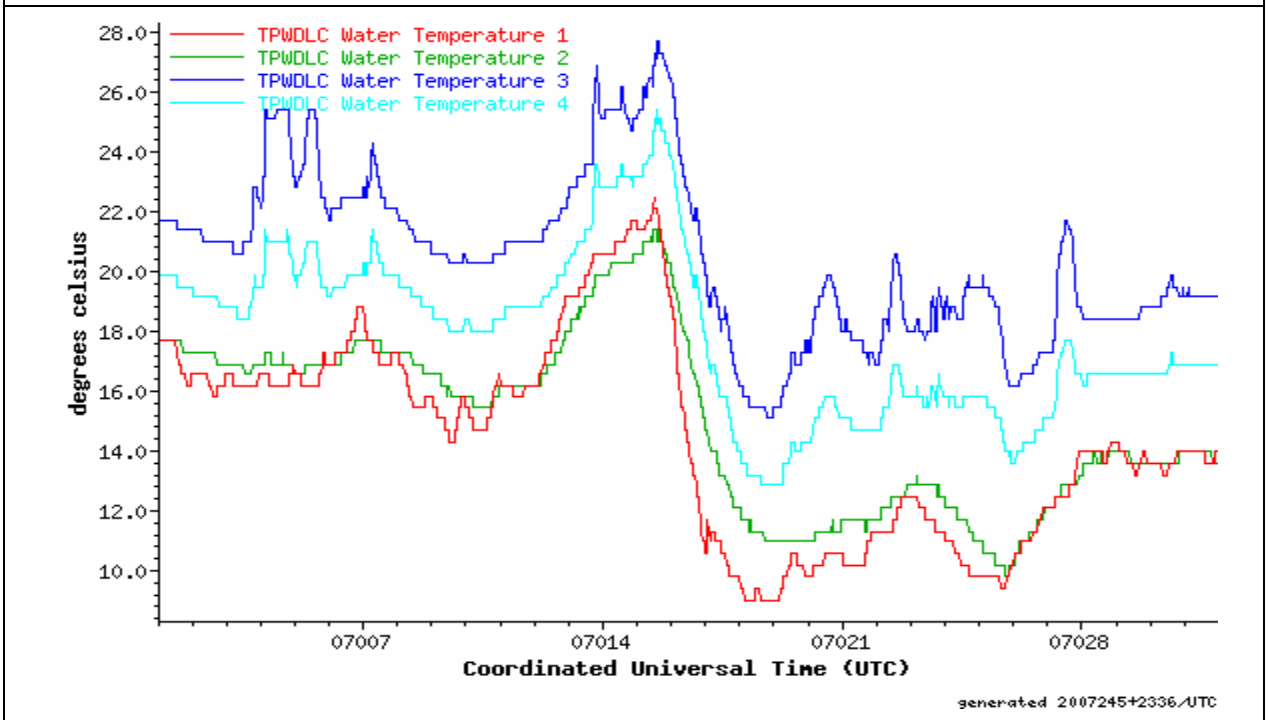

May 2007 Temperature records for the TPWD Land Cut Station

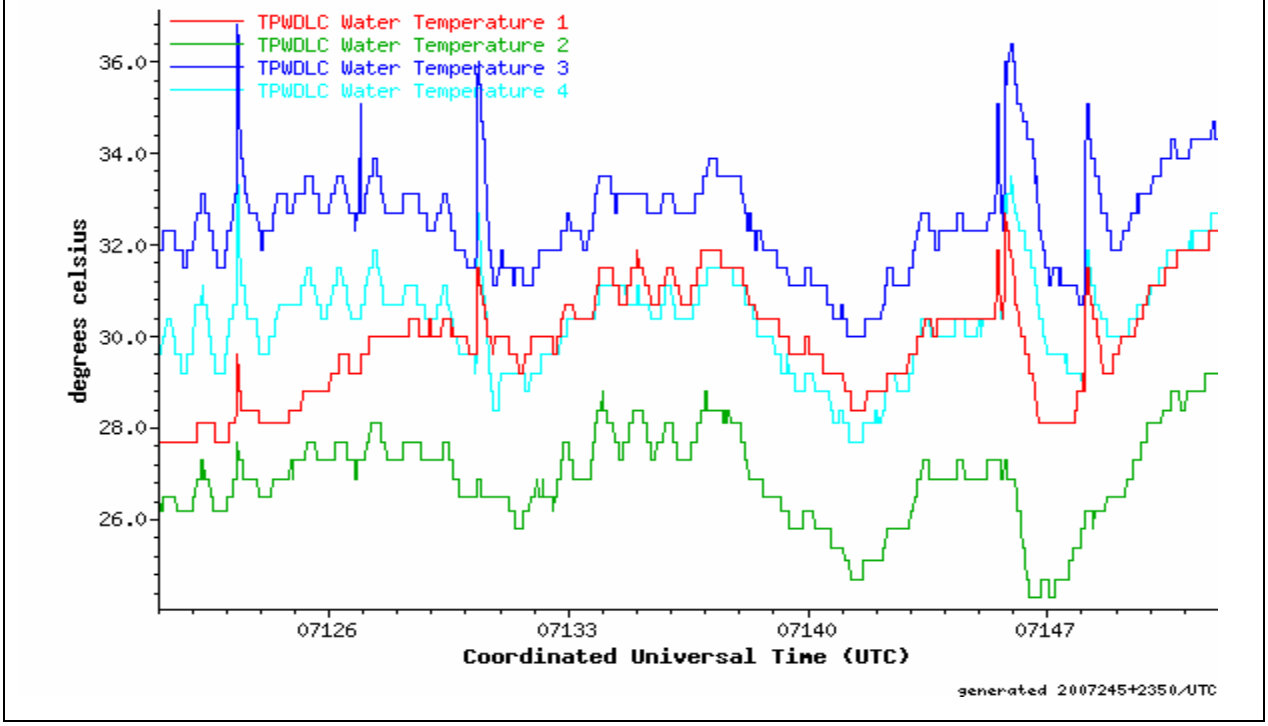

Table 3 cont. (full records in Appendix II).

July 2007 Temperature records for the TPWD Land Cut Station
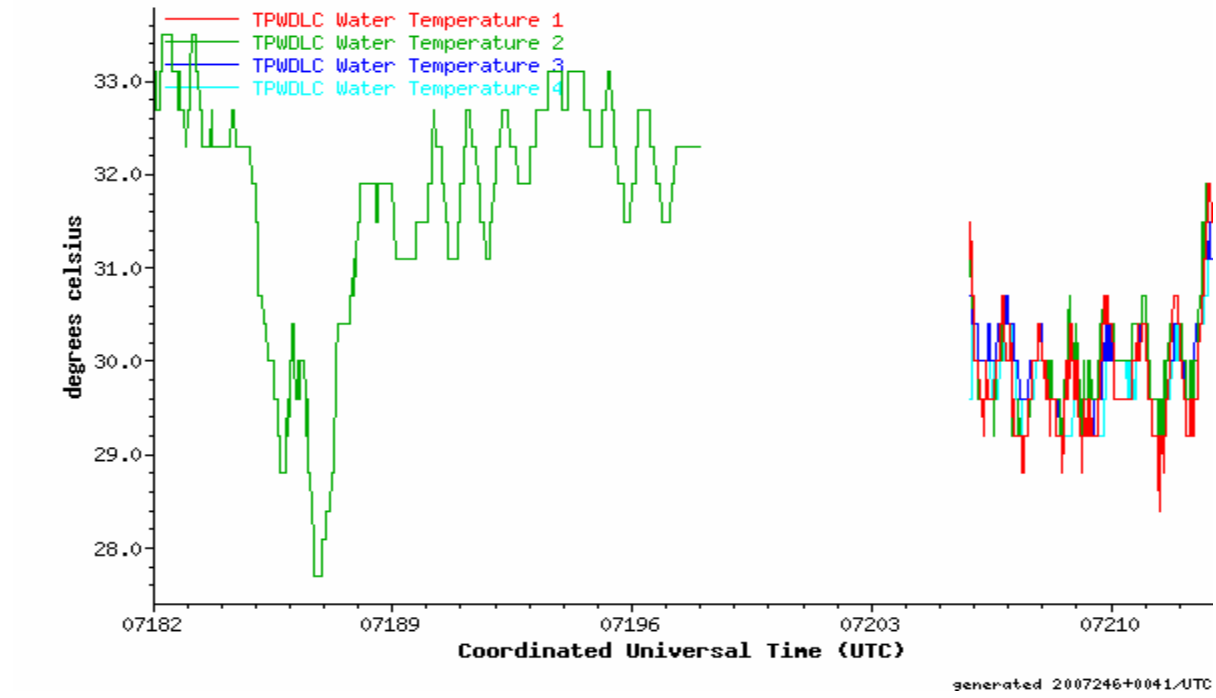
August 2007 Temperature records for the TPWD Land Cut Station
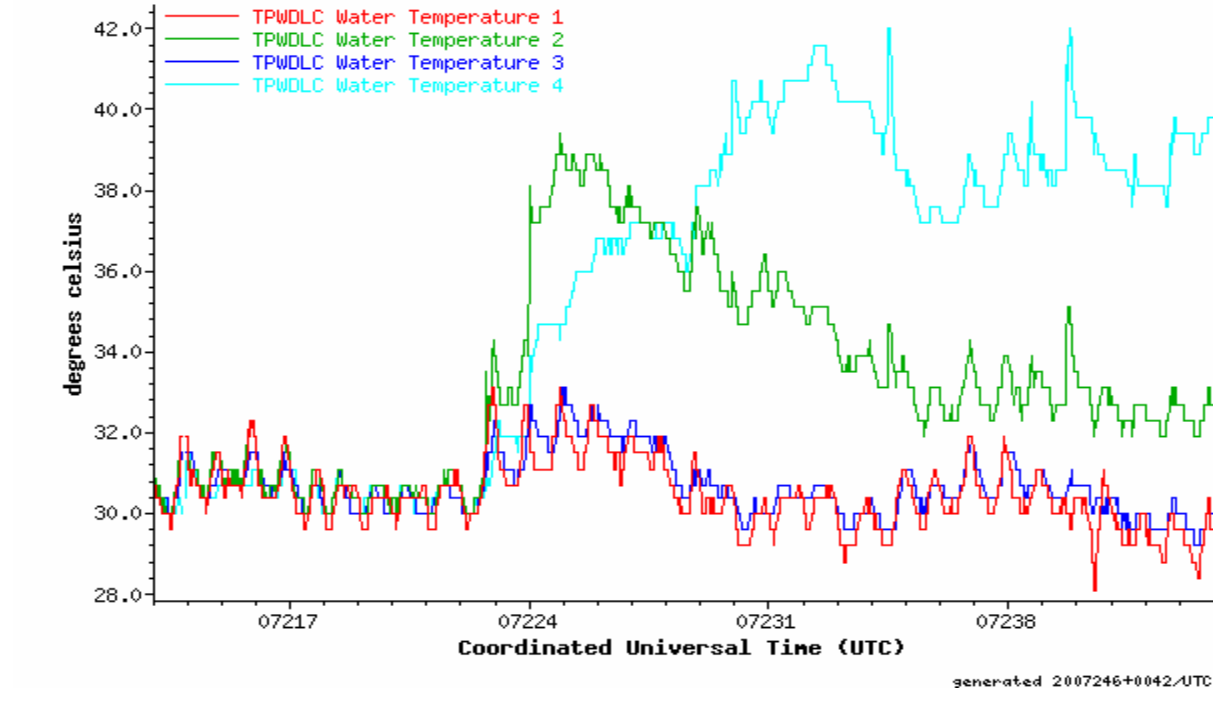

decrease during the fall and first portion of the winter months and increase during the spring with the exact temperature dynamic depending on the intensity and number of cold fronts. The sharpest temperature drop during the project was observed in January 2007 with water temperatures decreasing from 22.5°C at 7:00 PM on January 15 down to 4.6°C on January 18 at 7:00 AM or about 18°C in 60 hours.

The four water temperature time series for the Rincon Station functioned virtually uninterrupted during the project. Quality control was kept to a minimum for this exploratory data. For operational stations spikes and data from drifting sensors are typically removed as part of the DNR QA/QC daily process. For the Rincon station only data from sensor #4 or bottom sensor was removed from September 2006 to December 2006 as it became clear that the data did not longer make physical sense. The sensor started drifting to temperatures considerably above the other 3 sensors at the beginning of September 2006. The measurements from sensor 4 were therefore disabled until the problem could be corrected in December 2006. The Rincon sensor 4 or bottom temperature sensor had actually started drifting uncharacteristically from the readings of the other sensors in mid May 2006. For the analysis the period of mid May 2006 to mid December 2006 is not included to avoid the influence of a potentially malfunctioning sensor.

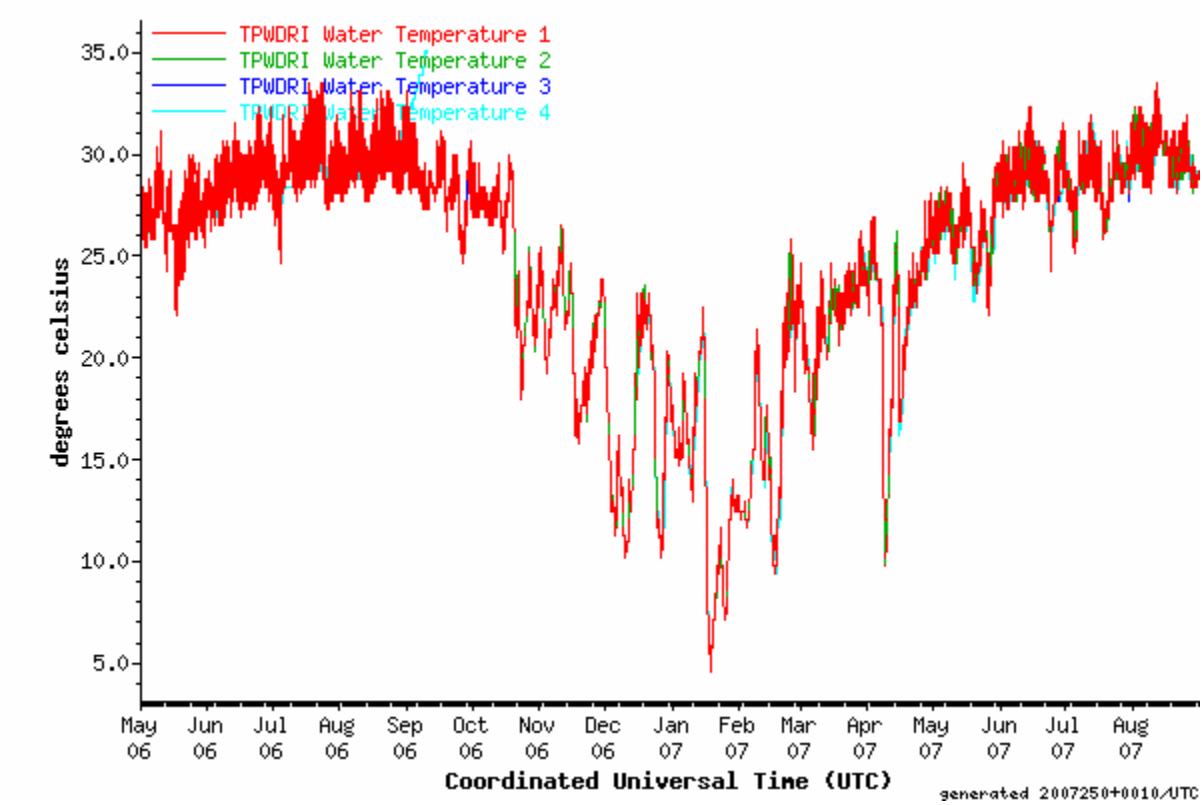

Figure 4. Water temperature measurements (3-hr frequency) for the 4 water temperature sensors at the TPWD Rincon station for the May 2006 to August 2007 period..

When considering the three other time series during the total project duration, no significant temperature differences could be observed except for a small number of hourly spikes observed

for the temperature sensor 1, the top sensor. These spikes will be analyzed later at the end of this paragraph. Except for these few spikes the temperatures of the three sensors stay virtually identical during the project duration as can be observed in the graphs of Table 2. Looking at the numbers rather than the graph reveals that there is no difference whatsoever between the measurements of these three sensors. Our first observation is that there is no water temperature gradient for most of the water column at the Rincon station within the resolution of the water temperature sensors (.1°C). As the top sensor is generally about 3' below the sea surface, this statement does not cover potential thin surface lenses of different temperature.

The only noticeable differences where observed for sensor #4 or bottom sensor. The sensor is located about 12' below the sea surface and therefore possibly up to 2'- 3' above the deepest location in the ICW channel. Temperature differences are typically smaller than 0.5°C and observed during warming trends. During sharp temperature rises temperature differences above 1°C can be observed for a few hours. A few cases of temperature differences above 1°C were observed during all seasons. A temperature difference of 3.4°C was measured on January 5, 7:00 PM, between sensor 4 and the other sensors (left portion of Figure 5). This temperature difference was back to within 0.5°C within 7 hours. For the project period, the largest temperature difference of 5.1°C was observed on February 20th, 2007 at 7:00 PM. For that event as well the bottom temperature gradient disappeared after 8 hours.

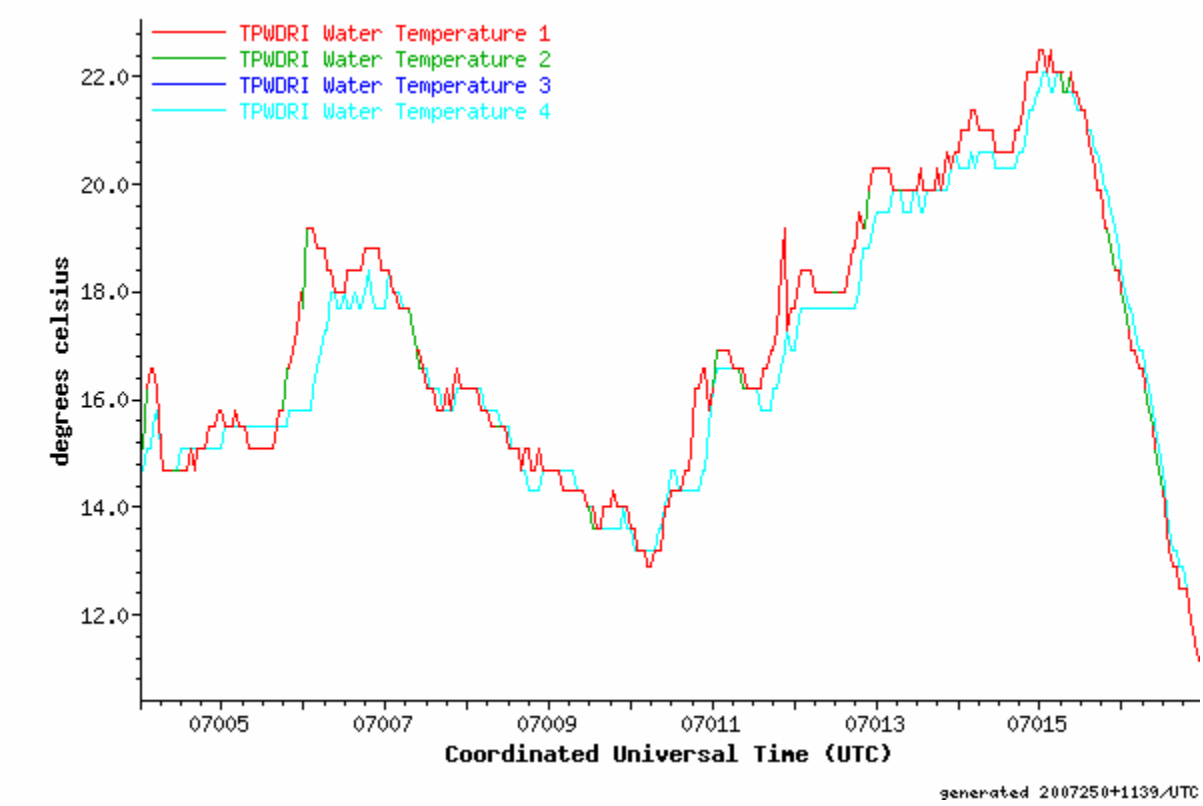

Figure 5. Water temperature measurements (1-hr frequency) for the 4 water temperature sensors at the TPWD Rincon station from January.

On occasions sensor temperatures were observed to be higher for sensor 4 than for sensor 3. The number of such cases was substantially lower than cases for which sensor 4 temperatures were

below sensor 3 temperatures. Figure 6 illustrates the distribution of cases with positive and negative temperature gradients between the two sensors. For the vast majority of cases the temperatures are within 1°C with some cases with temperature differences up to 5°C and a substantially smaller number of cases with negative temperature gradients with gradients as low as -2°C .

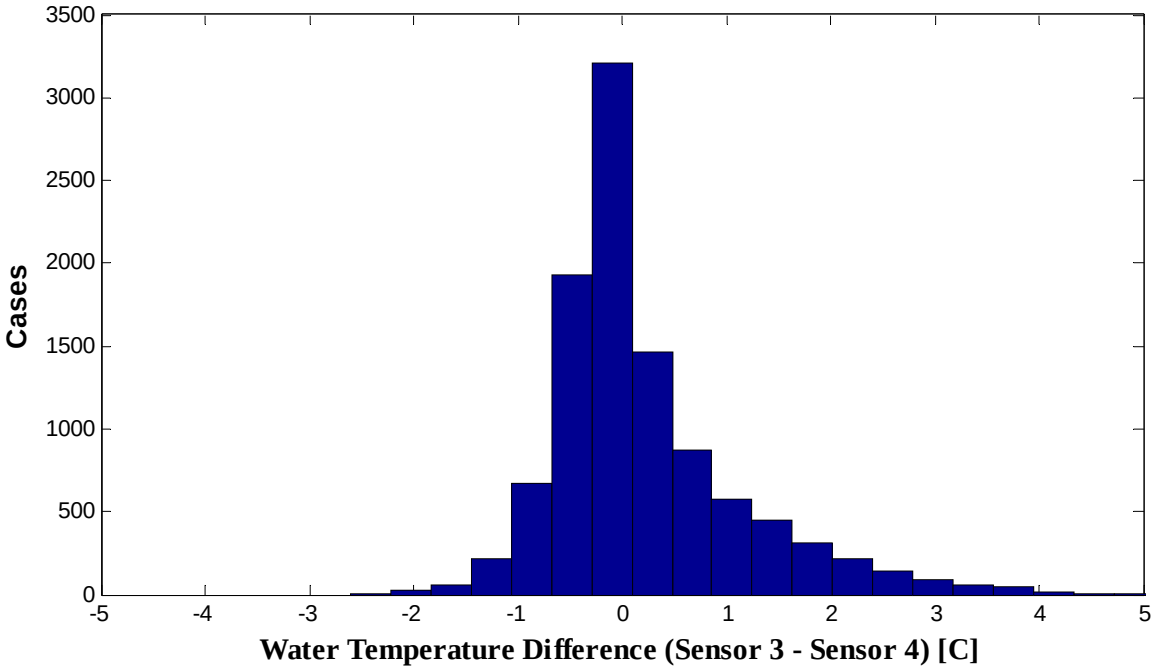

Figure 6. Frequency of water temperature differences between sensor 3 and sensor 4 for hourly temperature measurements.

Of particular interest to this study is the temperature gradient during low temperature events. No temperature differences could be observed during the largest temperature drop of January 15-18, 2007 as well as during the other substantial temperature drops, e.g. December 06 and April 07. The lack of a measured gradient during the cold front passages is likely due to the stronger winds associated with a frontal passage resulting in a faster/better mixing of the water column. Also in the absence of wind a possible temperature gradient would lead to lower temperatures at the surface (cooled by the colder air temperature) and the higher density of the colder surface waters would then lead to buoyancy driven currents and the homogenization of the temperature profile.

The water temperature time series of the 4 sensors of the Rincon station indicate that the water column is largely homogenous temperature wise with likely a small moderating effect at the bottom of the channel particularly during sharp temperature rises. This moderating effect is however not observed during the sharp temperature decreases observed during frontal passages. As the water temperature sensors were all located 8”-10” the water temperatures in the muddy bottom layer were not measured and could show stronger gradients. Such measurements will be discussed for a possible follow up study.

The last issue to be discussed for the Rincon station is the occurrence of temperature spikes, i.e. sharp rises, typically of a few degrees and up to 18°C for one or two data points. These spikes

were observed almost exclusively for sensor #1 (the top sensor). The largest numbers of temperature spikes were observed August 2007 (~ 12 spikes) and in November 2006 (~ 6 spikes). Such spikes can occur for all types of instruments due to a variety of reasons including communication problems, electrical problems, sensor malfunction etc. They are typically removed as part of the DNR QA/QC process. Spike data was however not removed for these stations to verify that the spikes were indeed caused by spurious problems. Given that sensor #1 is the top sensor, it seemed appropriate to make sure that the spikes were not related to the low water levels for example. Note also that raw data stays permanently in the DNR database and that when labeled spike or otherwise unreliable data is only removed from the record accessible to the public but can always be retrieved if necessary. To verify the spurious nature of these spikes, water temperatures were compared other parameters in figures 8 & 9. As can be seen there is no correlation with water levels, water level standard deviation, air temperature or wind speed. Consequently these spikes were removed from the accessible record i.e. a reader consulting the stations records online will now see water time series without spikes.

2.4.2 TPWD Land Cut Station

The Land Cut station installation was completed on December 13, 2005. The Land Cut and Rincon sensor # 2 temperature records are compared in Figure 9. Overall the records are very similar with differences observed only during the major cold events of January, and April 2007. Figure 10 compares sensor #1 & #2 readings at the two stations during these cold events. For the January event the minimum temperature reached by both Rincon sensors was 4.6°C while the minimum temperatures reached by Land Cut sensors #1 and #2 were respectively 9.0°C and 11.0°C. The difference is important for this study as the readings are below and above the cutoff temperature of 7.2° (45F) for likely physiological damage to local marine life. For the April cold event, both Rincon sensor minimum readings were 9.8°C while the minimum Land Cut readings were both 14.7°C although sensor #2 reached 14.7°C 10 hours after sensor #1. These differences must however be considered with caution as measurement problems, described later in this

Table 4. minimum temperatures reached at the project locations and other nearby locations (listed North-South) in the Laguna Madre during the January 15-18, 2007 cold front passage.

Station	Minimum Temperature reached		Time minimum temperature first reached during the cold event
Bob Hall Pier (Gulf side)	9.8°C	49.6F	January 17 - 10 AM
Packery Channel	6.4°C	43.5F	January 17 - 5 AM
TCOON Bird Island	6.0°C	42.8F	January 18 - 7 AM
TCOON Baffin Bay	6.7°C	44.1F	January 18 - 7 AM
TPWD Land Cut Sensor #1	9.0°C	48.2F	January 17 – 10 PM
TPWD Land Cut Sensor #2	11.0°C	51.8F	January 18 – 12 PM
TPWD Rincon Sensor #1	4.6°C	40.3F	January 18 - 7 AM
TPWD Rincon Sensor #2	4.6°C	40.3F	January 18 – 7 AM
TCOON Port Mansfield	10.3°C	50.5F	January 19 - 1 PM
S. Padre Island Coast Guard Station	4.8°C	40.6F	January 17 - 10 AM

section, were encountered for the Land Cut Station. The Rincon and Land Cut minimum temperatures reached are compared to other Laguna Madre stations and Bob Hall Pier in Table 4.

The minimum temperatures at the nearby similar stations, Bird Island and Baffin Bay, are respectively 6.0°C and 6.7°C reached both January 18, 7 AM. Measurements from these stations match well with the Rincon station readings. The other stations listed for reference are Bob Hall Pier, Packery Channel, Port Mansfield and the South Padre Island Coast Guard station. The first station indicates the Gulf signal which as expected indicates a higher minimum temperature reached and also a minimum temperature reached 1 day before the portion of the Laguna Madre monitored. The stations of Packery Channel and the South Padre Island Coast Guard Station reach their minimum temperatures earlier as well, likely due to their connection to the Gulf of Mexico. The Port Mansfield station also reaches a higher minimum temperature (10.3°C) due to its connection to the warmer nearby Gulf of Mexico. Based on this analysis the TPWD Land Cut measurements should be taken cautiously and possible significant differences in temperature profiles during cold events will continue to be investigated.

Selected monthly records of all 4 Land Cut sensors are displayed in Table 3. While the temperature records for all 4 sensors match from its onset in December 2005 to mid July 2006 and from late July 2007 to early August 2007. Starting mid July 2006 sensor # started recording higher temperatures by up to 3°C than the other sensors. By September 2006 all sensors start measuring different temperatures with sensors #1 & #2 systematically recording lower temperatures than sensors #1 and #2 with a temperature range for the 4 sensors of about 4°C to 6°C. The thermistor string was replaced in July 24, 2007. Following this replacement, all sensors measured the same water temperatures within 1°C up to August 1PM. From that point on the sensor readings drifted a part. Examination of the thermistor string removed on July 24th revealed considerable barnacle build-up but no other specific damage to the instrumentation. Investigation of the instrumentation problem at the Land Cut station is still ongoing. For this report the months for which the Land Cut water temperature sensors showed different readings will be discounted due to sensor related problems and the Land Cut station readings will be considered to behave very similar to the Rincon station. This was the case during the months for which the sensor readings were not considered problematic. Possible difference could still be observed during the sharp decreases related to cold front passages but additional data will be needed for further analysis. Also equipment alternative are considered such as different themistors to solve the Land Cut station recurring problem.

Finally figure 9 comparing the Rincon and Land Cut water temperature time series shows larger short term variability at the Rincon station as compared to the Land Cut station. It is not clear if the effect is indeed physical i.e. related to small differences in local water temperature dynamics or due to sensor performance or sensor installation.

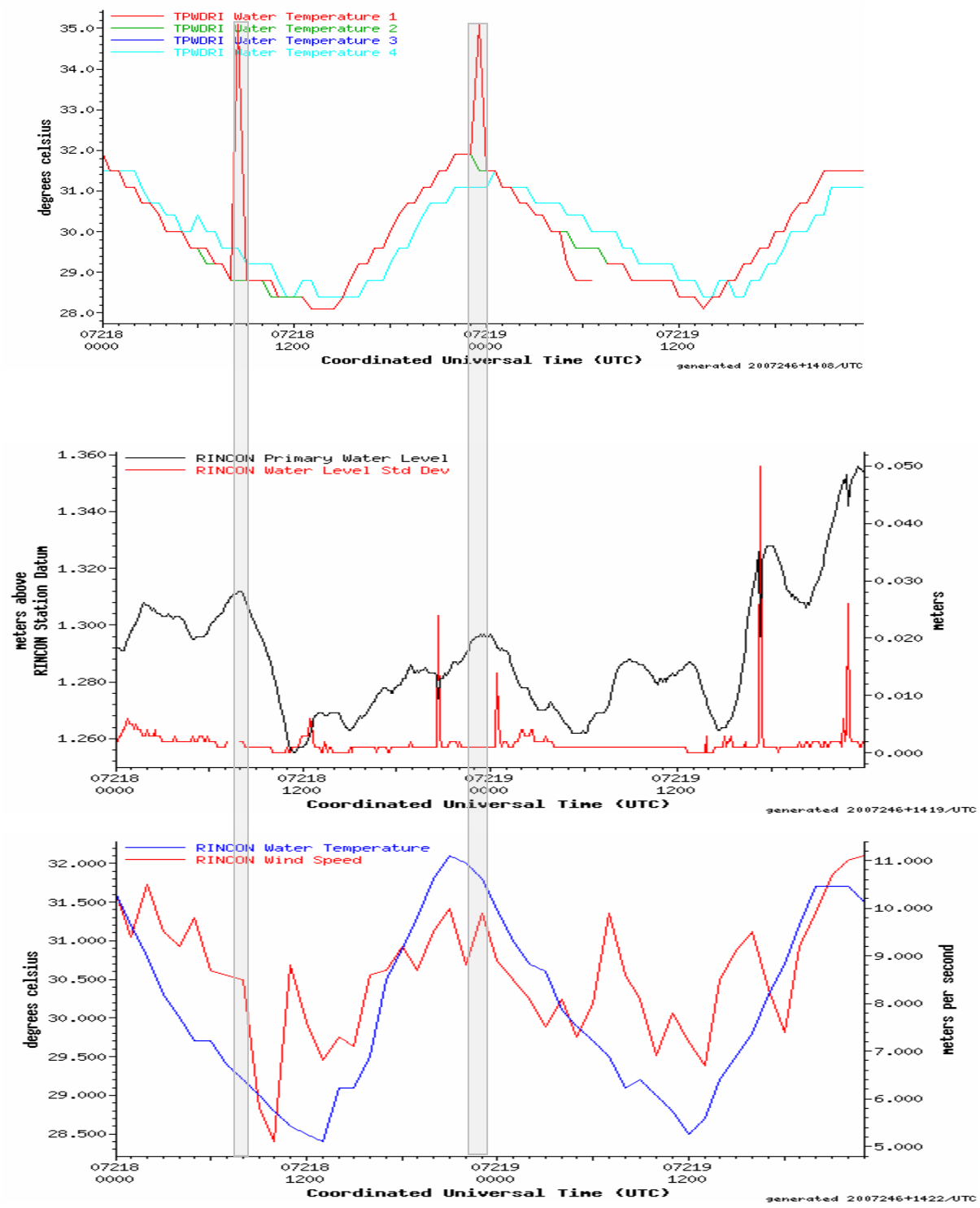

Figure 7. Water temperature measurements (top graph) comparison with water level, water level standard deviation (middle graph), air temperature and wind speed (bottom graph) for the Rincon station (August 2007). The timing of the spikes is highlighted throughout the graphs.

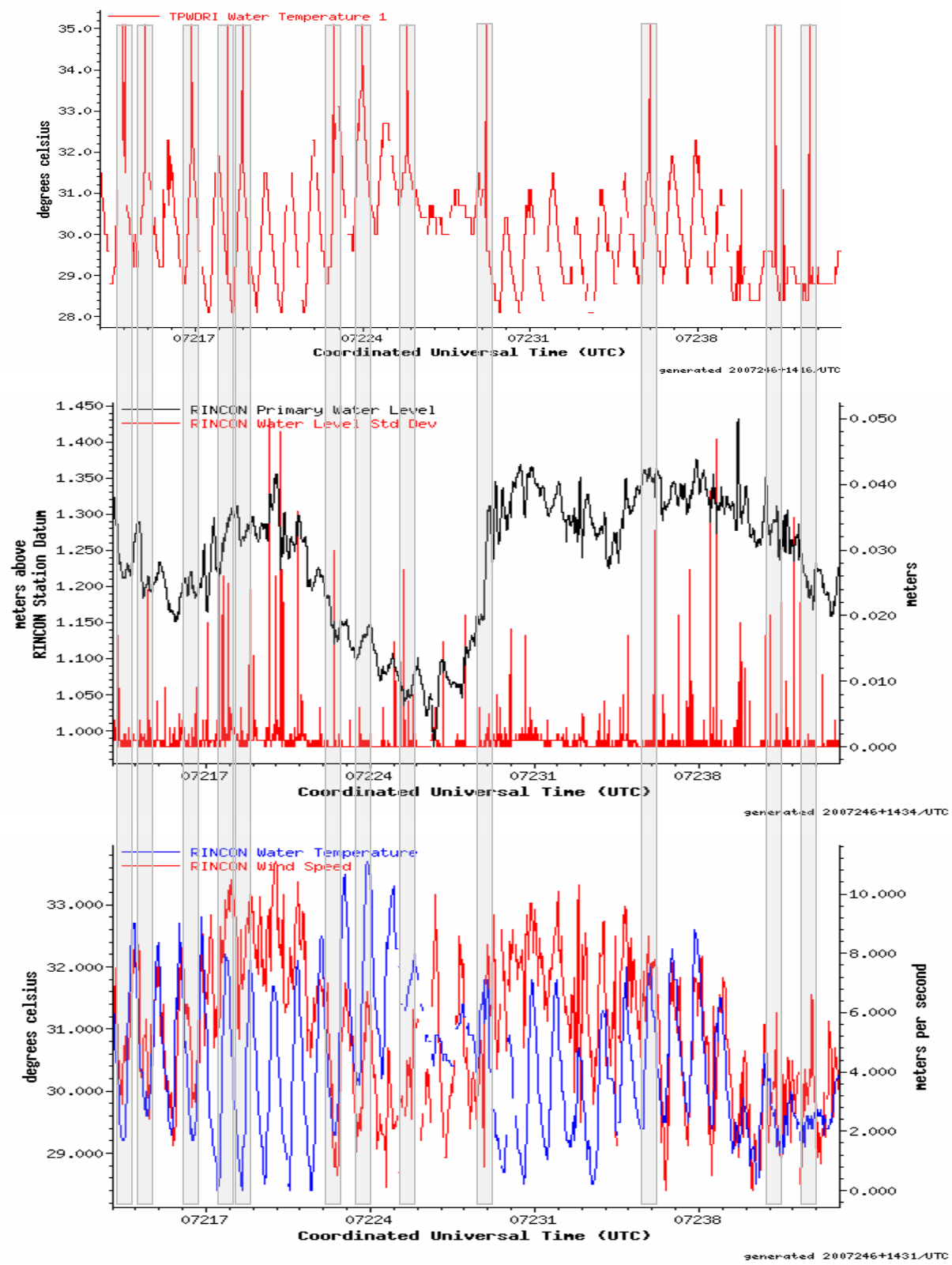

Figure 8. Water temperature measurements (top graph) comparison with water level, water level standard deviation (middle graph), air temperature and wind speed (bottom graph) for the Rincon station (August 2007). The timing of the spikes is highlighted throughout the graphs.

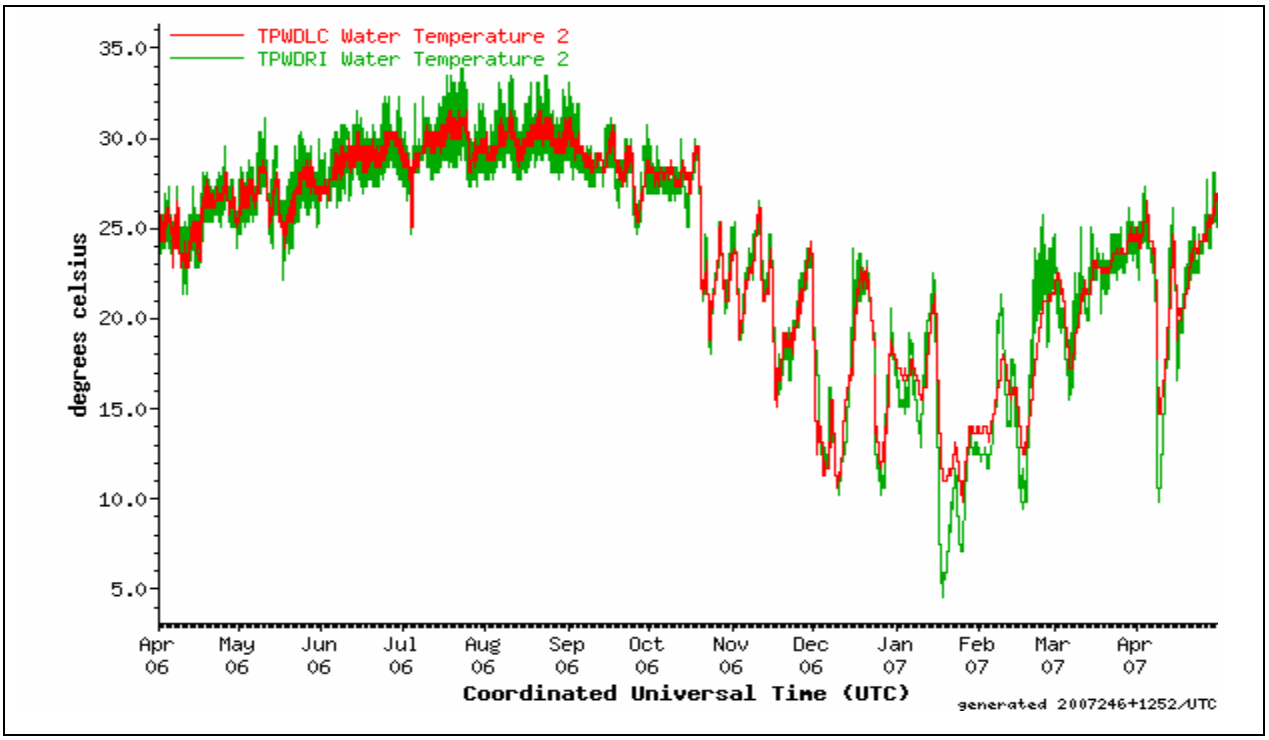

Figure 9. Comparison of water temperature measurements for sensor #2 at the Rincon (green) and Land Cut (red) stations for April 2006 to April 2007.

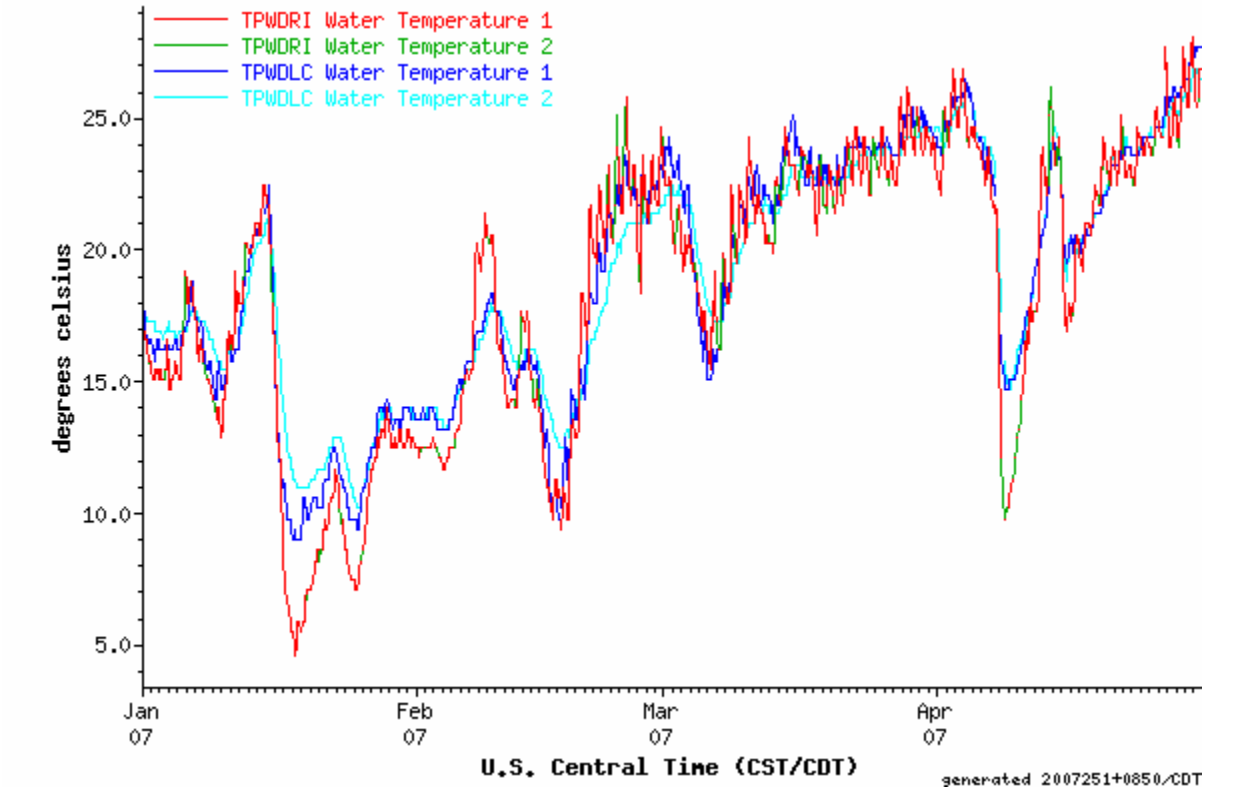

Figure 10. Comparison of water temperature measurements for sensors #1 & #2 at the Rincon and Land Cut stations for the duration for January to April 2007.

3. Design of Predictive Water Temperature Model

3.1 Introduction to modeling work

The goal of the modeling portion of this work is to design, optimize, assess the performance and implement on the World Wide Web a water temperature prediction model for the middle portion of the Laguna Madre. This portion of the report is mostly extracted from the work of Texas A&M University-Corpus Christi Masters of Science in Mathematics student Robyn Ball. At the time of this report Ms. Ball is finishing her thesis work exploring the applicability and performance of random forest modeling to the prediction of water temperatures, particularly during cold events. Her full work compares the different modeling techniques including the Artificial Neural Network model implemented as part of this work and will be shortly available as Masters of Science in Mathematics thesis. The text below is based on her analysis with additional or modified discussions focused on the applicability of the model and its relationship to the local environment.

As will be explained in the following section, the predictive model could not be designed and optimized directly based on the stations project data due to the short time series available. The implemented real time model uses National Centers for Environmental Predictions (NCEP) air temperature predictions transmitted 4 times a day by the National Weather Service. However the model had to be initially calibrated using measurements as forecasts to have sufficient data and cases were available for the calibration (perfect prog methodology, see Wilks 2006). Portions of the modeling work therefore involves checking the transportability of the model from the Bird Island Station to the project stations and the use of NCEP predictions instead of measurements for the forecasts as well as possible biases, time lags or other corrections. The overall modeling work plan is described in Figure 11.

3.2 Model target station selection& model data

To create a reliable model it is essential to have a substantial temperature history to calibrate, test and evaluate the model. The recently installed project stations did not have sufficient time series to do so, especially for the rare low temperature events of particular interest to this study. The TCOON South Bird Island Station selected to build the predictive model is located south of Corpus Christi Bay in the Upper Laguna Madre, North of the two project locations. The site was selected because of its northern location, which should lead to somewhat cooler temperatures, and especially the availability of extensive records of archived measurements. Data from other stations was included to account for the possible influence of nearby water bodies, i.e. Corpus Christi Bay and the Gulf of Mexico. Bob Hall Pier station is located on the shores of the Gulf of Mexico and Ingleside Station is located on the North shore of Corpus Christi Bay. The location of all study stations is illustrated in Figure 12.

Types of data available and their quality is presented for the Bird Island station in Table 5. For this project eleven yearly records (1995 to 2005) of air and water temperature were considered. For the training and optimization of the models and the calculation of correlation coefficients the yearly data sets of 1995, 1996, 2000, and 2001 were selected. For these 4 years yearly data sets from the nearby Bob Hall Pier and Ingleside Stations were included as well to test for possible correlations. These data sets consist of air temperature, water temperature, wind speed and wind direction, as well as measured and harmonically predicted water levels. Table 5 lists the data quality for each of the variables/stations.

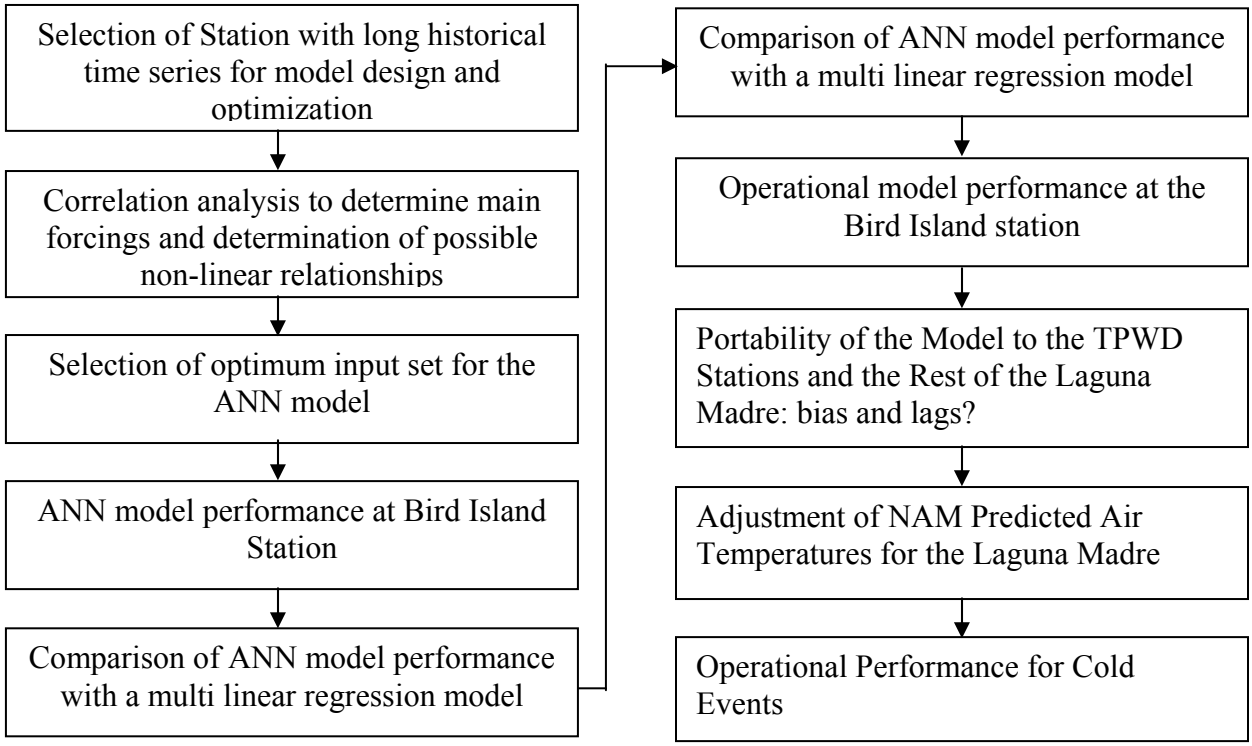

Figure 11. Schematic of the overall modeling approach for the study.

Figure 12. Map of TCOON Stations used in ANN optimization.

Table 5. Data Quality. wtp = water temperature. atp = air temperature. wpl = primary water level. harmwl = harmonic predicted water level. wsd = wind speed. wdr = wind direction.

Data Quality

Station/Year	% wtp missing	% atp missing	% pwl missing	%wsd missing	%wdr missing
S. Bird Island (wtp, atp, pwl, harmwl, wsd, wdr)					
1995	2.91	2.83	0.57	2.63	5.73
1996	4.09	3.96	1.74	3.9	5.51
1997	4.52	4.73	2.07	4.65	5.03
1998	2.81	2	0.42	2.8	3.45
1999	2.12	2.27	0.62	2.1	2.55
2000	1.07	1.07	0.77	1.06	1.3
2001	7.03	5.06	4.54	5.05	5.2
2002	0.92	0.94	0.37	0.95	0.96
2003	0.18	0.18	0.07	0.19	0.18
2004	1.96	1.96	0.39	2	2.13
2005	14.8	3.74	1.02	14.8	15.36
Bob Hall Pier (wtp, atp, pwl)					
1995	28.9	3.02	3.05		
1996	2.3	2.34	1.67		
2000	0.24	0.24	0.08		
2001	0.26	0.26	0.06		
Ingleside (wtp)					
1995	1.59				
1996	14.41				
2000	1.49				
2001	1.1				

The water temperature measurement sensors of these stations (other than the project stations) are located mid-depth in the water column. The harmonic water level forecasts are computed using DNR harman & harmpred web based software (Mostella et al., 2002). The programs implement NOAA procedures (Schureman, 1958). The harmonic coefficient computations are based on one year of observations of water levels and a set of 26 harmonic constituents. Wind speed and wind direction are included in the model as squared winds along and across the local shoreline (angle of 25° from North). Gaps in the data used with the neural network models were filled using linear interpolation between the closest known measurements.

3.3 Definition and frequency of cold events

Of particular interest to the study is the measurement and prediction of cold events. For the purpose of this study, a cold event is defined as any period during two days with one or more occurrences of water temperature falling below 7.2°C (~45°F). This threshold value is based on the experience of scientists from the Texas Department of Parks & Wildlife regarding the onset of fish mortality. Another important parameter for the onset and severity of fish kills is the length of time the water temperature remains below 7.2°C. Between 1995 and 2005 at Bird Island 24

such cold water events occurred, 23 of them ranging in length from 1 to 110 hours. One event in January of 1997 lasted 214 hours (Figure 13) and resulted in significant fish mortality (TPWD, 1997).

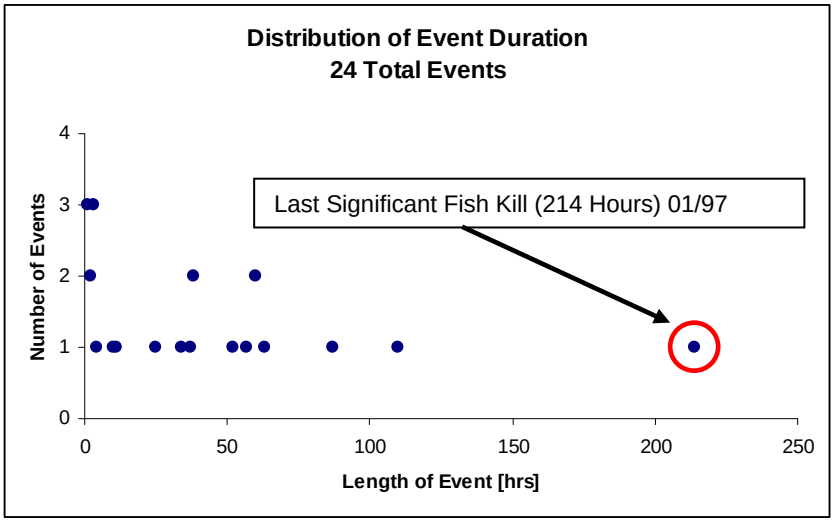

Figure 13. Distribution of event duration at Bird Island from 1995 to 2005.

3.3 Water temperature frequency analysis

To identify possible periodic components of the water temperature time series, a Fast Fourier Transform was implemented in Matlab using water temperatures at Bird Island from 1995 through 2005. The resulting power spectrum clearly shows 12, 24 hour and 1 year periodicities. We obtained the Fourier power spectrum (Figure 14) using the equation:

$$X(k) = \sum_{n=1}^{N} x(n) e^{-2\pi i \left(\frac{(n-1)(k-1)}{N} \right)}$$

The 12 hour and shorter periodicities likely appear as corrections/multiples of the 24 hour component. The most important periodicities are the yearly and daily cycles, with no other significant components.

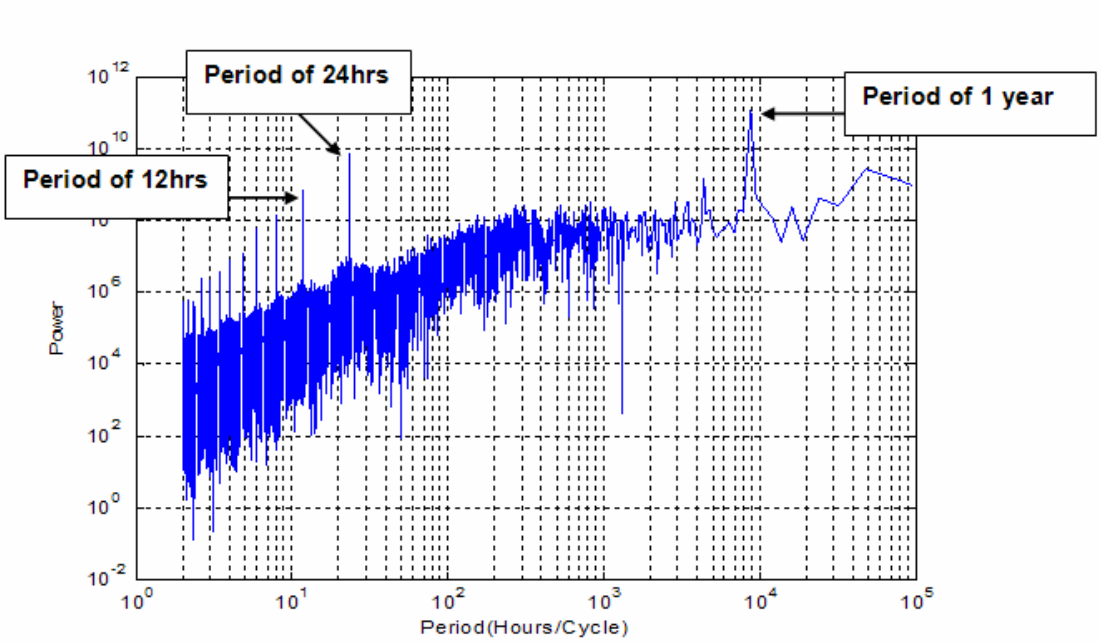

Figure 14. Fourier Power Spectrum

3.4 Statistical analysis of likely water temperature forcings

Statistical analysis was employed to gain a better understanding of the relationships between the target and possible input variables. Such relationships are important to design environmental models. Statistical analysis was employed to determine the strength of the relationship between water temperature at the Bird Island station and other possible inputs. These inputs were selected based on the physical understanding of the system as well as availability of data.

Possible inputs considered:

Atmospheric forcing of water temperature

- Previous air temperature at Bird Island
- Forecasted air temperature for Bird Island

Air/Water mixing

- Wind along and wind across shore squared at Bird Island

Heat input from nearby water bodies

- Primary water level at Bird Island
- Harmonic water level forecasts at Bird Island
- Water level difference between Bob Hall Pier and Bird Island Stations
- Previous water temperature measurements at Bob Hall Pier and Ingleside Stations

Day/night cycles

- 24 hour time stamp

For each of the possible inputs, the following series of statistical measures were computed:

Autocorrelation & Partial Autocorrelation (univariate analysis)

- Autocorrelation: tests the strength of the association between past and future events within the target time series
- Partial Autocorrelation: At lag k, the autocorrelation between x_t and x_{t-k} that is not accounted for by lags 1 through k-1.

Correlation with other inputs (bivariate analysis)

- Pearson's r correlation with other parameters
- Spearman's rank-order correlation with other parameters
- Kendall's τ correlation with other parameters

Pearson's r is used to determine characteristics of the relationships between water temperature and other parameters; however, because the relationship between water temperature and some variables will likely include non-linear relationships, Pearson's r cannot be used to conduct null hypothesis tests and can mask the true relationship. Thus, to further solidify the strength of relationship hypotheses, we also implemented the nonparametric indices Spearman's rank-order correlation and Kendall's τ, which require fewer assumptions.

Spearman's rank-order correlation is a measure of monotonic relationships when continuous variables are artificially converted into a set of ranks (Chen and Popovich, 2002). Since the functional relationship between some of the variables is not necessarily linear, Spearman's rank-order correlation is utilized to infer the strength and direction of the relationship between parameters.

Like Spearman's rank-order index, Kendall's τ is normally used to assess the relationship between two ordinal variables. Here, Kendall's τ is used as support to monotonic relationship hypotheses between variables. Kendall's τ measures the proportion of discrepancy between concordant and discordant pairs. Two pairs (X_i,Y_i) and $(X_j, Y_j)$are concordant if $Y_i < Y_j$ when $X_i < X_j$, if $Y_i > Y_j$ when $X_i > X_j$, or if $(X_i - X_j)(Y_i - Y_j) > 0$. Otherwise, the pairs are discordant (Chen and Popovich, 2002).

3.4.1 Water temperature autocorrelation and partial autocorrelation

The analysis of water temperatures illustrated in Figure 15 reveals strong autocorrelations throughout 60 hours of lags. The highest autocorrelation coefficient (acf) (0.998) occurs at 1 hour, steadily decreasing over the 60 hours, with local maxima occurring at 23 (0.959) and 47 hours (0.902), revealing the inherent 24 hour periodicity of the system. The partial autocorrelation peaks at 1 hour (0.998) but decreases sharply to -0.383 at 2 hours. Other than at 1 hour, the strongest partial autocorrelation coefficients occur at 8 and 16 hours with partial acf 0.134 and 0.128 respectively with local minima at 24 hours (-0.169). This result suggests that, in addition to 24 hour periodicity, there may be additional 8 and 16 hour periodicities. The strong correlation indicates that past water temperature should be part of the model input as expected and the lags give information as to the extent of the time series to be fed into the model.

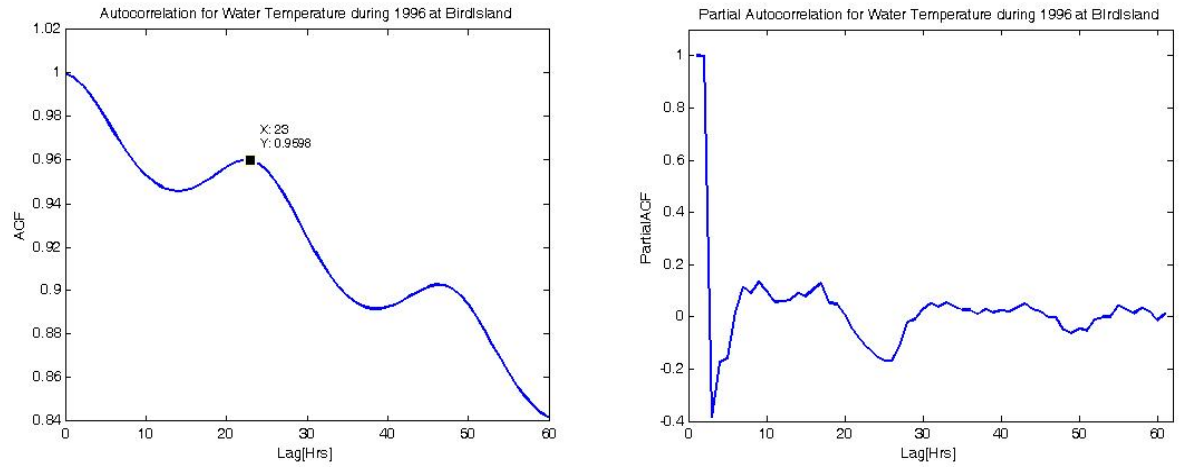

Figure 15. Autocorrelation and partial autocorrelation for Bird Island water temperature.

3.4.2 Correlation between air temperature and water temperature at the station

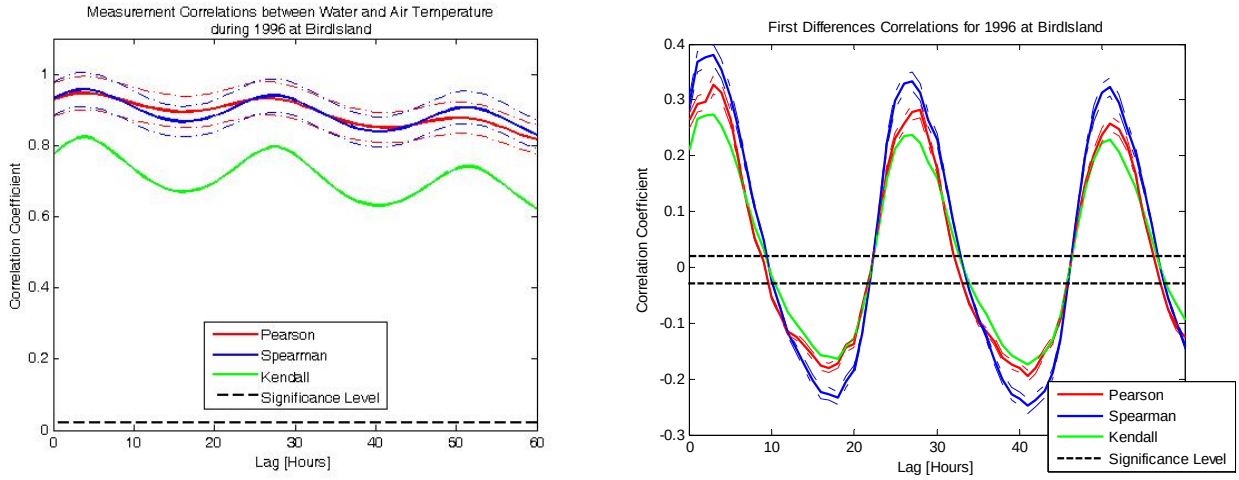

Figure 16. Correlation and first differences correlation between air temperature and water temperature at the Bird Island Station.

Figure 16 shows strong correlations between air temperature and water temperature at Bird Island with evident 24 hour periodicity. The maximum cross-correlation coefficient (ccf) (0.928) for all indices occurs at 4 hours, indicating that water temperature lags behind air temperature by approximately 4 hours. There are local maxima at 28 and 52 hours for Kendall, 27 and 52 hours for Spearman, and 26 and 50 hours for Pearson. The first differences correlation coefficients peak at 3 hours for all indices, have local maxima at 28 and 51 hours for Pearson, and at 27 and 51 hours for Spearman and Kendall. There are local minima between 17 and 18 hours and at 41 hours.

3.4.3 Correlation between water temperature at Bob Hall Pier and the target station

The highest measurement correlations between water temperature at Bird Island and water temperature at Bob Hall Pier occur at 0 hours for all indices and decrease gradually over the 60 hour lags. While Pearson decreases in a general linear fashion, Spearman has local maxima at 21 and 45 hours while Kendall has local maxima at 22 and 46 hours. Like measurement correlations, the largest first differences correlation coefficient occurs at 0 hours with maxima at 23 and 47 hours and local minima at approximately 9, 32, and 57 hours.

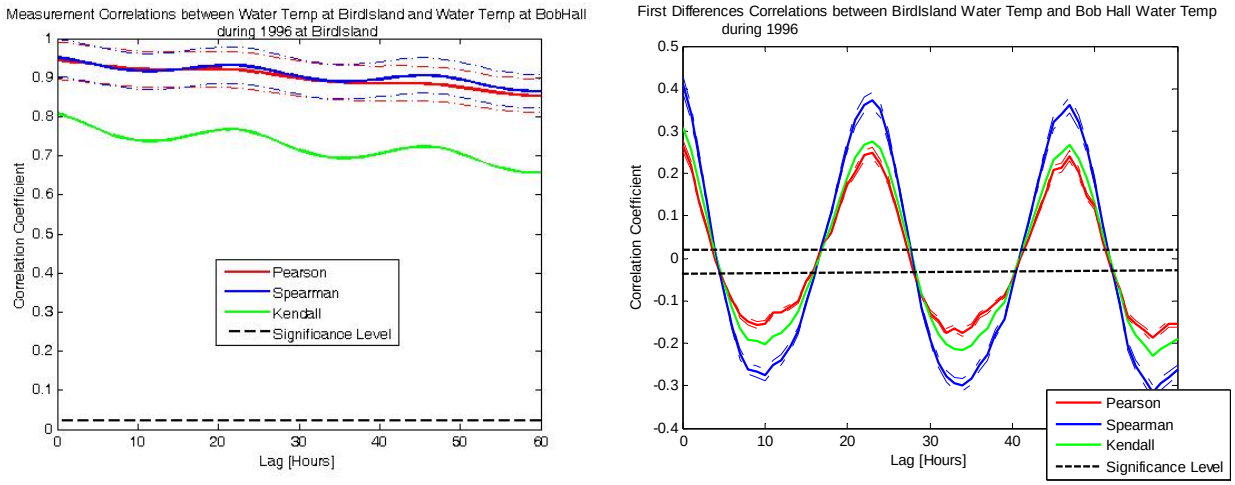

Figure 17. Correlation and first differences correlation between air temperature and water temperature at the Bird Island Station.

3.4.4 Correlation between water temperature at Ingleside and the target station

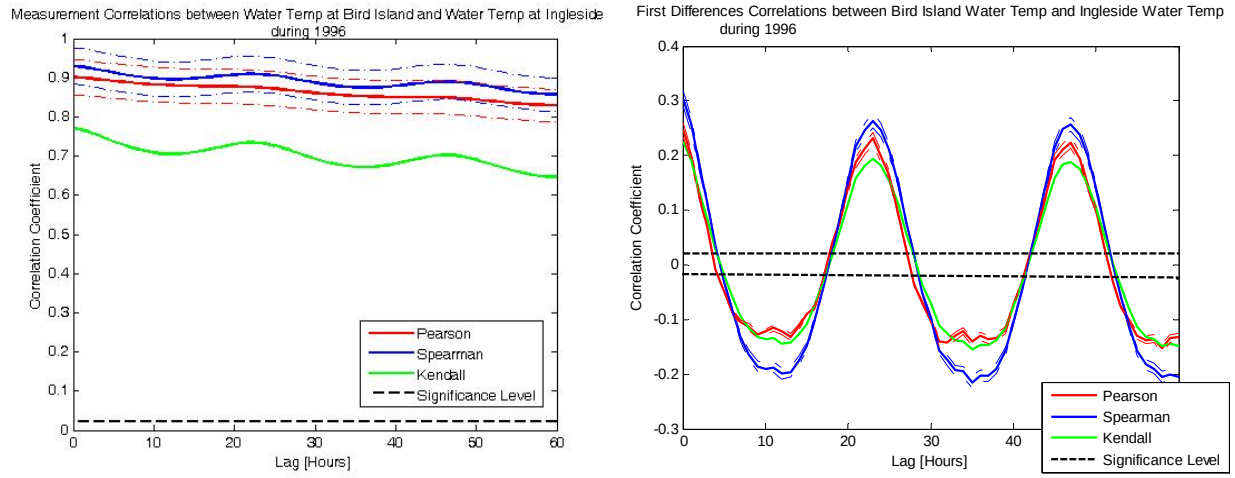

Figure 18. Correlation and first differences correlation between water temperature at the Ingleside station and the target station.

Like correlations with Bob Hall Pier water temperature, the correlation coefficients between water temperatures at Bird Island and at Ingleside occur at 0 hours with weak local maxima at 22 and 46 hours and local minima at approximately 13 and 35 hours for Spearman and Kendall. For the first differences, local maxima occur at 23 and 47 hours with local minima at approximately 13, 35, and 58 hours all consistent with the general daily periodicity of water temperatures. There is no indication in these results that water temperatures in the neighboring Corpus Christi Bay and Gulf of Mexico drive water temperatures at the Bird Island. It should be pointed out that this statistical analysis gives information on the average relationship between water temperatures at the different stations and that a possible different dynamic during the more rare cold water events may not be elucidated by this analysis.

3.4.5 Correlation between wind along shore and the target station

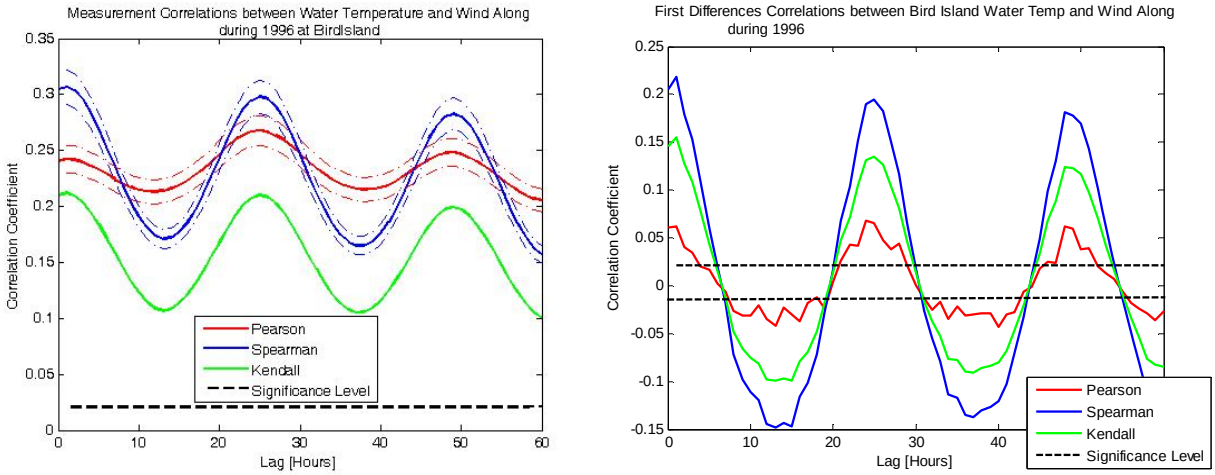

Figure 19. Correlation and first differences correlation between wind along shore and water temperature at the target station.

The greatest measurement correlation coefficient between water temperature at Bird Island and wind along shore squared occurs at 1 hour with local maxima at 25 and 49 hours and local minima at 13, 37, and 60 hours for Spearman and Kendall and at 12, 38, and 60 hours for Pearson. Similar to the measurement correlations, the greatest first differences correlation coefficient occurs at 1 hour. Local maxima occur at approximately 25 and 50 hours and local minima at approximately 16, 38, and 60 hours. In this case the Spearman index achieved significantly higher positive and negative correlations as compared to the correlation measured by the Pearson correlation indicating a substantial non-linear component to the relationship between water temperature and wind.

3.4.6 Correlation between wind across shore and the target station

Similar to wind along shore squared, the greatest measurement correlation coefficient between water temperature at Bird Island and wind across shore squared occurs at 1 hour with local maxima at 28 and approximately 50 hours and local minima at approximately 13, 38, and 60 hours. Similar to measurement correlations, the greatest first differences correlation coefficient occurs at 1 hour. Local maxima occur at approximately 25 and 50 hours and local minima at approximately 15, 39, and 60 hours. As with wind along shore, the Spearman index achieved

both the highest positive and negative correlation, underlining the nonlinear relationship between the target and wind.

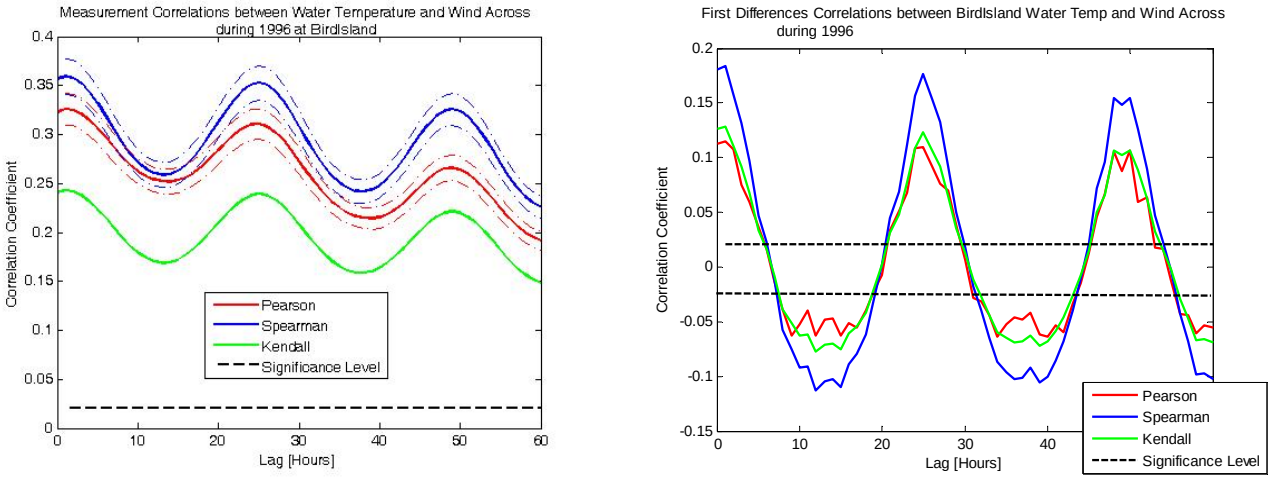

Figure 20. Correlation and first differences correlation between wind across shore and water temperature at the target station.

For both wind along and across shore, the maxima and minima correlation coefficients occur in 24 hour intervals, illustrating the 24 hour periodicity. This is likely linked to the 24 hour periodicity of the sea/land breeze which is a strong component of the overall weather forcing of the Laguna Madre during most of the year. The highest correlation coefficient is for 1 hour increasing from the 0 hour correlation and decreasing thereafter. This likely indicates a short lag between changes in the wind pattern and its effect on the water temperature, likely through mixing of the water column and water currents in the Laguna Madre.

3.4.7 Correlation between primary water levels and water temperature

For all three statistical correlation indices there are only negative correlations between measurements of water temperature and water level at Bird Island. There are local minima at approximately 18, 40 and 60 hours for Spearman and Kendall and at 21 and 44 hours for Pearson but they are all very weak. The first differences have local maxima correlation coefficients at approximately 6, 30, and 53 hours with local minima at 20 and 43 hours. The first differences correlation suggests that the change in water level 6 hours ago is most strongly correlated with the current change in water temperature. While the strength of the correlation coefficients for the first differences is weak, it is statistically significant and indicates that this input should be considered for the ANN model.

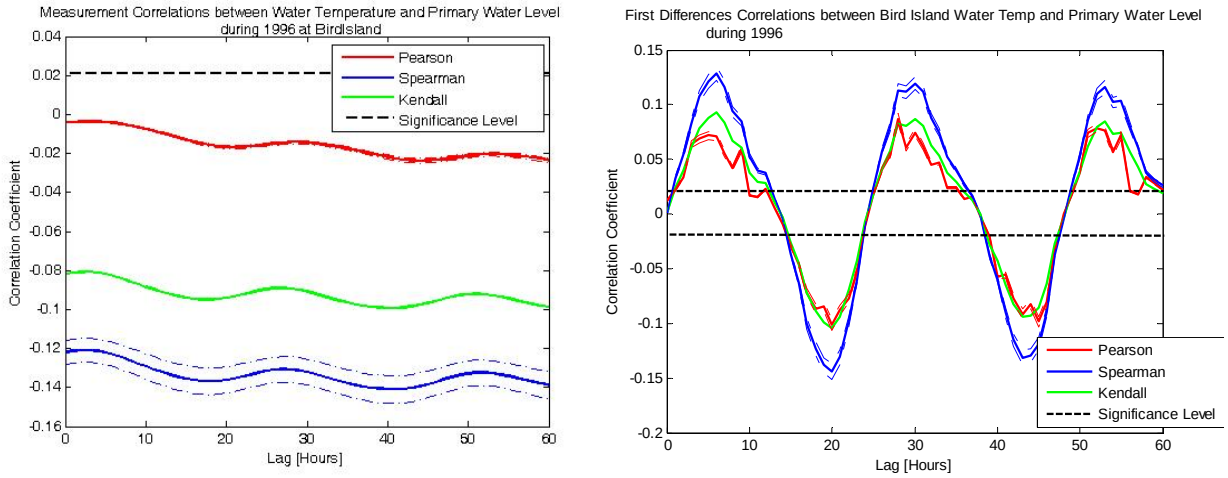

Figure 21. Correlation and first differences correlation between primary water levels and water temperature at the target station.

3.4.8 Correlation between Water Level Difference at Bob Hall Pier and water temperature at the target station

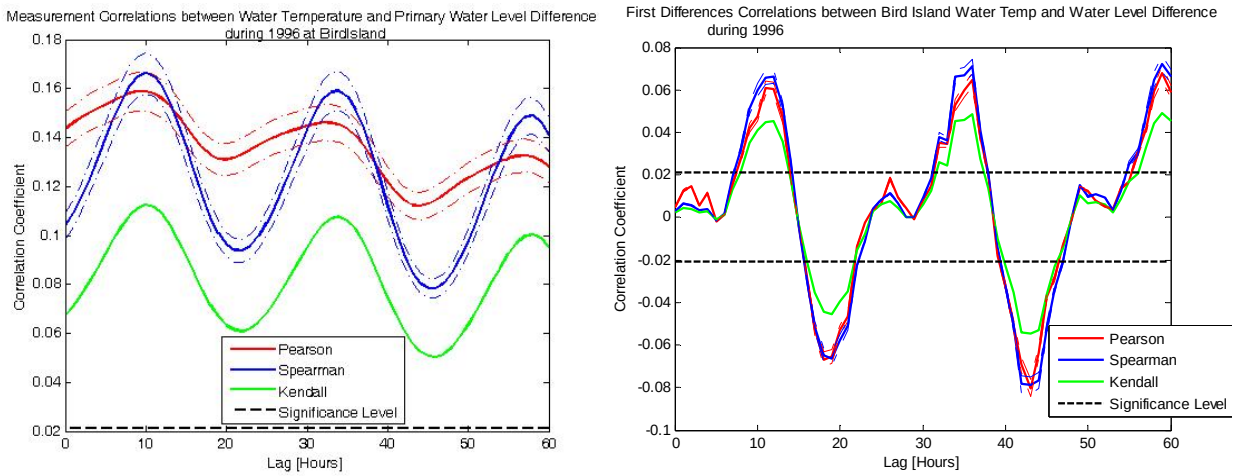

Figure 22. Correlation and first differences correlation between primary water level differences at the Bob Hall Pier Station and water temperature at the target station.

The highest measurement correlation coefficient between water temperature at Bird Island and the water level difference between Bob Hall and Bird Island occurs at approximately 10 hours with local maxima at 34 and 58 hours for Spearman and Kendall and at 32 and 57 hours for Pearson. Local minima occur at 0, 22, and 46 hours for Spearman and Kendall and at 0, 20, and 44 hours for Pearson. Maxima correlation coefficients for first differences occur at approximately 12, 36, and 59 hours with local minima near 20 and 43 hours. This result is consistent with the 24 hour periodicity of water level fluctuations but also suggests that there is approximately a 10 hour lag between the change in water level between Bird Island and Bob Hall and water temperature.

3.4.10 Statistical Analysis Conclusions

There are significant correlations between all the possible input variables and water temperature at Bird Island. The strongest correlations occur between water temperature at nearby locations and air temperature at Bird Island. Consequently all inputs will be successively tested as possible input to the model.

3.5 Model input selection

The main modeling technique selected to predict water temperatures was Artificial Neural Networks. The technique was selected because of the non-linear nature of some of the relationships between forcings and water temperatures and because of the implementation capabilities of DNR. A neural net model was also selected for this work over other techniques because of its robustness to noisy data, and generic modeling capability (Hagan, et al., 1996, Rumelhart and Chauvin, 1995). The ANN model is compared with a multi linear regression model at the end of section 3 to estimate the advantage of having selected this modeling technique.

The ANN model design for input selection follows a stepwise method (Wilks, 2006), i.e. progressively adding and comparing possible inputs to the model to determine the optimal number of previous measurements to include in the model. Rather than experimenting with the number of neurons and the number of hidden layers, our initial model follows the approach taken by Tissot, et al. This study found that simple [1,1] neural networks performed best for predictive modeling of water levels at the same location (Tissot et al., 2003). More complex neural network structures were tested once the [1,1] model was optimized. For the initial model a tansig function was used for the hidden layer neuron and a purelin function for the output layer neuron (tansig/purelin). All other possible combinations of transfer functions were also tested with the (tansig/purelin) model providing similar or better performance. A comparison with the (tansig/purelin) model with a (purelin/purelin) model is presented in section 3.7.1. The ANN models were developed, trained, and tested within the Matlab R2006b computational environment, utilizing the Neural Network Toolbox (The MathWorks, Inc., 2006). All ANN models were trained using the Levenberg-Marquardt algorithm.

The next key choice for the model set-up is to establish a training-testing strategy. The presence of a variety of cold events led to the selection of 1996 as the main training set. 1996 saw six cold water events ranging from 2 to 110 hours. A full year was selected to the training data set for the model to include a sufficient amount of data for the training and to include all seasonal patterns. 1997 was another possibility but a significant amount of missing measurements during the cold water event of 1997, which resulted in a significant fish kill, ruled out that year for both training and testing. We selected three test years: 1995 with two cold water events (60 and 63 hrs), 2000 with four events (1, 3, 3, and 39 hrs), and 2001 with three events (3, 10, and 87 hrs).

The inputs to the neural networks consist of time series of the various parameters measured and described in section 3.4. These time series are previous water and air temperature measurements at Bird Island, water temperature measurements at Bob Hall Pier, and forecasted air temperature at Bird Island. The selection of the number of previous measurements and air temperature predictions is described later in this section. A schematic of the neural network model is presented in Figure 23. First each element of the input set is multiplied by a weight (to be determined by the training procedure). All the weighted inputs are then summed and transformed

by the first neuron. The result is then multiplied by another weight and transformed by the second neuron. The result is the forecasted water temperature.

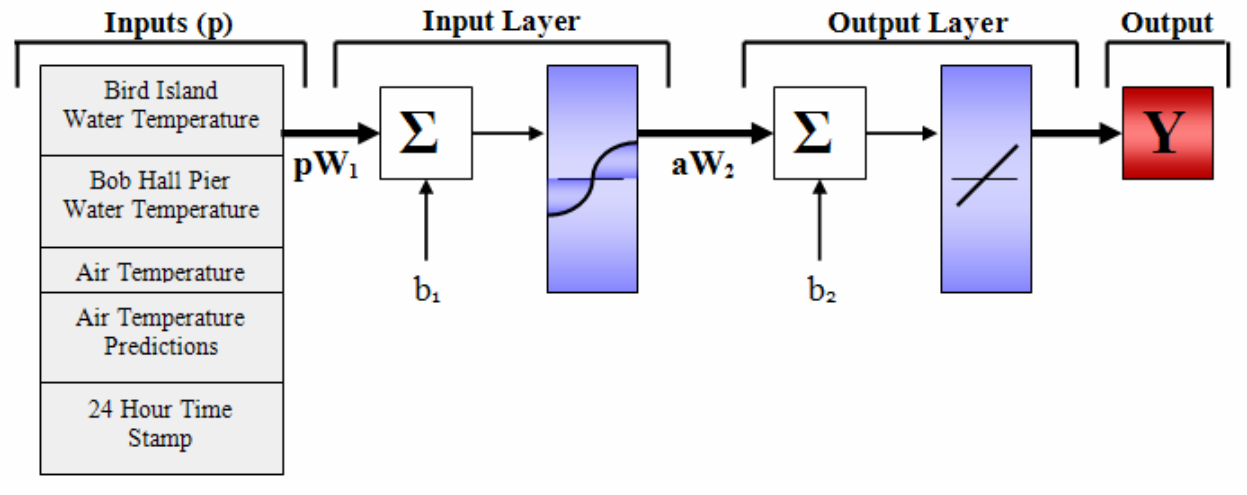

Figure 23. Schematic of ANN model. Tansig transfer function for input layer and a purelin transfer function for the output layer. $b_{1,2}$ are the biases and $\mathbf{W}_{1,2}$ are weight matrices for the respective layers.

In training the model, forecasted air temperatures are replaced by measured air temperatures at Bird Island. For model implementation, air temperature predictions are provided by the local National Weather Service office. Sets of NAM (North American Model) predictions have been provided four times daily to DNR since 2002 allowing the model designers in a forthcoming section to test the model with actual forecasts. Although we are most interested in accurately predicting cold events, the ANN models are initially optimized based on training and testing over yearly data sets. This methodology was adopted in large part because the cold events are sparse. Once the model is optimized, this initial approach is also compared to seasonal training. The ability of the ANN models to perform well, as compared to linear models during both regular and cold event situations, is also tested. The model performance is computed for both average and cold water event conditions and is assessed by the average absolute error $E_{absavg} = (1/N)\sum_{i=1}^{N}|e_i|$ over the full data sets, one year of water temperature measurements, and by the same computation for cold water events.

Based on the autocorrelation coefficients indicating the persistence of water temperatures, initial input selection for the ANN included only previous water temperatures at Bird Island Station. During the optimization process, it was observed that short-term (3 and 12 hour) forecasts behaved similarly. Longer term (24 and 48 hour) forecasts, while dissimilar to short-term forecasts, compared well to one another. Based on this observation, one model was designed for short 3 and 12 hour forecasts and another model was optimized for longer 24 and 48 hour forecasts. Starting by using only the latest water temperature (wtp(0)) measurement as input to the model, up to 60 hours of previous water temperature measurements were consecutively added. This process produces a series of 61 water temperature models: wtp(0), wtp(0:1), wtp(0:2)…wtp(0:60). In total, for previous water temperature measurements, 244 possible

models (Figure 24) were compared. For each forecast interval (3, 12, 24 and 48 hour) the model performances are graphed for the training and testing sets. For both short term and long term forecasts model improvements are measurable up to the inclusion of the previous 26 hours of water temperature measurements (wtp(0:26)).

Once the basic ANN model is constructed, the next step is to select and test other possible models against this base model (wtp(0:26)) and determine whether including other inputs will lead to a significant performance improvement.

As presented in section 3.4 the statistical analysis revealed that there are significant correlations between the target and all the possible inputs considered. For this reason, we tested all of the possible inputs to determine whether their inclusion increased the performance of the model. For each of the additional possible inputs, new models were assembled by adding their input to previous water temperatures (wtp(0:26)). These other models were evaluated one at a time. The same stepwise method discussed previously was utilized for each of these other models with the number of previous measurements progressively increased to include up to 60 hours of previous measurements. The possible input models were assessed based on the average absolute error reduction. To justify adding an input time series, results from all test years are compared. Additional inputs are included if there is a substantial improvement (average absolute temperature difference of 0.02°C or larger) for the majority of the test years.

3.5.1 Previous water temperature inputs at Bird Island Station

For previous water temperature input (see Figure 24), the model's average absolute error continues to decrease over the entire 60 hours of added inputs for every test year. The 48 hour forecast errors decrease in a linear fashion, while the other forecast errors steeply decrease between approximately 0 and 5 and 15 to 20 hours. The error levels off after approximately 26 hours of previous measurements. Based on these results, 26 hours of previous water temperature at Bird Island are included in all ANN models.

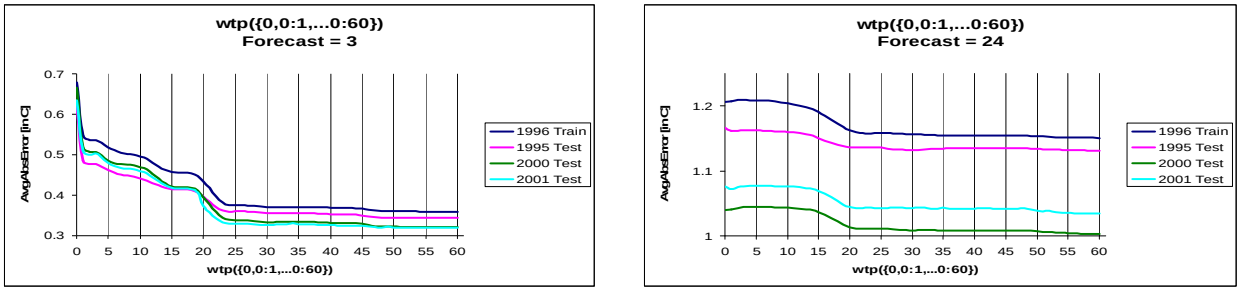

Figure 24. Average absolute errors for 3 and 24 hour forecasts. Previous water temperatures at Bird Island (ranging from 0 to the past 60 hours) are the only inputs.

3.5.2 Previous and future air temperature inputs

The most interesting results from a predictive modeling standpoint came when adding to the model past air temperature measurements and air temperature predictions. The impact of air temperatures on the model was expected as the statistical studies presented in the previous section showed a high correlation between changes in air temperature and changes in water temperature as well as a peak for the correlation coefficient for a lag of 4 hours. As previously

mentioned the predictions are actual air temperature measurements during the training/testing portion of the model development. Differences between using measurements as predictions (perfect prog) and the operational predictions will be discussed.

Similarly to the water temperature case, a sharp decrease in the prediction error is observed when increasing the number of past temperature measurements between approximately 20 and 25 hours. No significant decrease in predictive error is observed when adding more than the past 26 hours of past water temperature measurements. The change in predictive errors with and without the inclusion of the past 26 hours of air temperatures is presented in Table 6. When forecasted air temperatures are added to previous air temperatures, the error further decreases dramatically for the longer prediction times, in some cases by more than 60%. Table 7 compares the predictive errors decrease when including air temperature predictions. Table 8 shows the percent decrease in the error when air temperature predictions, along with the previous 26 hours of air temperature measurements, are added as inputs to the model.

Table 6. Comparison of Average Absolute Error [°C] between the base model and the base model with past air temperature measurements.

Comparison of Average Absolute Error [°C]

Base Model [wtp(0:26)] and Base Model with Air Temperature Measurements [wtp(0:26) & atp(0:26)]

	1996	1996	1995	1995	2000	2000	2001	2001
Forecast	Base Model	With Air Temp	Base Model	With Air Temp	Base Model	With Air Temp	Base Model	With Air Temp
3	0.38	0.34	0.36	0.32	0.34	0.30	0.33	0.30
12	0.88	0.81	0.88	0.82	0.79	0.71	0.80	0.76
24	1.16	1.09	1.14	1.08	1.01	0.95	1.04	1.04
48	1.90	1.82	1.81	1.78	1.61	1.54	1.66	1.66

Table 7. Comparison of Average Absolute Error [°C] between the model with past air temperature measurements and model including air temperature predictions.

Comparison of Average Absolute Error [°C]

Base Model with Air Temperature Measurements [wtp(0:26) & atp(0:26)] and Base Model with Air Temperature Measurements and Predictions [wtp(0:26) & atp(0:26) & atp predictions]

	1996	1996	1995	1995	2000	2000	2001	2001
Forecast	Air Temp	With Predictions	Air Temp	With Predictions	Air Temp	With Predictions	Air Temp	With Predictions
3	0.34	0.32	0.32	0.30	0.30	0.29	0.30	0.29
12	0.81	0.56	0.82	0.54	0.71	0.49	0.76	0.55
24	1.09	0.60	1.08	0.56	0.95	0.53	1.04	0.63
48	1.82	0.73	1.78	0.66	1.54	0.64	1.66	0.82

Table 8. Percent Decrease in Average Absolute Error when air temperature predictions are added to the model.

Percent Decrease in Average Absolute Error When Adding Air Temperature Predictions

Forecast	1996	1995	2000	2001
3	7%	6%	3%	3%
12	31%	35%	31%	28%
24	45%	48%	44%	39%
48	60%	63%	58%	51%

3.5.3 Other inputs

Adding the current water temperature at Bob Hall Pier increased the performance of the ANN for long-term forecasts (24 and 48 hours) but did not produce significant improvement for short-term forecasts. The results for other possible input variables are represented in Table 9. The optimized ANN models include previous water and air temperature at Bird Island as well as forecasted air temperature at Bird Island. The short-term model (3 and 12 hour forecasts) also includes the previous 16 hours of a 24 hour time stamp [0.1,2.4] and the long-term model includes the current water temperature measurement at Bob Hall Pier. The performance of the final ANN model is presented in Table 10.

Table 9. Inputs and series of inputs considered during the model design.

	Series Included	
Possible Inputs Considered	**Short Term**	**Long Term**
Bird Island water temperature	previous 26 hrs	previous 26 hrs
Bird Island air temperature	previous 22 hrs	previous 16 hrs
Bird Island forecasted air temperature	ALL	ALL
Wind along and across shore	None	None
Bird Island primary water level	None	None
Bird Island harmonic predicted water level	None	None
Bird Island & Bob Hall water level difference	None	None
Bob Hall water temperature	None	Current
Ingleside water temperature	None	None
24 hr time stamp	previous 16 hrs	None

Some of the variables not included in the model sill had strong correlations with future Bird Island Station water temperatures such as the Ingleside water temperature (Figure 5). Although the strength of the correlation between these variables remains higher than 0.8 for Pearson and Spearman (over 60 hour lags), the addition of Ingleside water temperature did not make an improvement in the model's performance. This is likely due to the fact that past Bird Island water temperatures already include the model variance that past Ingleside station measurements could have elucidated. Similarly to multiple regression model design, this result suggests that strong correlations between the target variable and other possible inputs do not necessarily justify their inclusion in an ANN model.

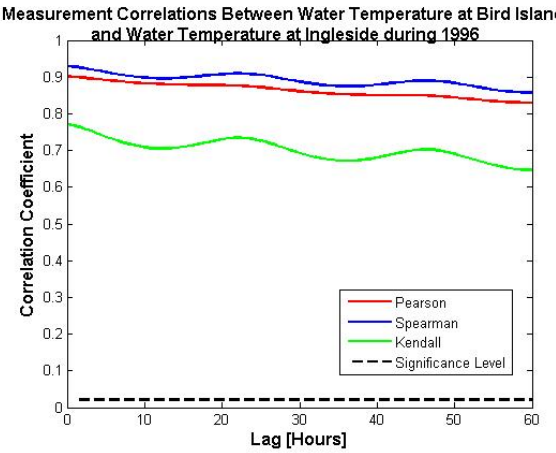

Figure 25. Cross-correlation between water temperature measurements at Bird Island and water temperature measurements at Ingleside.

3.6 Model training over different time periods

In the previous section the models were all trained and tested on yearly data sets. This method was also compared to training seasonally with the same inputs. Because of the distribution of events, the models were trained on data from December 1995 – April 1996, and included 6 cold events (2, 4, 38, 57, 63, and 110 hrs). Both seasonally trained and yearly trained models were tested on data from December 2000 – March 2001, also including 6 cold events (1, 3, 3, 3, 10, and 87 hrs). For average conditions, seasonally and yearly trained models yielded similar results for short-term forecasts. For longer term forecasts, the yearly trained model performed slightly better for average conditions. The seasonal model performance was mixed during cold events. Although the error decreased by more than 15% for 12 hour forecasts, the error increased by over 7% for 48 hour forecasts. However testing on cold events was limited as the testing data sets included only one season with a substantial number of cold events (6). More testing will be required to evaluate potential benefits of seasonally trained models and for the rest of this study model training is completed over yearly data sets.

3.7 ANN model performance at Bird Island

The optimized ANN model performance was evaluated for yearly performance for years 1995, 2000 and 2001. The results presented in Table 10 show that the accuracy of the model decreases from 0.3°C for 3 hour forecasts to between 0.6°C and 0.9°C for 48 hour forecasts. The table also lists the performance of the model when evaluated only during cold events, i.e. when predicting temperatures below 7.2°C (~45°F). Interestingly, the model is on average more accurate for cold water temperature predictions; there is however a large year to year and event to event variability. The variability is likely due to the smaller number of predictions as well as the variability in the intensity of the frontal passages generating these cold events. During cold events, the accuracy varies for the 3 testing years from 0.2°C to 0.4°C for 3 hour forecasts to 0.4°C to 0.5°C for 48 hour forecasts.

Table 10. Average absolute errors in the optimized ANN model for both the training year (1996) and test years (1995, 2000, 2001).

Average Absolute Error of Optimized ANN [in °C]

	Forecast	1996	1995	2000	2001
Year	3 hours	0.31	0.30	0.28	0.29
Cold Events		0.42	0.22	0.43	0.29
Year	12 hours	0.56	0.53	0.49	0.55
Cold Events		0.82	0.45	0.42	0.79
Year	24 hours	0.59	0.57	0.53	0.67
Cold Events		0.92	0.39	0.46	0.78
Year	48 hours	0.69	0.65	0.64	0.87
Cold Events		0.99	0.45	0.48	0.40

It is hypothesized that the better performance during cold events, as compared to the performance averaged over the yearly data set, is due to the more systematic behavior of the water temperature during such events. In particular, the water temperature is strongly correlated/driven by the air temperatures during cold events. Such correlation however leads to a model performance sensitive to the accuracy of air temperature predictions. To assess the importance of air temperature predictions the model was further tested without such predictions. Results are presented in Table 11.

As can be observed in Table 11, model accuracy for cold events is now considerably below average model performance. The average absolute errors increase dramatically during test years by 2.3°C to 4.7°C for 48 hour forecasts. The differences between the results with and without air temperature predictions emphasize the importance of this parameter, particularly during cold events. Note that the results in Table 11 were computed using measurements as forecasts for the inputs to the model.

Table 11. Average absolute errors in the optimized ANN model without air temperature predictions for both the training year (1996) and the test years (1995, 2000, 2001).

Average Absolute Error of Optimized ANN without Air Temperature Predictions [in °C]

	Forecast	1996	1995	2000	2001
Year	3 hours	0.33	0.32	0.29	0.31
Cold Events		0.44	0.25	0.46	0.30
Year	12 hours	0.78	0.77	0.67	0.75
Cold Events		1.21	0.93	0.92	1.07
Year	24 hours	1.09	1.07	0.94	1.02
Cold Events		2.07	1.74	1.59	0.90
Year	48 hours	1.81	1.72	1.51	1.59
Cold Events		5.28	4.06	4.75	2.26

3.8 Comparison of ANN model with linear models

In this section the ANN model is compared with two linear model alternatives to assess the hypothesized advantage of the non-linear ability of the ANN methodology. In section 3.8.1, the ANN methodology is used but only linear transfer functions are selected for the hidden and output neurons. In section 3.8.2 the ANN model is compared with a classic multi linear regression model.

3.8.1 Comparison with an ANN model with linear transfer functions

The (tansig/purelin) non linear model is compared here with a (purelin/purelin) linear model. The models are compared based on the average absolute error. The performance of the purelin/purelin model was similar to the nonlinear ANN design over the full yearly data sets. However the nonlinear model outperformed the linear model during cold events, as can be seen in Table 12. The mean of the average absolute error of all test years during cold events is lower for all forecast times and, as the forecast time increases, so does the difference in the error between the linear and nonlinear models.

Figure 26 further illustrates the better performance of the nonlinear model during cold events. The figures also suggest that the linear model is negatively biased for low temperatures. It is hypothesized that the modeling capability of the non linear ANN design allows for an unbiased or less biased prediction of water temperatures during cold events.

Table 12. Mean of 1995, 2000, and 2001 average absolute errors during cold events.

Mean of 1995, 2000, and 2001 Average Absolute Errors during Cold Events [in °C]				
Forecast	**3 hrs**	**12 hrs**	**24 hrs**	**48 hrs**
Tansig/Purelin	0.28	0.53	0.49	0.45
Purelin/Purelin	0.29	0.54	0.54	0.52

3.8.2 Comparison with multi-linear regression model

To better assess the performance of the ANN model, a comparative multi-linear regression model was also developed. Several methodologies were considered to select the "best" performing multi-linear regression model based on the available data. Possible multi-linear regression models were assessed on the average absolute error. The automated p-value based Matlab routine led to the best performing model when evaluated on test sets 1995, 2000, 2001. Initially, the model included all of the inputs in the optimized ANN model. The Matlab function stepwisefit was used to determine which of these inputs led to the best linear model. Inputs were selected or rejected based on the p-value. The p-value in this case is the probability that the coefficient for a particular input will be equal to zero. The maximum p-value for a predictor to be added is 0.05 and the minimum p-value for a predictor to be removed is 0.10. Like the ANN model, the linear model was trained on 1996 and tested on 1995, 2000, and 2001. Comparative results are presented in Table 13. The ANN model significantly outperforms the multilinear regression model. Other training procedures could be further tested for the multi linear regression model and may lead to better performance, however for the purpose of this study, the significant differences in table 13 are deemed sufficient to justify the choice of the ANN methodology.

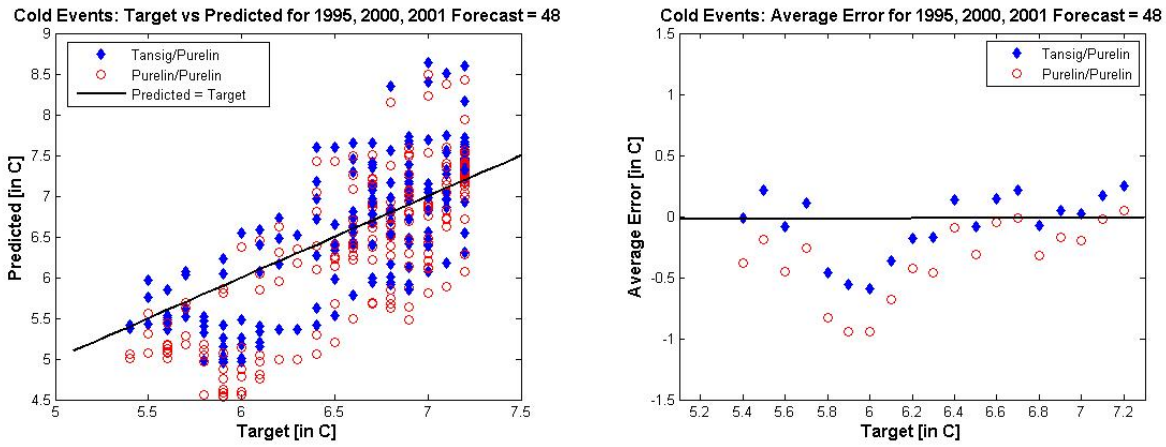

Figure 26. Target vs. predicted water temperatures for tansig/purelin and purelin/purelin transfer function models during 1995, 2000, and 2001 cold events (left figure) and models bias vs. target temperature (right) – all for 48 hour forecasts.

Table 13. Multi-linear vs. ANN. Mean of 1995, 2000, and 2001 average absolute errors during cold events.

Mean of 1995, 2000, and 2001 Average Absolute Errors during Cold Events [in °C]				
Forecast	**3 hrs**	**12 hrs**	**24 hrs**	**48 hrs**
Multi-linear	0.81	0.75	0.70	0.76
ANN	0.29	0.54	0.54	0.52

4. NAM Air Temperature Predictions & Adjustments for the Laguna Madre

As discussed in the previous sections we found that air temperature predictions greatly enhance the performance of the model. In the previous sections we trained the model using the "perfect prog" approach (Wilks, 2006), that is, we assumed the air temperature predictions are always accurate. With this assumption one can use air temperature measurements as predictions instead of actual air temperature predictions. This was in large part done because of the lack of available NWS predictions for the full training time period. In this section we analyze and compare the performance of the model when using measurements as predictions and when using actual predictions from the National Centers for Environmental Predictions (NCEP) Environmental Modeling Center (EMC) which is part of the National Weather Service (NOAA/NWS). The comparisons are computed only for the period for which such predictions are available. The models used by NCEP vary periodically including during our test period. We used predictions from two models, the NCEP MesoEta model from 2004 to June 2006 and the NCEP NAM-WRF model after June 2006.

The Eta-12 model or MesoEta model was a limited-area, numerical atmospheric model. The model integrated the primitive hydrostatic equations in three dimensions. The vertical coordinate was known as the Eta, obtained based on the modification of the terrain following sigma coordinate. The advantage of the eta coordinate was that the surfaces are quasi-horizontal, thus avoiding errors associated with steep slopes of the coordinate surfaces (Mesinger, 1984) and hence improving the solution over highly variable topography such as over the Western United States. Initial values to each Eta forecast model run were provided by the fully-cycled Eta Data Assimilation System (EDAS), which incorporated the 3-dimensional variational analysis (3D-VAR) technique. NCEP Eta surface data (from netCDF files containing Eta forecast output mapped to AWIPS Grid 215, which has a horizontal grid spacing of 20 km) were sent every six hours to TAMUCC-DNR starting in February 2002 with some interruptions. The forecast data were stored for a set of about 40 locations including the TCOON Bird Island station. MesoEta Predictions will be identified as MESO2 predictions in the text below.

The NCEP NAM-WRF model was developed collaboratively between a number of organizations including the Mesoscale, Microscale, and Meteorology Division of the National Center for Atmospheric Research (NCAR/MMM),NOAA/NWS, the Forecast Systems Laboratory (NOAA/FSL), the Oklahoma University Center for Analysis and Prediction of Storms, and the Air Force Weather Agency. The philosophy behind the development of this model was to create an advanced mesoscale community (non-proprietary) model and data assimilation system. The WRF is a non-hydrostatic, limited-area, numerical model in which the domain and physics parameterizations can be chosen amongst several options. The current WRF contains several options for explicit microphysics, cumulus parameterization, planetary boundary layer radiation, and parameterization of the surface. The NAM-WRF predictions have been made available to DNR from the local National Weather Service since June of 2006 and are the predictions used by the present operational model. More specifically the operational model uses the NAM-WRF air temperature predictions at Bird Island released every 6 hours and

typically transmitted to DNR 3.5 hours after their computation. The predictions are for 3, 6, 9... up to 48 hours in the future. Thus, the "span" of the prediction is therefore at most 48 hours.

4.1 Performance with NAM-WRF Predictions

To determine the accuracy of NAM air temperature predictions, we first looked for biases. While we computed the biases for the full 0-48 hrs range of predictions, we will only present the results for 6, 12, 24, and 48 hour predictions. The first comparison consists of measured and NAM predicted air temperatures from June 2006 through March 2007 at the Bird Island Station. Over the entire range of temperatures, no clear bias emerged however a significant positive bias was found for measured air temperatures below 15˚C (see in Table 14). For such cases the predicted air temperature is consistently higher by an average of more than 3˚C than the corresponding measurements. Figures 27 through 30 illustrate this positive bias for the low temperature range. The left sides of the figures illustrate the bias between predictions and measurements for the entire temperature range while the right portions of the figures illustrate the significant bias for measured air temperatures below 15˚C.

Table 14. Average bias of NAM-WRF model when measured air temperature is less than15˚C.

NAM-WRF Average Bias When Measured Air Temperature is Less Than 15˚C

Age of Prediction	Average Bias [˚C]
6	3.1
12	3.8
24	3.2
48	3.3

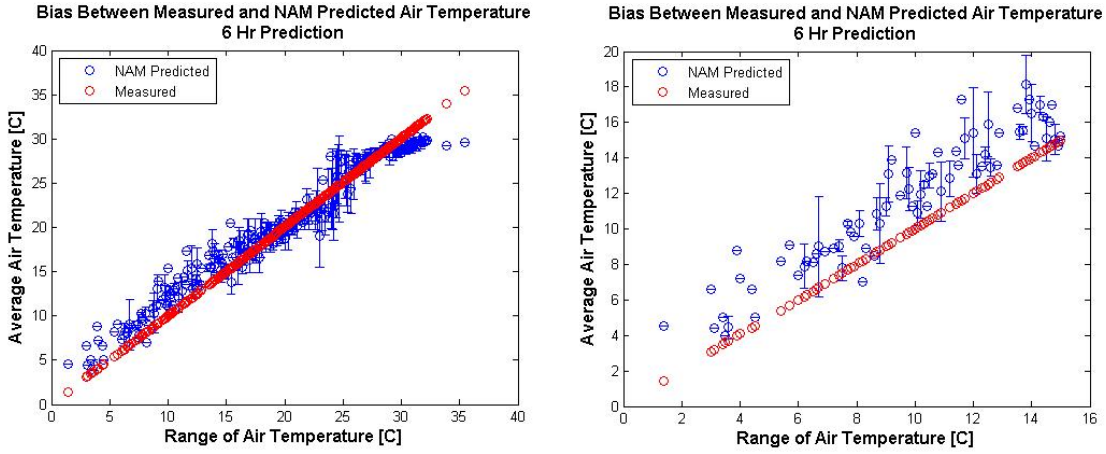

Figures 27. Biases between measured and NAM predicted air temperature at Bird Island for 6-hour predictions. The error bars represent the respective standard deviation.

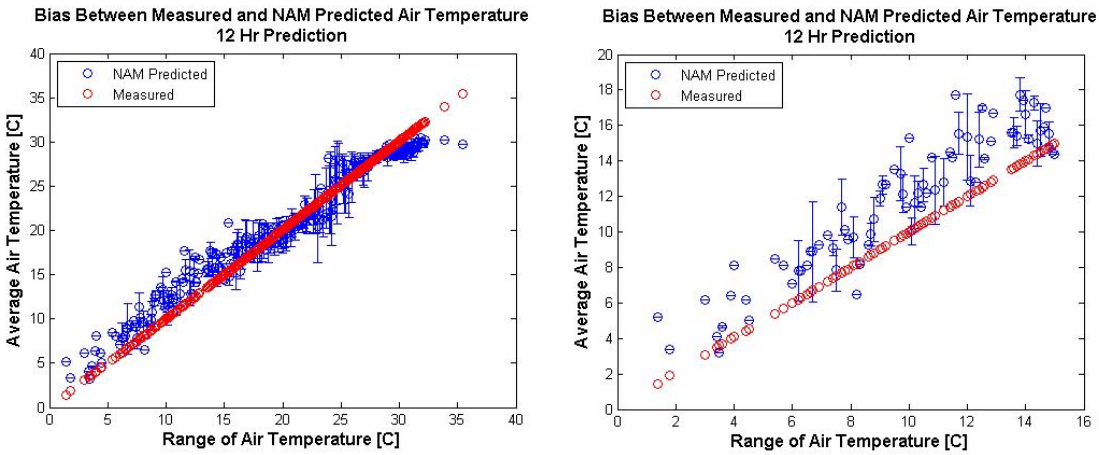

Figures 28. Biases between measured and NAM predicted air temperature at Bird Island for 12-hour predictions. The error bars represent the respective standard deviation.

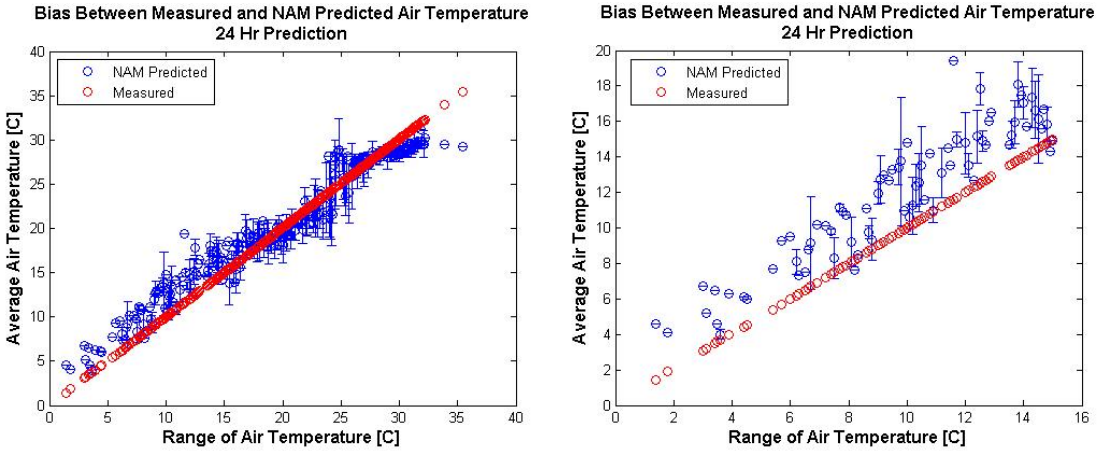

Figures 29. Biases between measured and NAM predicted air temperature at Bird Island for 24-hour predictions. The error bars represent the respective standard deviation.

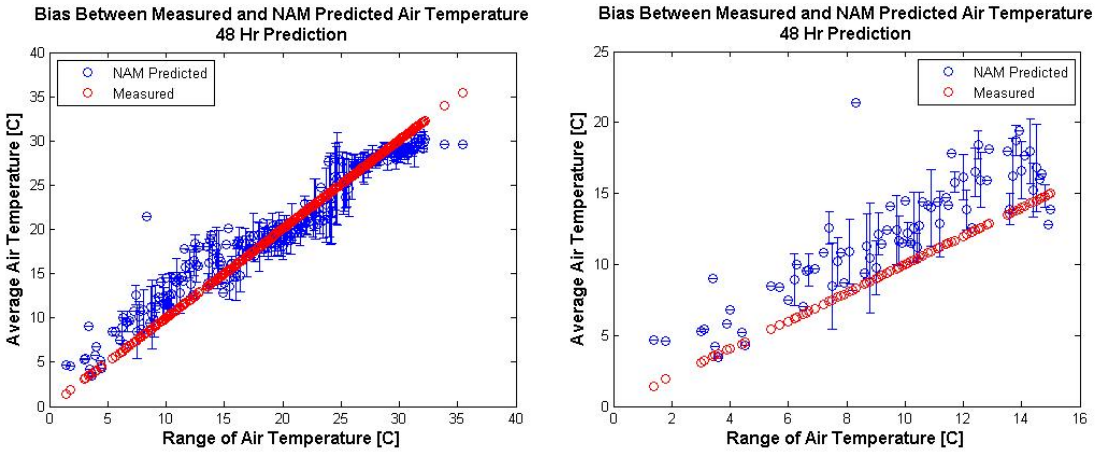

Figures 30. Biases between measured and NAM predicted air temperature at Bird Island for 48-hour predictions. The error bars represent the respective standard deviation.

Since the predictive model was found to be highly dependent on the accuracy of air temperature predictions different methods were compared to correct the air predictions for temperatures below 15˚C. A linear adjustment for all prediction times was computed (3, 6, 9,...48 hours). The respective linear adjustments for each prediction time are compared in Table 15 to simply subtracting the respective average biases. The mean, average absolute and largest prediction errors are compared. A quadratic transformation was also tested to improve the predictions but no significant improvement was observed as compared to the linear adjustment. A linear adjustment was therefore implemented such that when NAM predicted air temperatures are equal to or below 18˚C, a linear transformation is used to adjust the prediction.

Table 15. Comparison of linear and bias model for adjusting NAM air temperature predictions.

Comparison of Linear vs. Bias Model for Adjusting NAM-WRF Predictions [°C]

Prediction Age	Model	Mean	Average Absolute	Largest Error
6	Linear	0.0	2.2	7.4
	Bias	2.2	3.1	9.7
12	Linear	0.0	2.2	7.1
	Bias	2.9	3.6	9.8
24	Linear	0.0	2.2	6.3
	Bias	2.4	3.3	9.3
48	Linear	0.0	2.6	7.4
	Bias	2.3	3.5	9.6

4.2 Performance with MESO2 Predictions

Since we also wanted to test events in 2003 and 2004, we evaluated the accuracy of the MESO Eta or MESO2 air temperature predictions, the predictions available for this time frame. As can be seen in Table 16, similarly to the NAM_WRF model the MESO2 model consistently predicted warmer air temperatures for the Bird Island station particularly when measured air temperatures are less than 15˚C. MESO2 has however a higher positive bias than does the NAM-WRF model, in some cases as much as 8.7˚C.

Table16. Average bias of MESO2 model when measured air temperature is less than 15˚C.

MESO2 Average Bias When Measured Air Temperature is Less Than 15˚C

Age of Prediction	Average Bias [˚C]
6	4.0
12	3.6
24	3.0
48	5.0

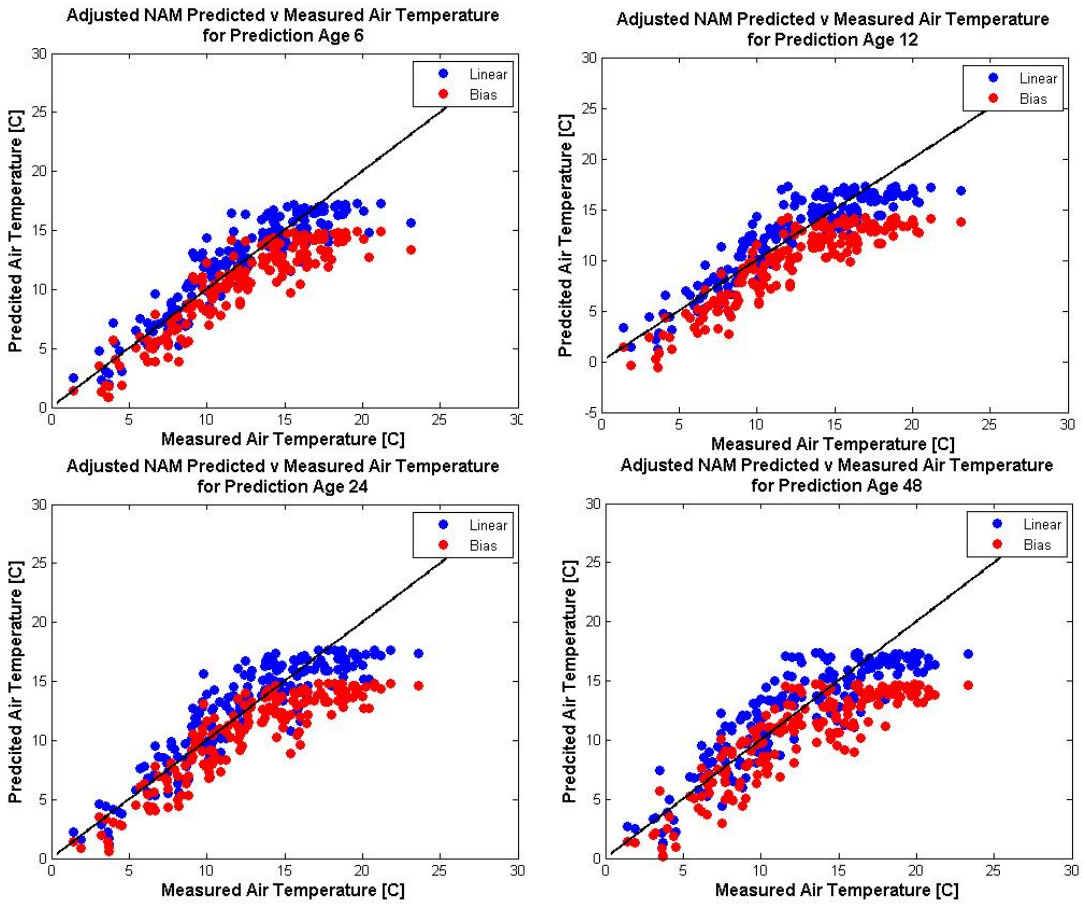

Figures 31. Comparison of linear transformation versus subtracting the bias for the NAM-WRF model. Predictions are for 6, 12, 24, and 48 hours, respectively.

Figures 32 through 35 illustrate the positive bias of the MESO2 predicted air temperatures as compared to measured air temperatures. The left sides of the figures illustrate the bias for the entire temperature range while the right side of the figures show the significant bias when the measured air temperatures are less than 20˚C. Since the average bias over all prediction times is higher for the MESO2 model than NAM-WRF, the correction threshold was increased from 18˚C to 20˚C. The same procedure was then followed to determine the best method to adjust for this bias. The comparison between a linear transformation correction and the subtraction of a bias is presented in Figure 36 and Table 17. Similarly to the NAM-WRF case predictions corrected with a linear correction are more accurate than when subtracting the respective biases. The linear transformation correction was therefore implemented.

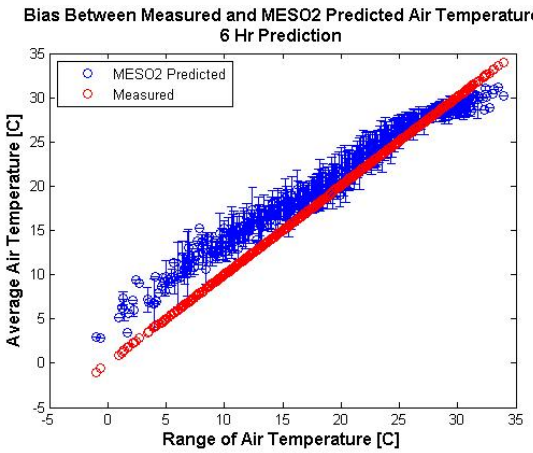

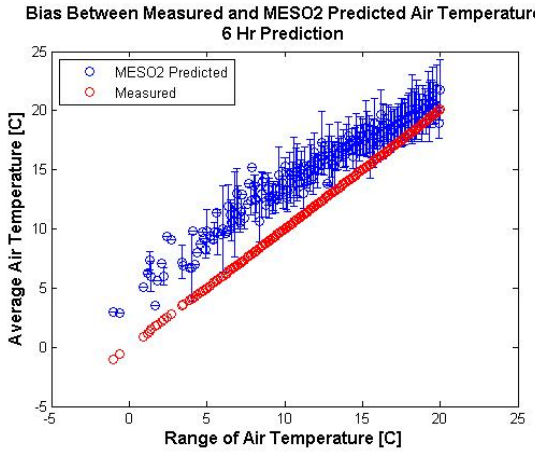

Figures 32. Biases between measured and MESO2 predicted air temperature at Bird Island for 6 hour predictions. Error bars represent standard deviation.

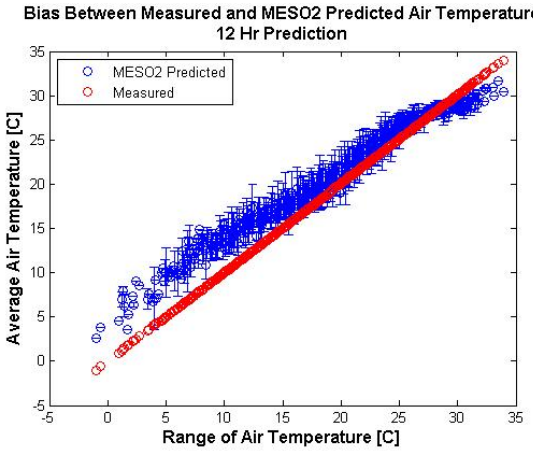

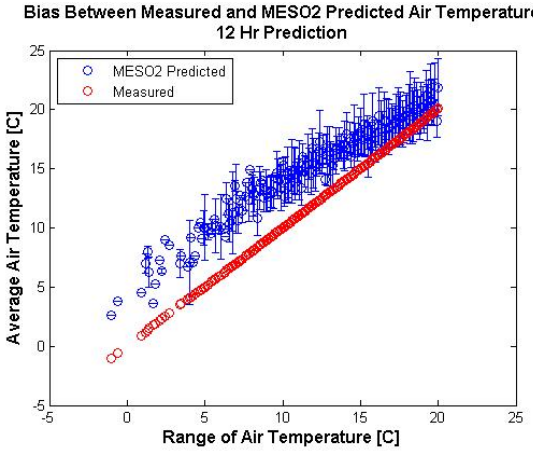

Figures 33. Biases between measured and MESO2 predicted air temperature at Bird Island for 12 hour predictions. Error bars represent standard deviation.

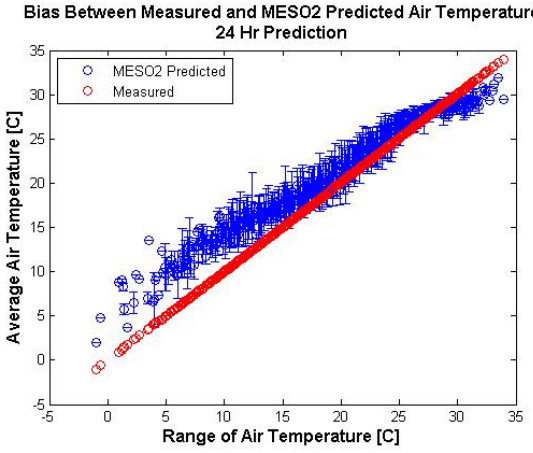

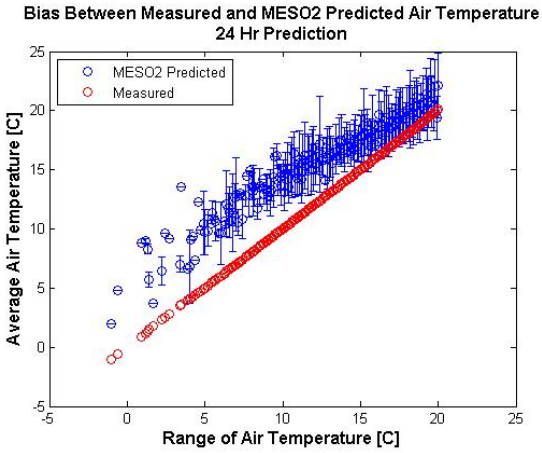

Figures 34. Biases between measured and MESO2 predicted air temperature at Bird Island for 24 hour predictions. Error bars represent standard deviation.

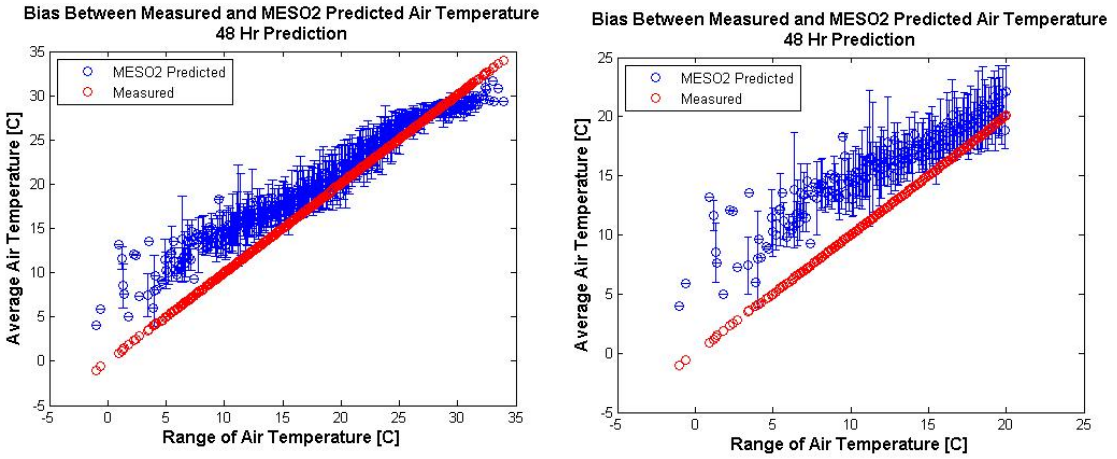

Figures 35. Bias between measured and MESO2 predicted air temperature at Bird Island for 48 hour predictions. Error bars represent standard deviation.

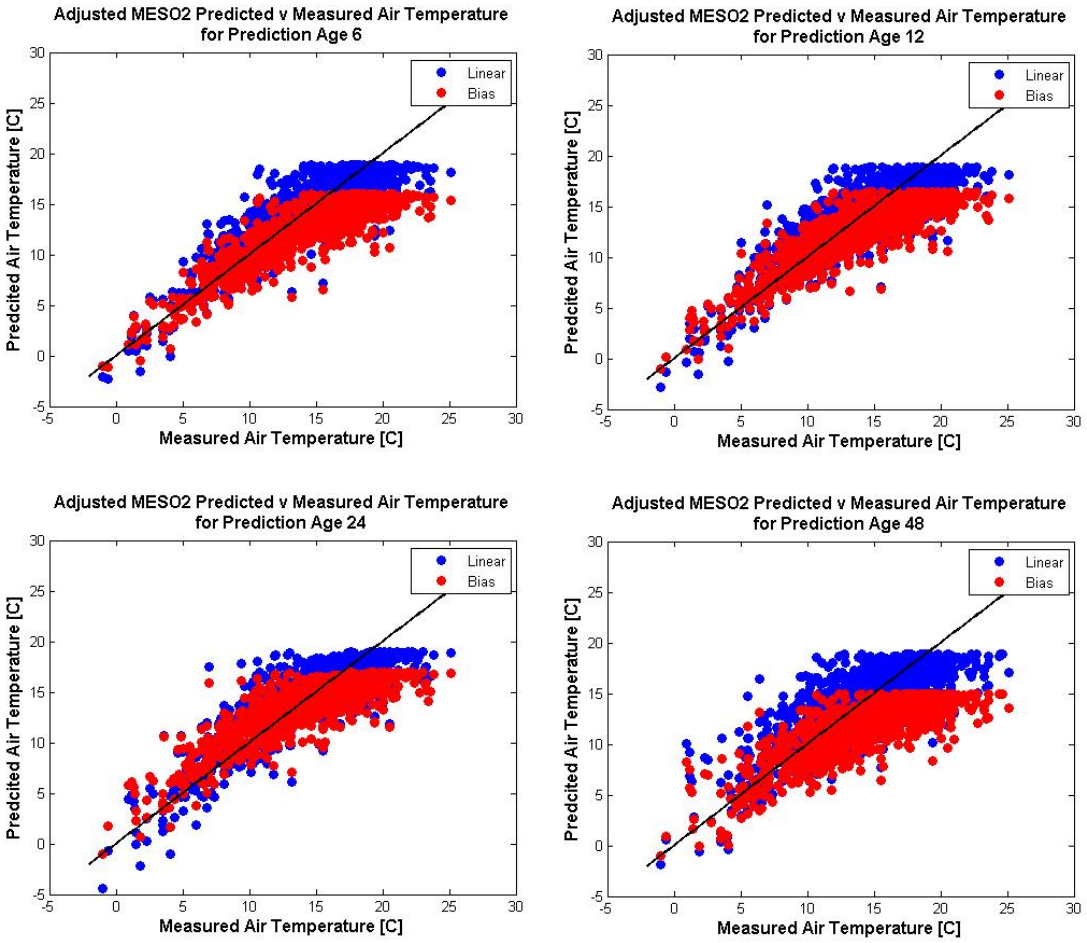

Figures 36. Comparison of linear transformation versus subtracting the bias for the MESO2 model for 6, 12, 24, and 48 hour predictions, respectively.

Table 17. Comparison of linear and bias model adjustments for MESO2 air temperature predictions.

Comparison of Linear vs. Bias Model for Adjusting MESO2 Predictions [°C]

Prediction Age	Model	Mean	Average Absolute	Largest Error
6	Linear	0.0	1.6	8.3
	Bias	2.0	2.4	9.8
12	Linear	0.0	1.7	8.8
	Bias	1.5	2.2	9.9
24	Linear	0.0	1.8	10.5
	Bias	0.9	2.1	9.3
48	Linear	0.0	2.1	10.0
	Bias	2.8	3.3	11.5

5. Operational Performance for Bird Island Station Predictions

To test the performance of the operational model at the Bird Island Station four recent cold water events were selected. The list of these events is presented in Table 18. The table includes the events minimum air and water temperatures measured. Predictions for 3, 12, 24 and 48 predictions were computed using both the perfect prog approach and actual air temperature predictions provided by the National Weather Service, i.e. MESO2 predictions for the 2003 & 2004 events and NAM-WRF predictions for the 2007 events. For all cases the predictions were adjusted using the linear transformations discussed in section 5 when the air temperatures were predicted to be below the respective model thresholds. The model was tested on the event data with water temperature below 45F with an additional 3 days prior and after the first and last water temperature measurement below 45F.

Table 18. Table of Events used in the testing of the model. MinWtp is the minimum water temperature reached and MinAtp is the minimum air temperature reached during the event.

Table of Events

Event	Year	Start Day	Length [hrs]	MinWtp [°C]	MinAtp [°C]
1	2003	17-Jan	38	7.4	2.1
2	2004	24-Dec	79	4	-1.2
3	2007	16-Jan	93	6	1.2
4	2007	16-Feb	7	7.9	2.7

Figures 37 through 44 illustrate the performance of the model for 3, 12, 24 and 48 hour water temperature predictions. The predictions are computed when using both perfect prog and NAM air temperature predictions. The results for the models using NAM predictions are on the right side while the models based on perfect prog predictions are on the left side. Tables 19 and 20 display the average absolute error for all conditions as well as for cold water temperatures both when using the perfect prog approach as well as the NAM WRF actual air temperature predictions. In this case as well as for tables 21, 22 and 23 the cut off for cold water temperature performance was increase to 9°C. Table 21 compares side by side the model mean average absolute errors when using the perfect prog approach and the NAM WRF actual air temperature predictions. Table 22 displays an event by event comparison of absolute error between measured and predicted air temperatures during cold water events and Table 23 compares the maximum error between measured and predicted air temperatures during cold events. The accuracy of the air temperature predictions is the main driving factor in the accuracy of the water temperature predictions for the model. Figures 45 through compare in a different format measured and predicted water temperatures for the four selected events and for 3, 12, 24 and 48 hour predictions. The graphs show that the prediction accuracy does not vary substantially for different temperature range but vary mostly from event to event. If the future atmospheric conditions are accurately predicted the water temperature predictions will be more accurate and show less variability. The impact of the air temperature predictions on the water temperature prediction accuracies is finally illustrated in figure 49 where the difference between predicted and measured air temperature is displayed for

12 hour prediction during event 2. The difficulty of the atmospheric model to predict air temperatures between hours 150 and 250 results in successive highs and lows in the prediction error. This error is in turn affecting the water temperature predictions as can be observed in Figure 40. The error in the water temperature predictions directly reflect the succession of the over and under predictions in the air temperatures. The effect can also be seen in Figure 46. For the other 3 events, air temperature prediction errors did not show such variability and neither did the water temperature predictions. For the 2007 cold water events, events 3 and 4, measured temperatures are available for the project Rincon station and displayed. For event 3, the water temperatures at the Rincon station show a short consistent lag throughout the event while no significant systematic trend is observed during event 4. As will be discussed in section 6 no significant differences in water temperatures were observed between the two stations when comparing all data. As more data becomes available project scientists will continue to compare water temperatures at the project stations, the Bird Island stations and other Laguna Madre station during cold water events.

Event 1: Data from January 14 – January 22, 2003

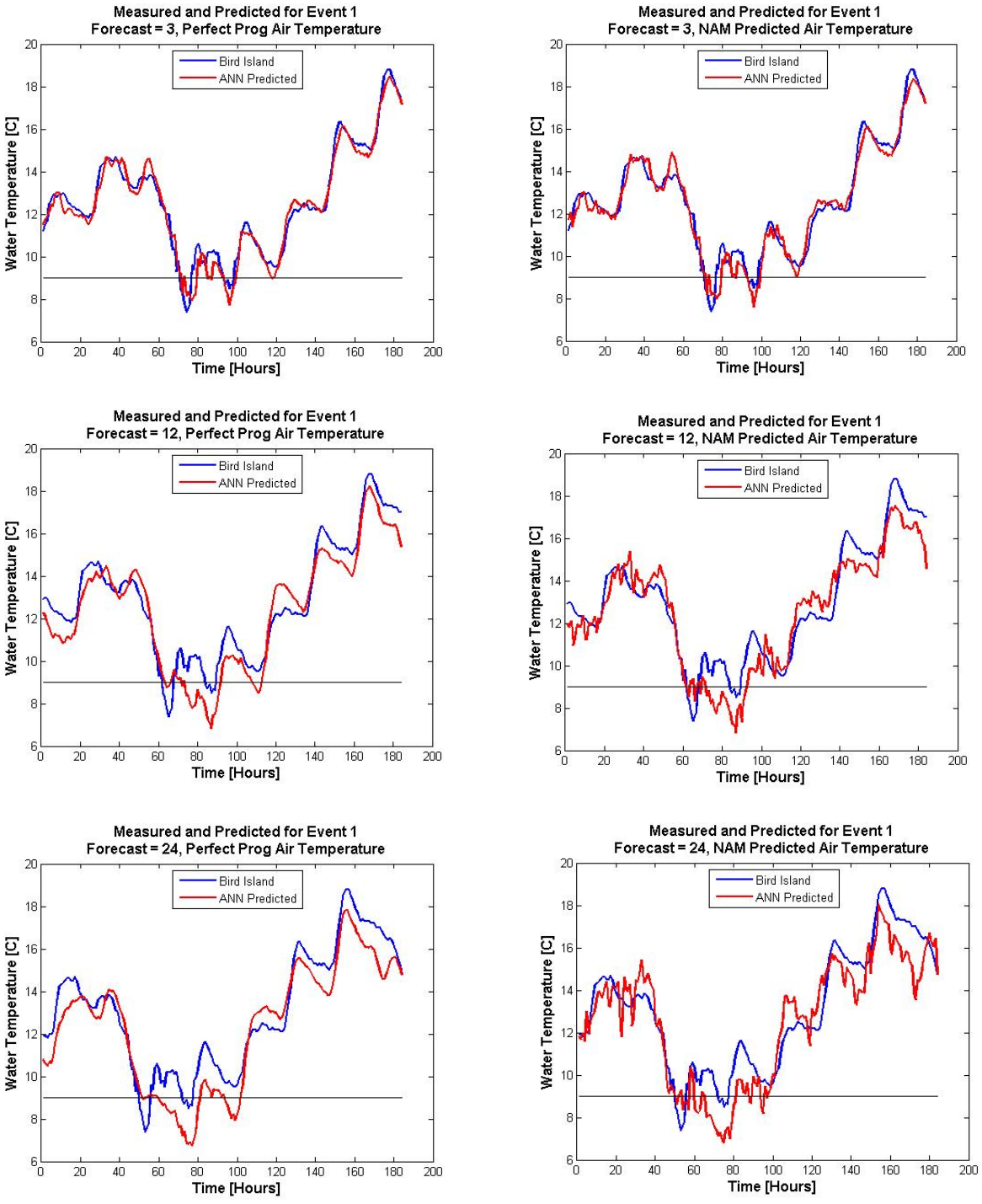

Figure 37. Comparison of Measured and Predicted water temperatures for Event 1 using perfect prog air temperature predictions (left) and MESO2 predictions (right). The predictions are for 3, 12, and 24 hours.

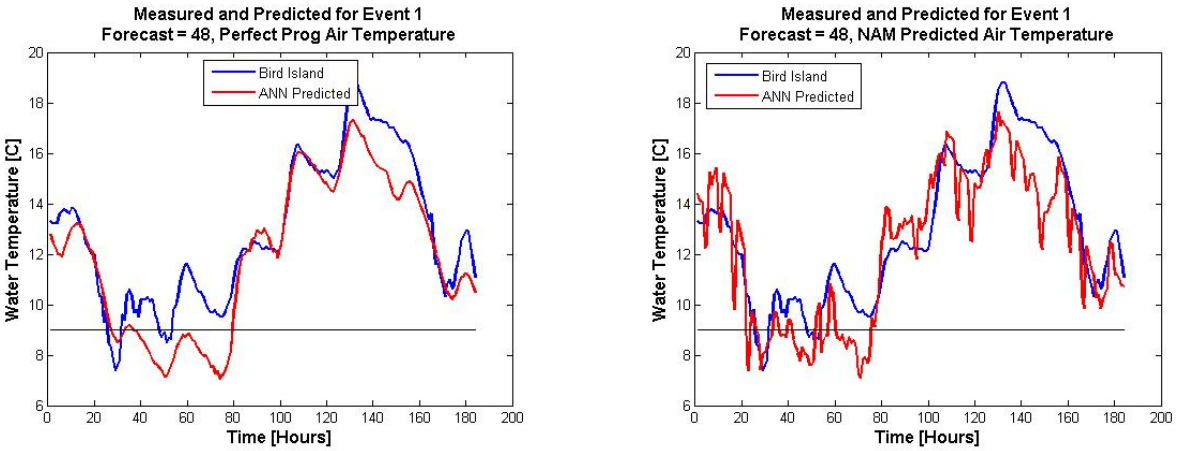

Figure 38. Comparison of Measured and Predicted water temperatures for Event 1 using perfect prog air temperature predictions (left) and MESO2 predictions (right). The predictions are for 3, 12, and 24 hours.

Event 2: Data from December 21 – December 29, 2004

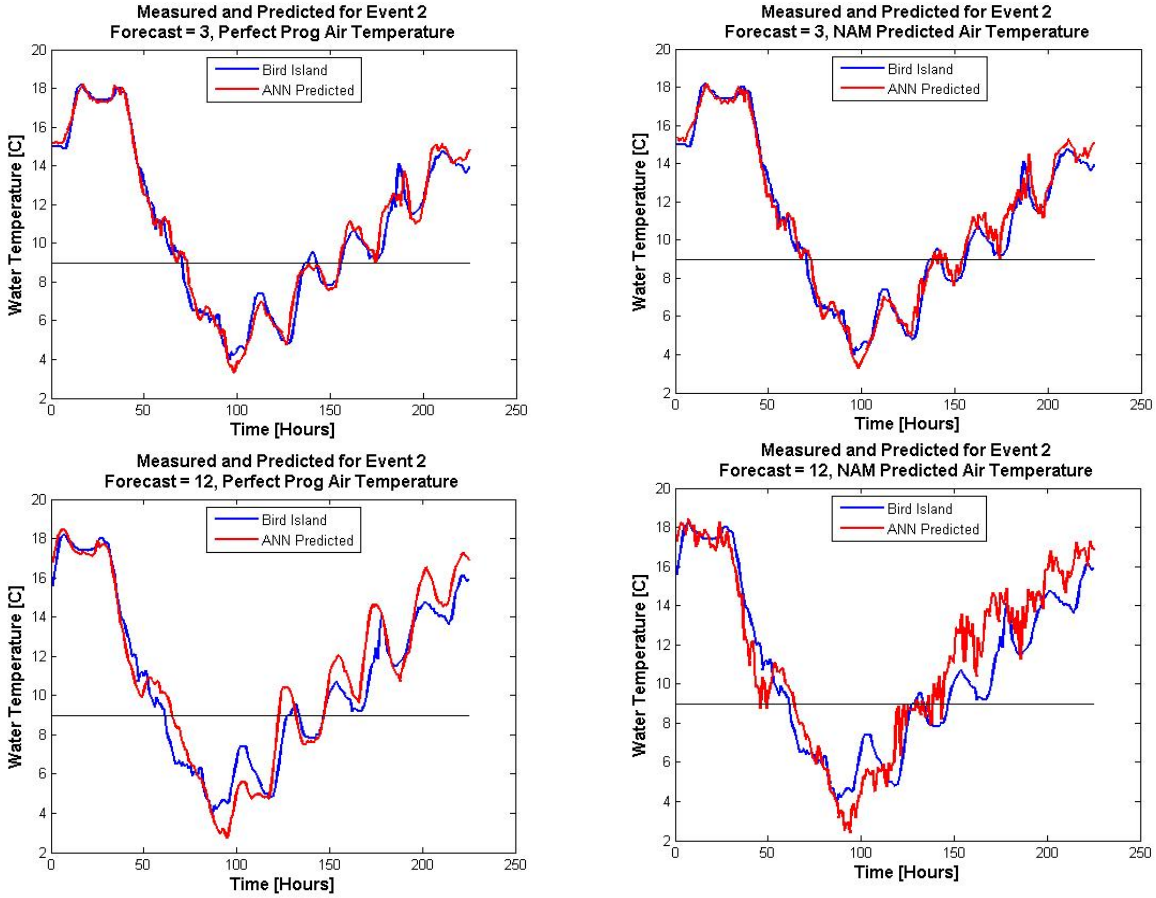

Figure 39. Comparison of Measured and Predicted water temperatures for Event 2 using perfect prog air temperature predictions (left) and MESO2 predictions (right). The predictions are for 3 and12 hours.

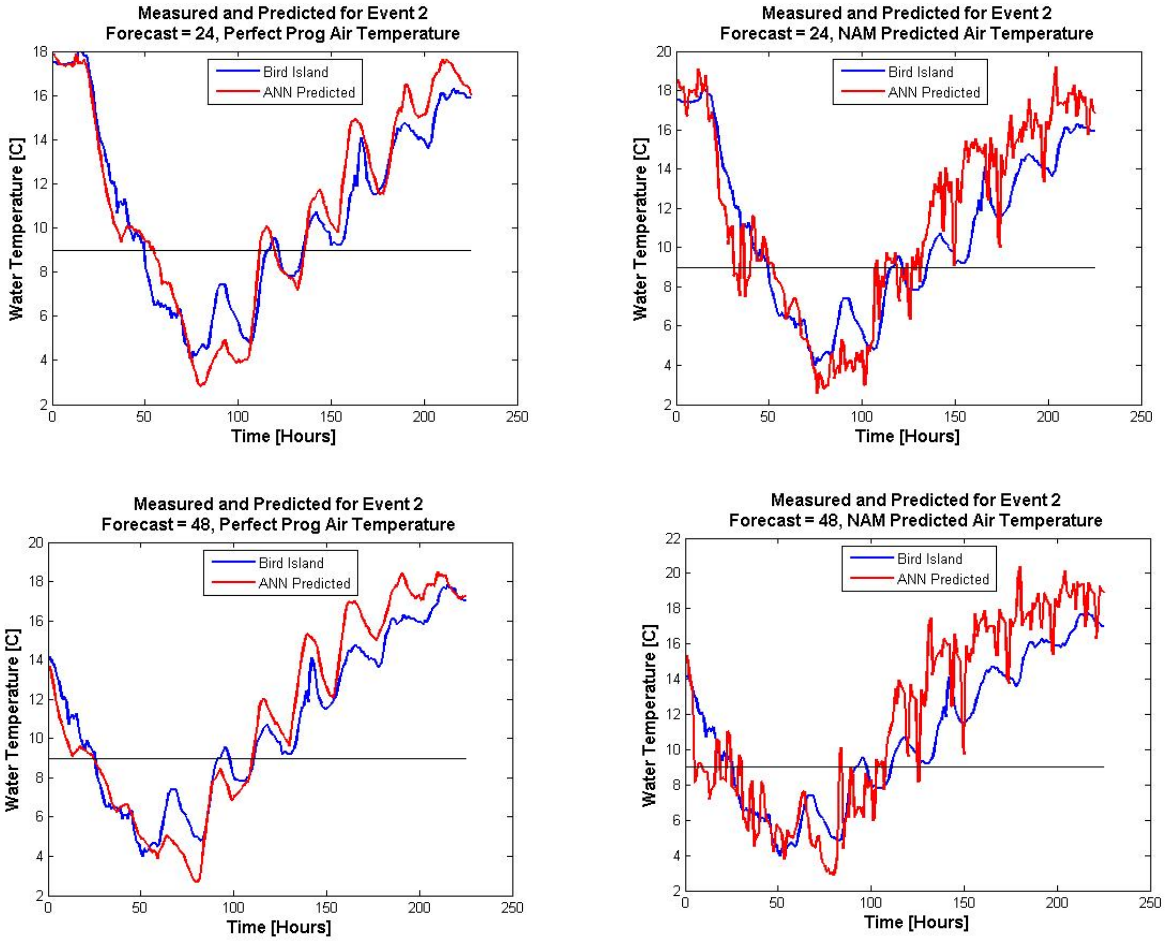

Figure 40. Comparison of Measured and Predicted water temperatures for Event 2 using perfect prog air temperature predictions (left) and MESO2 predictions (right). The predictions are for 24 and 48 hours.

Event 3: Data from January 13 – January 23, 2007

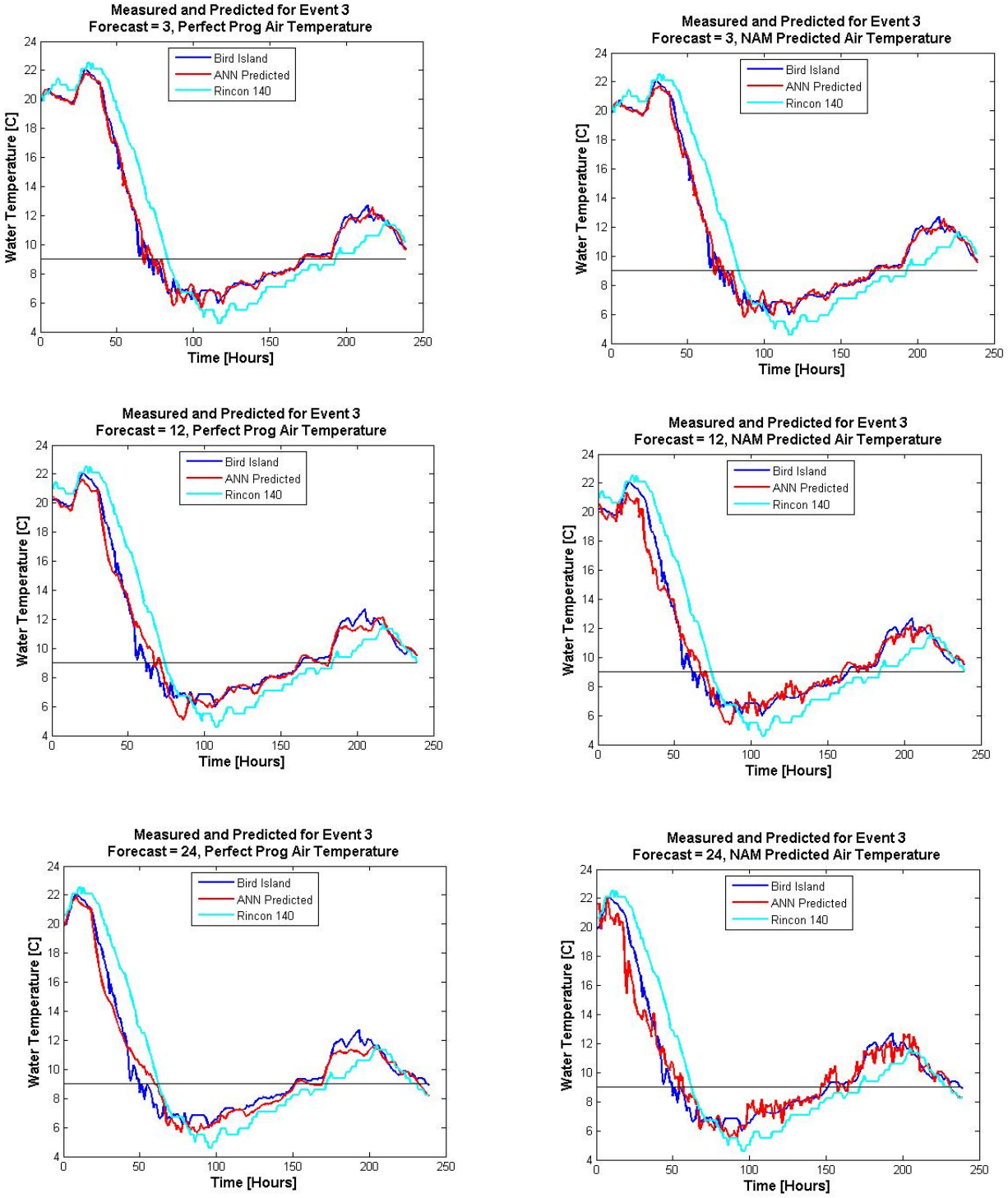

Figure 41. Comparison of Measured and Predicted water temperatures for Event 3 using perfect prog air temperature predictions (left) and MESO2 predictions (right). The predictions are for 3, 12 and 24 hours.

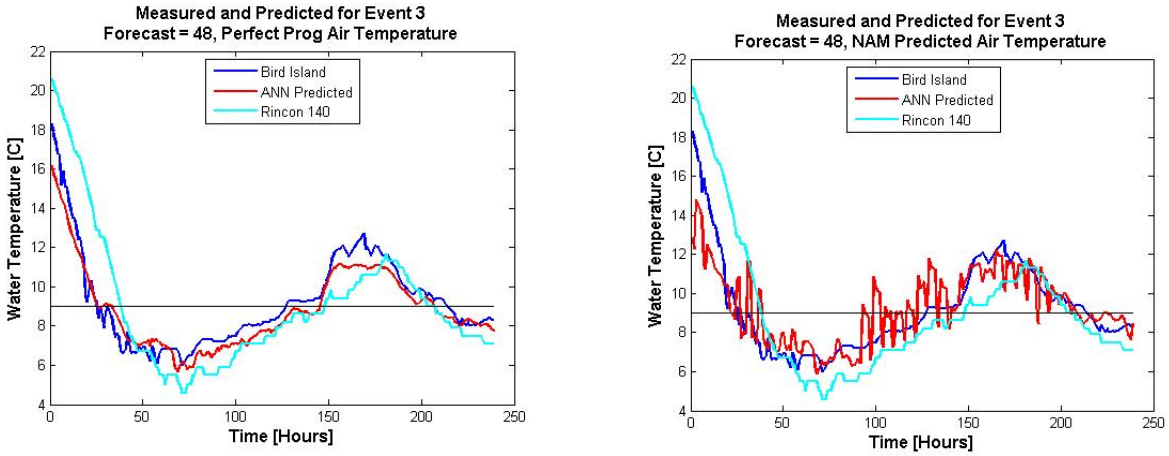

Figure 42. Comparison of Measured and Predicted water temperatures for Event 3 using perfect prog air temperature predictions (left) and MESO2 predictions (right). The predictions are for 48 hours

Event 4: Data from February 13 – February 19, 2007

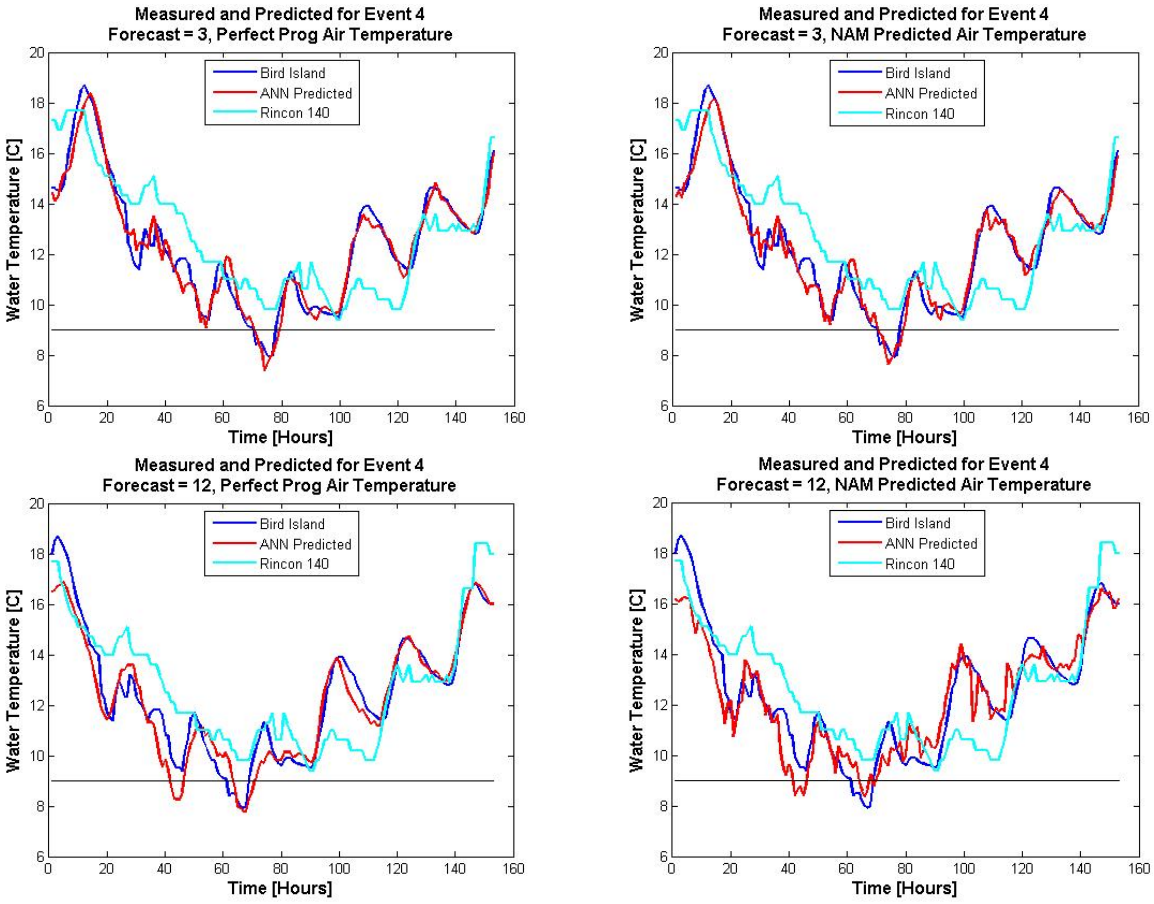

Figure 43. Comparison of Measured and Predicted water temperatures for Event 4 using perfect prog air temperature predictions (left) and MESO2 predictions (right). The predictions are for 3 and 12 hours.

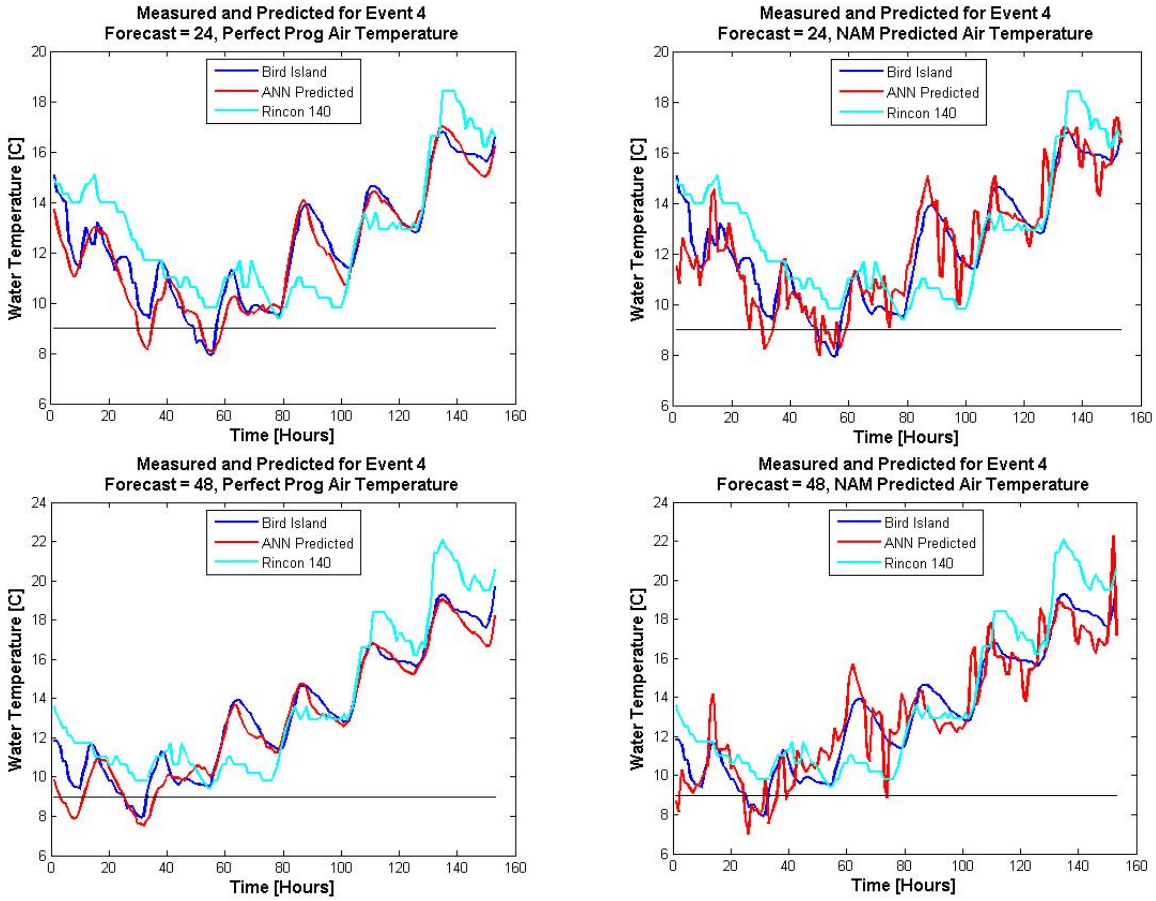

Figure 44. Comparison of Measured and Predicted water temperatures for Event 4 using perfect prog air temperature predictions (left) and MESO2 predictions (right). The predictions are for 24 and 48 hours.

Table 19. Average absolute error during the events when using perfect prog air temperature predictions.

Average Absolute Errors [°C] During Events: Perfect Prog Air Temperatures

	Event 1		Event 2		Event 3		Event 4	
Forecast	All Data	Cold Hours	All Data	Cold Hours	All Data	Cold Hours	All Data	Cold Hours
3	0.4	0.5	0.4	0.5	0.3	0.3	0.4	0.3
12	0.8	1.0	0.9	1.1	0.5	0.5	0.6	0.4
24	1.0	1.5	1.0	1.2	0.6	0.6	0.5	0.4
48	1.1	1.1	1.2	1.0	0.6	0.5	0.6	0.3

Table 20. Average absolute error during the events when using NAM air temperature predictions.

Average Absolute Errors [°C] During Events: NAM Predicted Air Temperatures

	Event 1		Event 2		Event 3		Event 4	
Forecast	All Data	Cold Hours	All Data	Cold Hours	All Data	Cold Hours	All Data	Cold Hours
3	0.4	0.5	0.5	0.5	0.3	0.3	0.4	0.3
12	0.9	1.0	1.3	1.1	0.6	0.5	0.8	0.8
24	1.0	1.2	1.7	1.3	0.7	0.5	0.8	0.7
48	1.3	0.8	2.1	1.4	0.9	0.8	1.0	0.6

Table 21. Comparison of mean average absolute errors during all events when using perfect prog and NAM air temperature predictions.

Mean Average Absolute Error [°C] Over All Events

	Using Perfect Prog Predictions		Using NAM Predictions	
Forecast	All Data	Cold Hours	All Data	Cold Hours
3	0.4	0.4	0.3	0.4
12	0.7	0.8	0.9	0.9
24	0.8	0.9	1.1	0.9
48	0.9	0.7	1.3	0.9

Table 22. Average absolute error between measured and predicted air temperatures during cold water events.

Average Absolute Error [°C] Between Measured and Predicted Air Temperature During Events

Prediction Age	Event 1	Event 2	Event 3	Event 4
3	1.4	2.5	1.0	1.3
12	1.5	2.6	1.1	1.3
24	1.4	2.6	1.2	1.4
48	1.8	2.5	1.9	1.7

Table 23. Maximum error between measured and predicted air temperatures during cold events.

Maximum Absolute Error [°C] Between Measured and Predicted Air Temperature During Events

Prediction Age	Event 1	Event 2	Event 3	Event 4
3	4.8	9.3	7.4	4.6
12	4.4	9.9	7.4	5.0
24	4.2	8.6	5.2	5.1
48	8.5	9.3	6.5	6.4

Event 1: Measured vs. Predicted Air Temperature

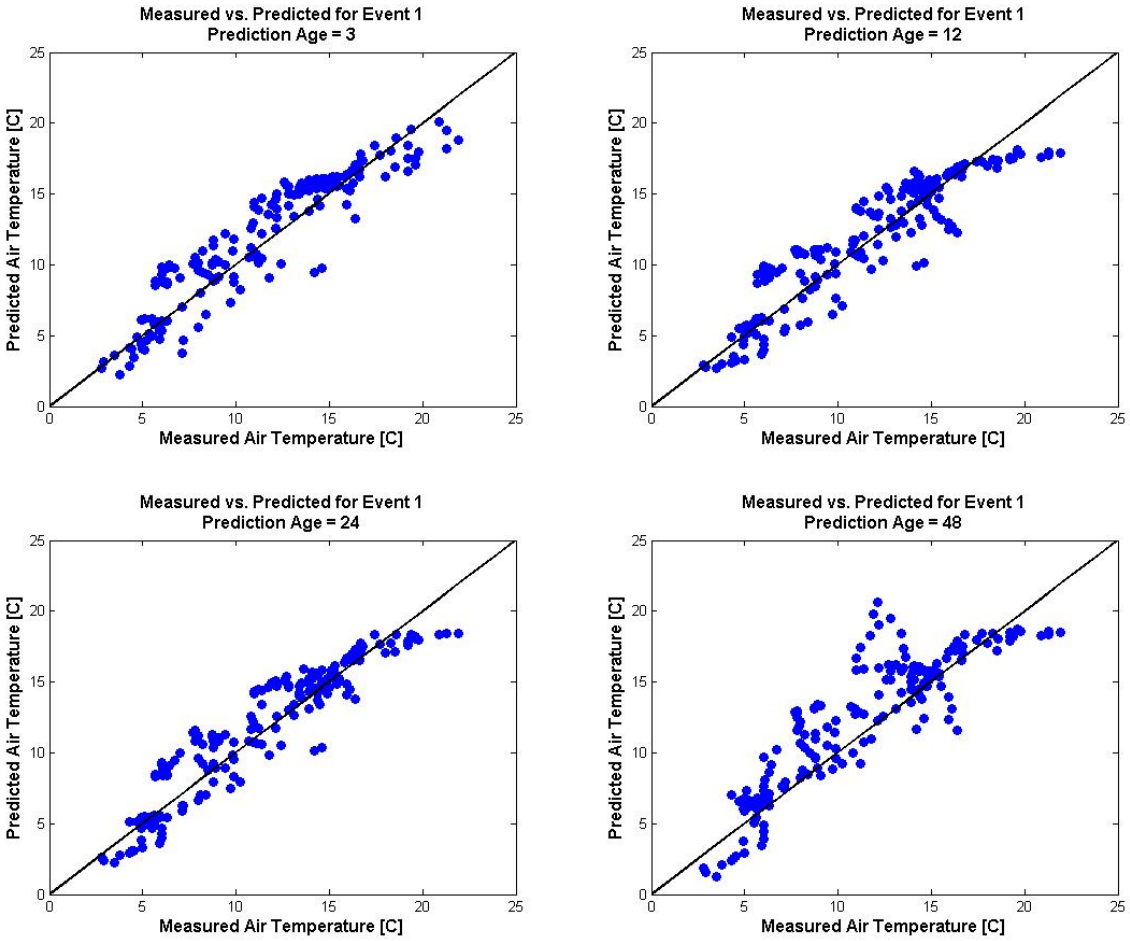

Figure 45. Comparison of measured and predicted water temperatures for event 1 for 3, 12, 24 and 48 hour predictions.

Event 2: Measured vs. Predicted Air Temperature

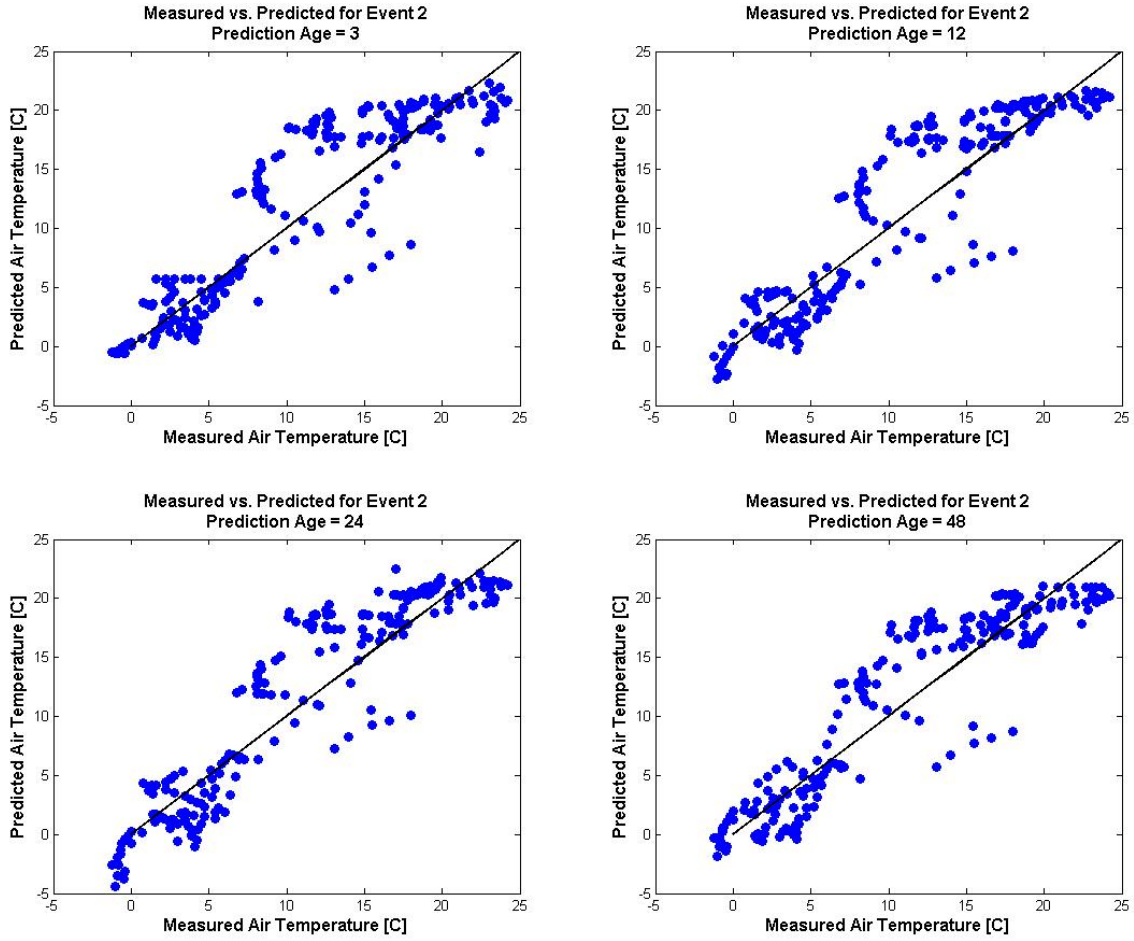

Figure 46. Comparison of Measured and Predicted water temperatures for Event 2 for 3, 12, 24 and 48 hour predictions.

Event 3: Measured vs. Predicted Air Temperature

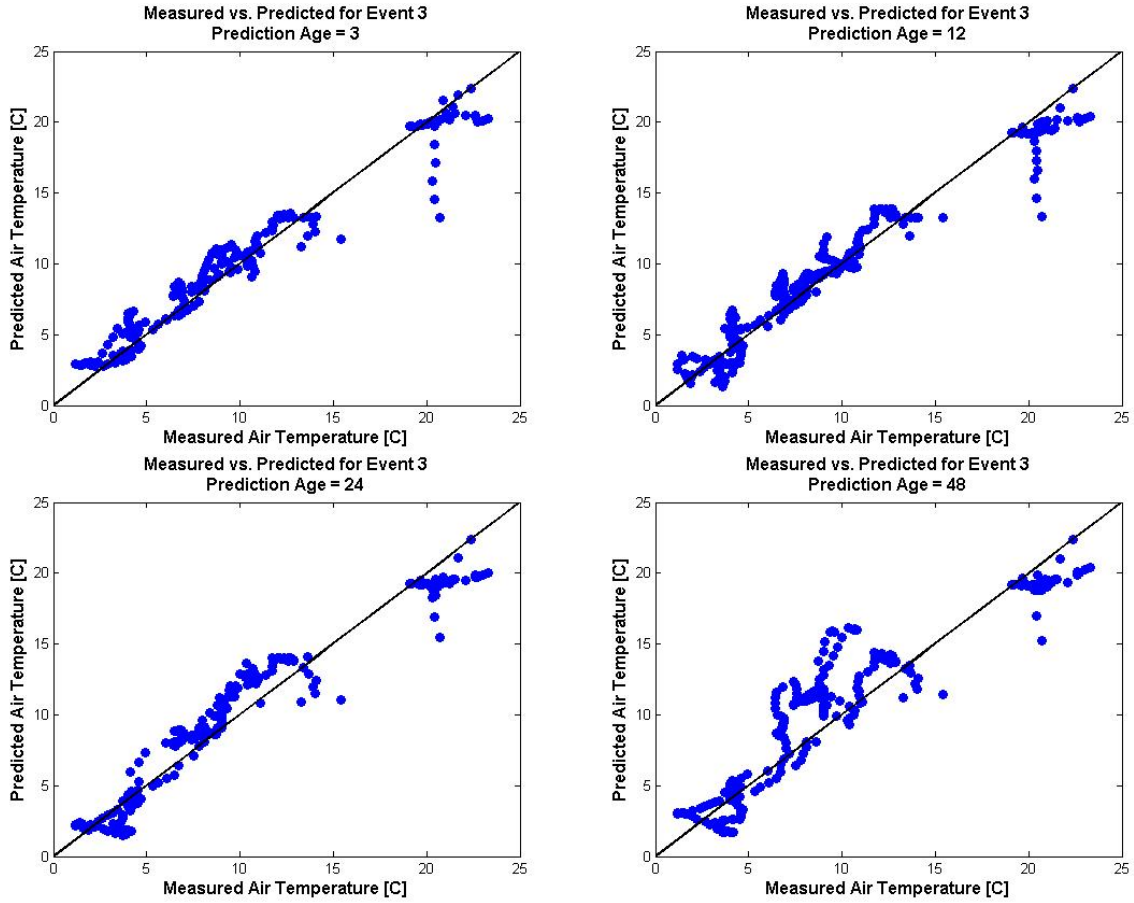

Figure 47. Comparison of Measured and Predicted water temperatures for Event 3 for 3, 12, 24 and 48 hour predictions.

Event 4: Measured vs. Predicted Air Temperature

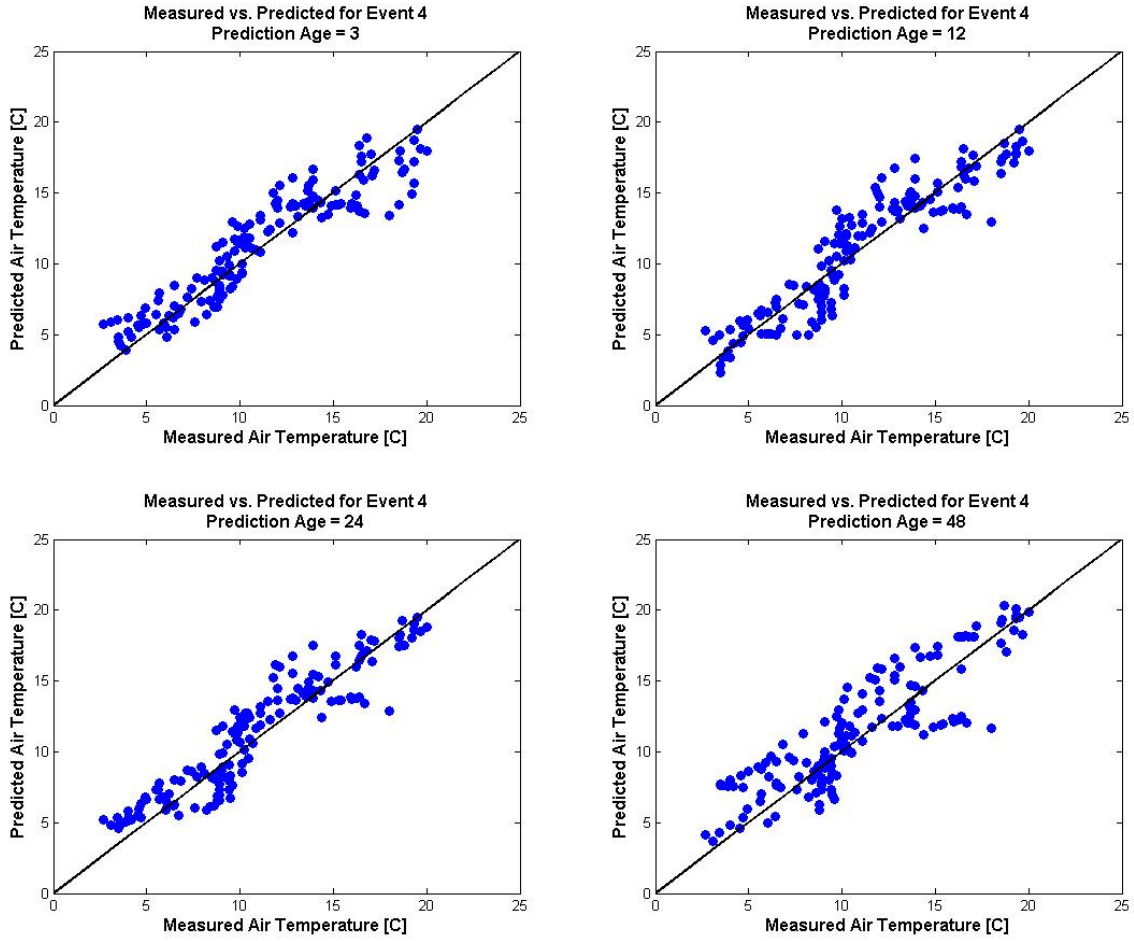

Figure 48. Comparison of Measured and Predicted water temperatures for Event 4 for 3, 12, 24 and 48 hour predictions.

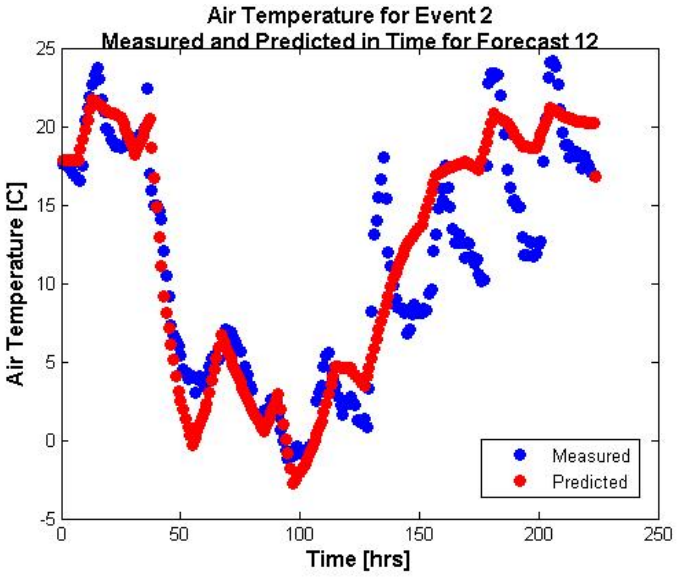

Figure 49. Detailed view for event 2, or example of how air temperature predictions affect water temperature prediction predictions - 12 forecasts during event 2.

6. Portability of the Model to the TPWD Stations and the Rest of the Laguna Madre

So far in this study, the water temperature predictions were computed for the Bird Island station located in the northern portion of the Laguna Madre. The Bird Island station was selected to design and test the model over the project stations because of the considerably longer time series available. This section of the report addresses the portability of the model to the project stations and other Laguna Madre stations by first testing for possible biases in water temperatures and then for possible lags in the water temperature dynamic.

The data used to analyze possible biases and lags included hourly water temperature measurements from the Bird Island, Rincon, Port Mansfield, and Port Isabel stations from March 2006 to March 2007. The locations of the stations are illustrated in figure 50. It was established in an earlier portion of this report that no significant temperature differences could be observed between the TPWD Landcut station and the TPWD Rincon station for the available measurements. The case of the Landcut station was therefore only addressed peripherally in this report for December 15, 2006 to June 2007 to confirm the previous observation and also to avoid using part of the data set that included likely sensor drifts.

Figure 50. Map of stations analyzed for biases and lags.

Our main interest here is how the Rincon and Bird Island station water temperatures compare. However possible biases and lags were also computed for other stations than the project stations to assess the overall homogeneity of water temperatures in the Laguna Madre.

6.1 Possible water temperature biases between Bird Island and other locations

To compute possible biases, the range of water temperatures was divided into bins, each with a bin size of 0.1°C. When the water temperature at Rincon falls within a certain bin, the average and the standard deviation of the water temperature at the comparison station are then computed for this bin. The results are graphed allowing for a visual identification of possible biases.

6.1.1 Comparison of water temperatures at the Rincon and Bird Island Stations

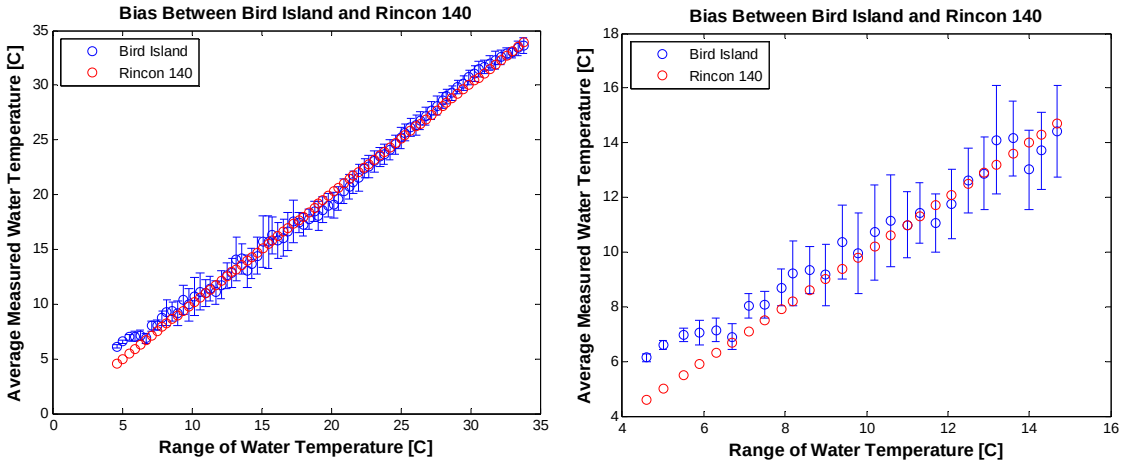

(a) (b)

Figure 51. Graphical analysis of possible biases between Bird Island and Rincon water temperatures for the full water temperature range (a) and for the low water temperature cases (b). The error bars represent the standard deviation of the respective water temperature distributions.

As can be observed in Figure 51 water temperatures are unbiased for most of the water temperature range. For the lower water temperatures Bird Island water temperatures are warmer than the Rincon water temperatures. However, it must be noted that we have only very few measurements for these cold water temperatures. Measurements between 4.6 - 6°C occurred during only one event at Rincon 140. At the writing of this report observational data is insufficient to conclude that significant water temperature differences can take place between stations during cold events. More observations will be needed to conclude and possibly adjust the operational model. The number of measurements for Bird Island and Rincon are illustrated in Figure 52 for the full range of temperatures measured. During the entire year of measurements Rincon station is, on average, 0.13°C cooler than Bird Island measurements. When the water temperature is

below 15°C, water temperatures at Rincon 140 are, on average, 0.44°C cooler that Bird Island water temperatures.

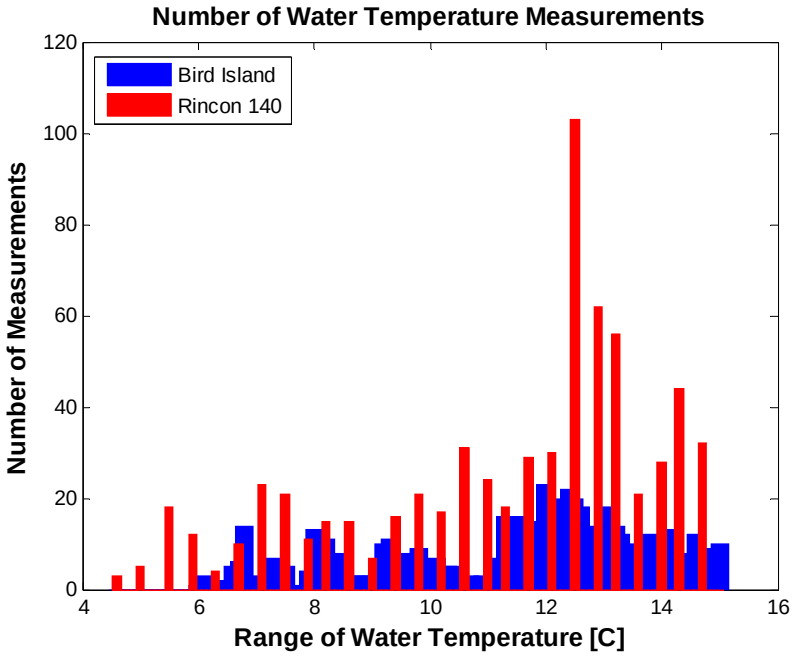

Figure 52. Number of Water Temperature Measurements for Rincon 140. Ranges from 4.6°C to 15°C.

6.1.2 Comparison of water temperatures at the Rincon, Port Mansfield, and Port Isabel stations

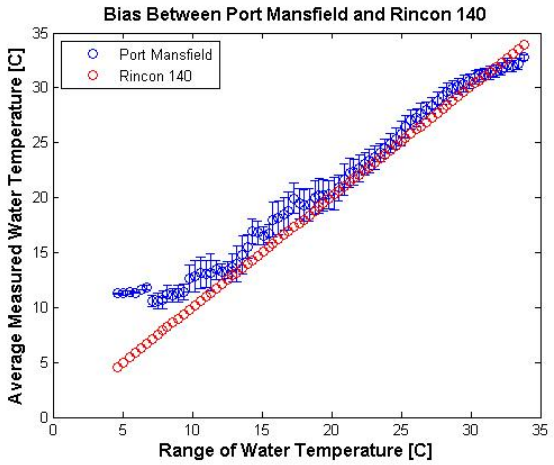

Figure 53. Measurement Biases Between Port Mansfield and Rincon 140. Error bars represent standard deviation.

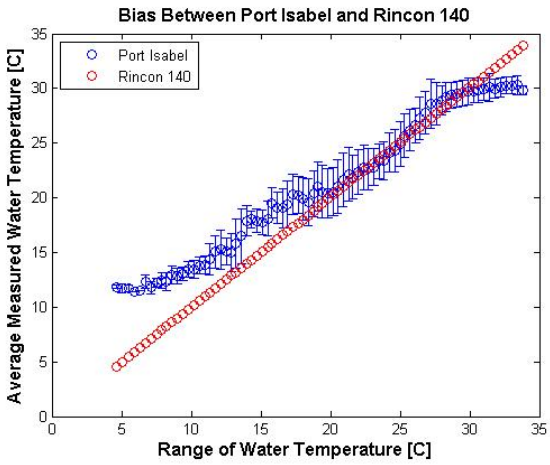

Figure 54. Measurement Biases Between Port Isabel and Rincon 140. Error bars represent standard deviation.

Statistical analysis of the data presented in Figures 53 indicates that Port Mansfield water temperatures are, on average, 1°C cooler than water temperatures at the Rincon project station. When the water temperature is less than 15°C at the Rincon station, water temperatures at Port Mansfield are 6.7°C warmer on average but this is again based on a very small number of measurements and therefore more observations are needed to provide significant figures for low water temperature cases. The warmer water temperatures at the Port Mansfield station are however to be expected as the ship channel provides a more direct link to the warmer waters of the Gulf of Mexico during cold front passages. The dynamic of the water temperatures at all locations close to ship channels are different then the Laguna Madre stations with higher lows and lower highs due to the moderating effect of the Gulf of Mexico waters.

The same comparison is conducted for the Port Isabel station at the southern end of the Laguna Madre and the same pattern is observed due to the presence of the nearby Brownsville ship channel and deeper waters at the station location. On average, Port Isabel water temperatures are 0.8°C warmer than Rincon water temperatures. When the water temperature at Rincon is less than 15°C, water temperatures at Port Isabel are 7.3°C warmer on average with the same caveat that very few water temperature measurements are available for the Rincon project station. That said it is not

6.1.3 Comparison of water temperatures at the Rincon and Landcut 141 stations

To analyze possible biases between Bird Island and the Landcut station, we used only data from December 15, 2006 to June 2007. Bird Island and Landcut water temperatures compare very well, both during regular and cooler water temperatures. Over the 6 month time period, water temperatures at the Landcut station are on average only 0.13°C warmer than at Bird Island. When the water temperature at the Landcut station is less than 15°C, water temperatures at Bird Island are approximately 0.3°C cooler. The results of the analysis are displayed graphically in Figures 55 and 56 and the respective distribution of measurements at both stations is presented in Figure 57.

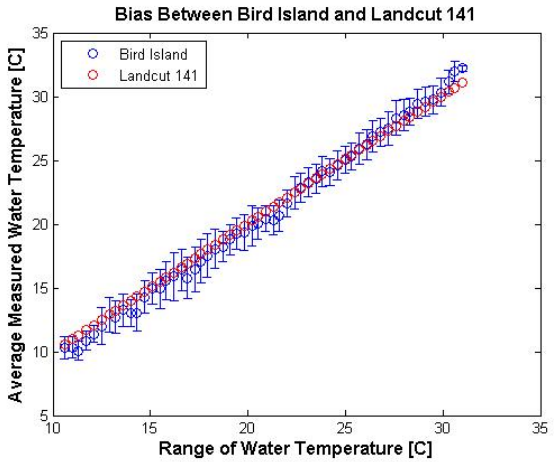

Figure 55. Measurement Biases Between Bird Island and Landcut 141. Error bars represent standard deviation.

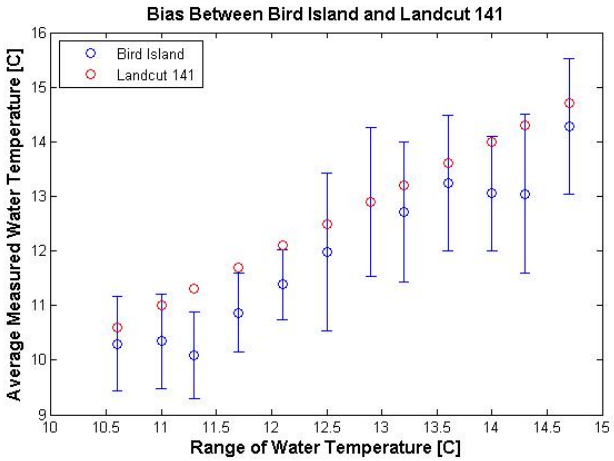

Figure 56. Measurement Biases During Cold Events Between Bird Island and Landcut 141. Error bars represent standard deviation.

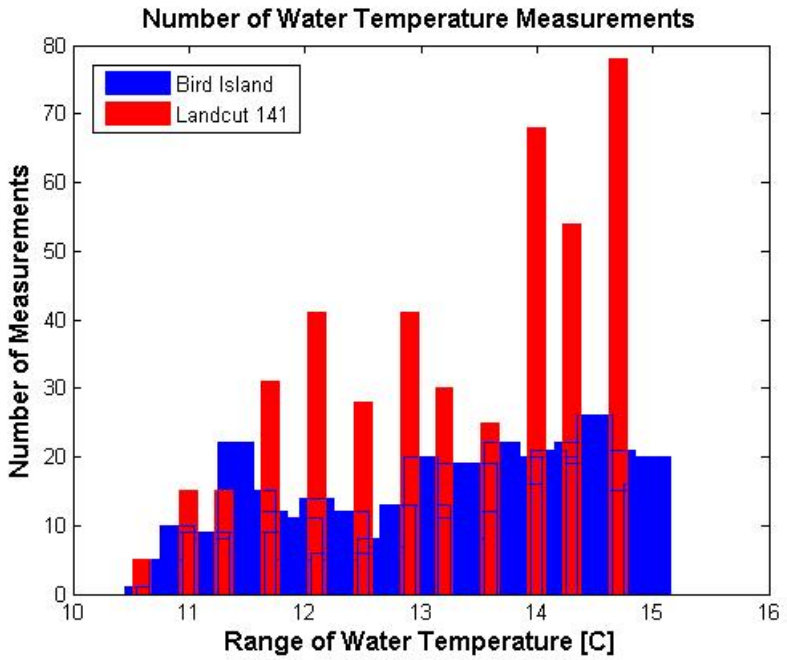

Figure 57. Number of Water Temperature Measurements for Bird Island and Landcut 141. Ranges from 10.6°C to 15°C.

6.2 Possible lags between water temperatures at Bird Island and other locations

The Rincon 140 station is located south of the Bird Island station in the Laguna Madre. Because of its southern location, the possibility that the changes in water temperature at Rincon lag behind Bird Island, particularly during cold events, was investigated. To assess this potential lag a series of cross correlations were computed. The data ranges from March 2006 to March 2007. No interpolation was done for missing measurements. Pearson cross correlations were computed for the entire year as well as during three cold events. The cold events included in the computations are listed in Table 24. Figure 58 display the results for all conditions. For the entire year, the strongest correlation occurs at 0 and 1 hours, with a correlation coefficient of 0.98. This indicates that the current water temperature at Bird Island strongly correlates with the current water temperature and water temperature one hour in the future at Rincon. Similar to the yearly correlations, the highest correlations when analyzing the data of the first cold event (Event 1, Figure 59) shows the highest correlation coefficients for 0 and 1 hours, with a correlation coefficient 0.94.

Table 24. Cold events used in this section of the study. MinWtp is the minimum water temperature and MinAtp is the Minimum air temperature reached during the event.

Table of Cold Events

Event	Year	Start Day	Length [hrs]	MinWtp [°C]	MinAtp [°C]
1	2007	16-Jan	93	6	1.2
2	2007	24-Jan	29	8	5.9
3	2007	16-Feb	7	7.9	2.7

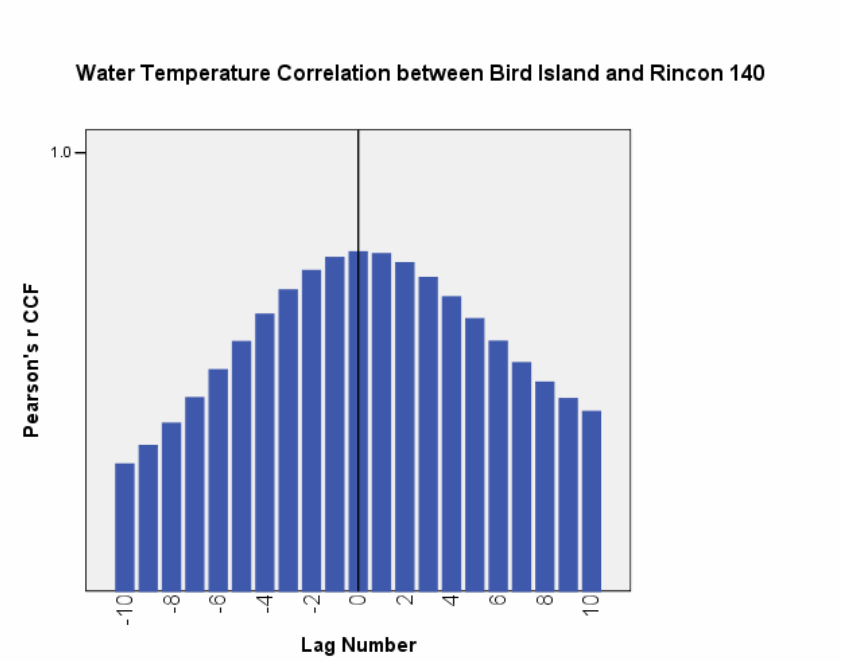

Figure 58. Water Temperature Correlation between Bird Island and Rincon 140. March 2006 – March 2007.

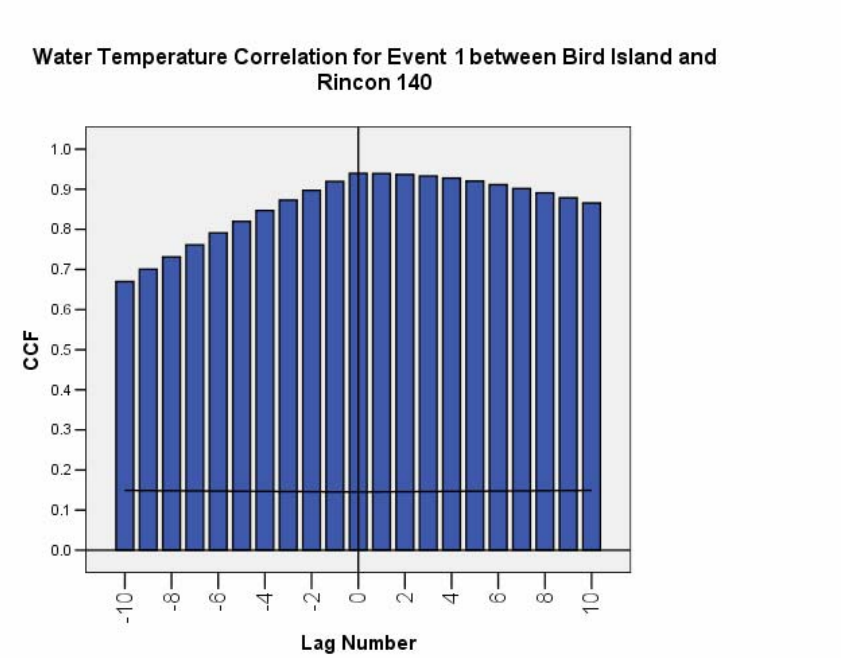

Figure 59. Water Temperature Correlation for Event 1 between Bird Island and Rincon 140. January 14 – January 22

When conducting the same analysis for Event 2 (Figure 60), the strongest correlation occurs at 1 hour, meaning that the current water temperature at Rincon is most highly correlated with water temperature in the previous hour at Bird Island. The correlation coefficient at 1 hour is 0.87.

For event 3 (Figure 61) the strongest correlation between water temperatures occurs at 0 hours, with a correlation coefficient of 0.49 and for event 4 the strongest correlation occurs at 1 hour (not shown). Given that the highest correlation between stations occurs for 0hrs for the entire year and that the strongest correlations are measured for no lag or 1 hr lags during the events no corrections were made to the model. Since there is no conclusive evidence of a bias or lag between Bird Island and Rincon 140, it is not necessary to linearly transform predictions for Bird Island.

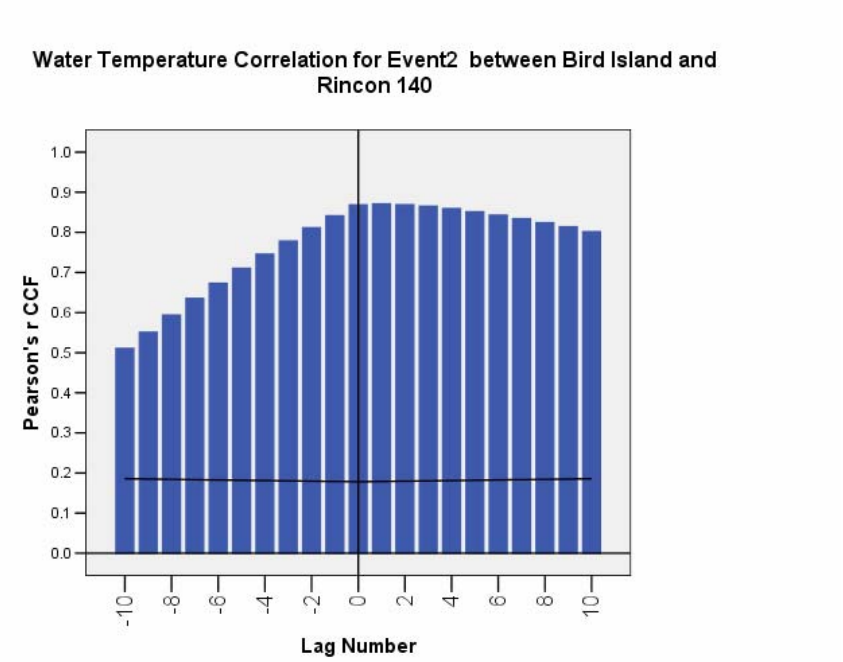

Figure 60. Water Temperature Correlation for Event 3 between Bird Island and Rincon 140. January 22 – January 27.

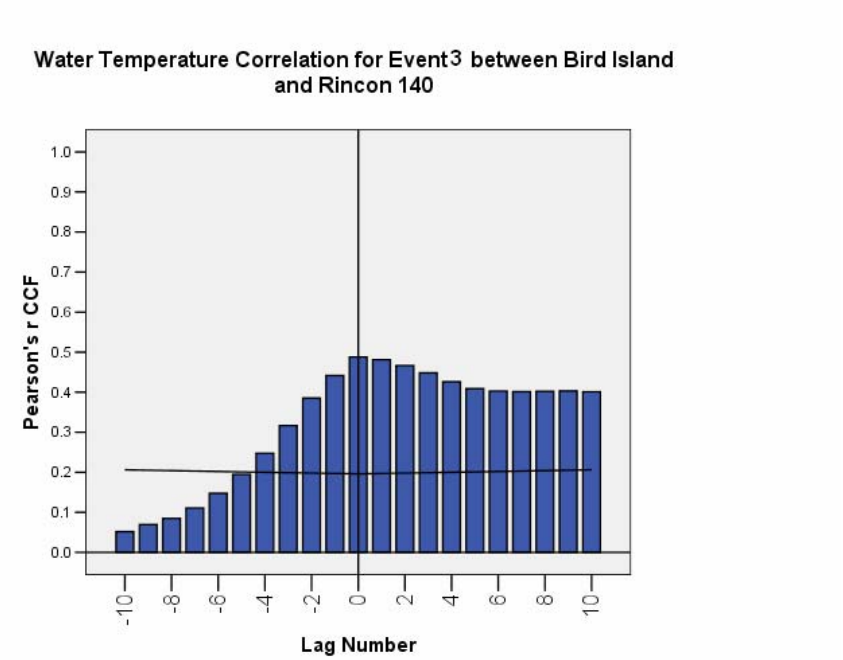

Figure 61. Water Temperature Correlation for Event 3 between Bird Island and Rincon 140. February 14 – February 18.

7. Operational Performance for Cold Events

This section is designed to help operational users assess the model accuracy for cold events. A set of tables was designed to address the typical operational cases. For these tables, a cold event is defined similarly to the rest of the study as an event during which the water temperatures are predicted and/or measured below 7.2°C. The results are based on test years 1995, 2000 and 2001 (the ones with the largest number of cold events and including the greatest variability of events i.e. length of the event, temperature gradients during the event). The probabilities for each case and for 4 forecasting target times are presented in the table below. If the model performance is perfect, the top row of the tables will have 1's while the bottom rows of the tables will have 0's.

Table 25. Operational cases considered and related event probabilities.

Events/Conditions	What are the probabilities that …	
A cold water event is predicted	The cold water event indeed takes place	A cold water event does not take place
A cold water event is not predicted	The cold water event still takes place	A cold water event indeed does not take place
A cold water event is observed	The cold water event had been predicted	The cold water event had not been predicted
A cold water event is not observed	The cold water event had been predicted	The cold water event had not been predicted

Model Performance when a Cold Event is Predicted

Forecasts:	3 hrs	12 hrs	24 hrs	48 hrs
Probability that the event will indeed occur	0.90	0.85	0.83	0.64
Probability that the event will not occur	0.10	0.15	0.17	0.36

Model Performance when a Cold Event is not Predicted

Forecasts:	3 hrs	12 hrs	24 hrs	48 hrs
Probability the event will indeed not occur	0.998	0.997	0.998	0.998
Probability that the event will occur	0.002	0.003	0.002	0.002

Model Performance when a Cold Event is Observed

Forecasts:	3 hrs	12 hrs	24 hrs	48 hrs
Probability that the event was predicted	0.79	0.69	0.74	0.72
Probability that the event was not predicted	0.21	0.31	0.26	0.28

Model Performance when a Cold Event is not Observed

Forecasts:	3 hrs	12 hrs	24 hrs	48 hrs
Probability that the event was not be predicted	0.999	0.999	0.999	0.997
Probability that the event was predicted	0.001	0.001	0.001	0.003

The results in the above tables indicate that if a cold event is not predicted by the model, the chances of such event taking place are virtually nil. Once an event is predicted, the chances that this event will indeed take place varies depending on the extent of the forecast from 90% for 3 hour predictions to 85%, 83% and 64% for 12, 24 and 40 hour predictions. A related question was also tested i.e. if a cold event occurs or does not occur what were the chances that it was predicted or not predicted. The results are displayed in the table above and indicate that if an event is not observed the chances that one was predicted are virtually nil and that if a cold water event takes place there is a 70% to 80% chance that the event was indeed predicted.

8. Web Based Implementation of the Predictive Model

The operational model is implemented as part of the DNR/TCOON website (http://lighthouse.tamucc.edu/) Forecasts portion. The underlying computational tools combine past air and water temperature measurements at the Bird Island station, the latest water temperature at Bob Hall Pier for predictions longer than 12 hours, a time stamp for predictions shorter than or equal to 12 hours and NAM WRF air temperature predictions for the Bird Island station (see Table 26.). The NAM WRF predictions are sent from the Corpus Christi Weather Forecasting Office to DNR four times per day. The predictions are sent 3.5 hours after their computations (00Z, 06Z, 12Z, 18Z). When including this delay, NAM WRF predictions are available as soon as 3.5 hrs after computations and with a delay as long as 9.5 hrs when including the 6 hrs between consecutive NAM WRF runs. While the model predictions are computed for the Bird Island station, section 6 demonstrated that these water temperature forecasts are also valid without any adjustments for the project stations. The model inputs are multiplied by their respective model coefficients and fed into the neural network every time a prediction is requested, i.e. displayed predictions are always computed with the latest information available in the DNR/TCOON database. While the training of the neural networks can be lengthy the operational computation once the models are optimized is virtually instantaneous. The prediction results are displayed at the following link which is part of the DNR/TCOON website Forecasts section: http://lighthouse.tamucc.edu/Forecasts/WaterLevelForecasts. The web layout of the predictions is presented in Figure 62 for the predictions. Clicking on prediction graph yields more information including the performance of the model for the past 7 days for 12, 24, and 48 hour predictions and the recent performance of the NAM-WRF air prediction model. Examples of past performance graphs are displayed in Figures 63 and 64 for 12 hour and 24 hour predictions

Table 26. Operational model inputs.

	Series Included	
Possible Inputs Considered	**Short Term**	**Long Term**
Bird Island water temperature	previous 26 hrs	previous 26 hrs
Bird Island air temperature	previous 22 hrs All available	previous 16 hrs All available
Bird Island forecasted air temperature	[max 45 hours]	[max 45 hours]
Bob Hall water temperature	None	latest
24 hr time stamp	previous 16 hrs	None

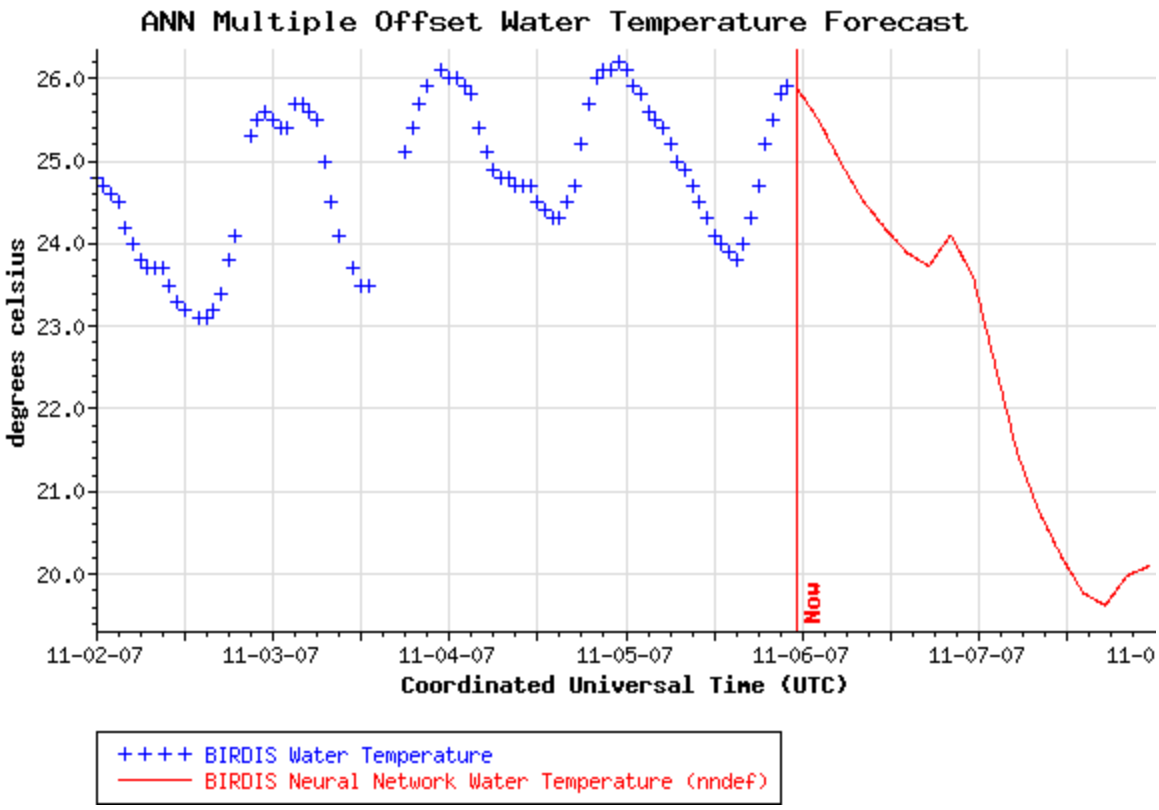

Figure 62. Web layout for the water temperature predictions. The graph presents the water temperature predictions ahead of the passage of the November 6, 2007 cold front.

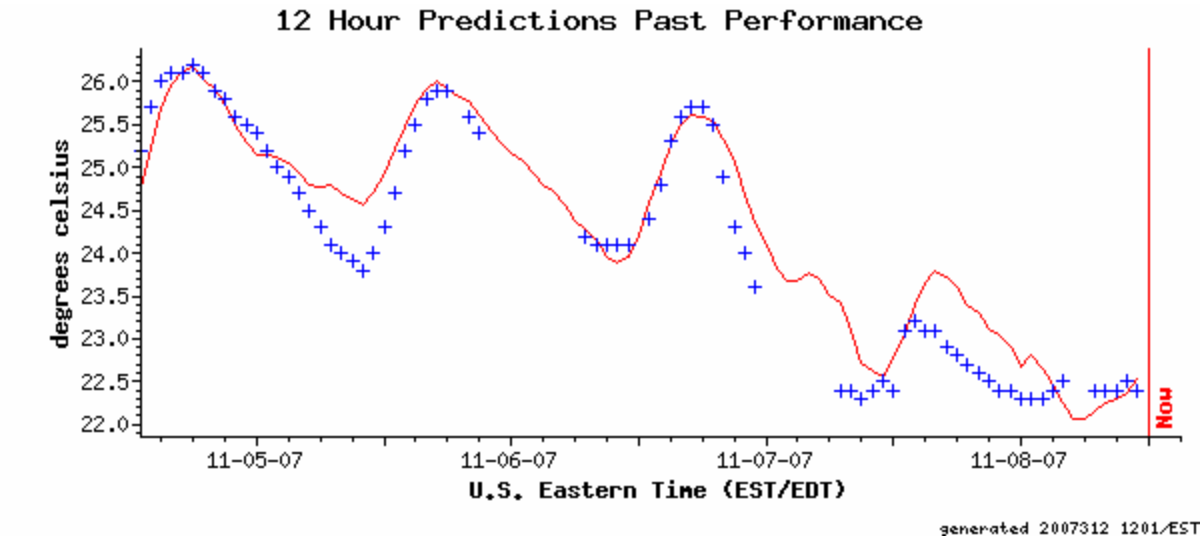

Figure 63. Web layout for the water temperature predictions performance for 12-hour predictions. The graph illustrates the model performance 2 ½ days after the predictions illustrated in Figure 62.

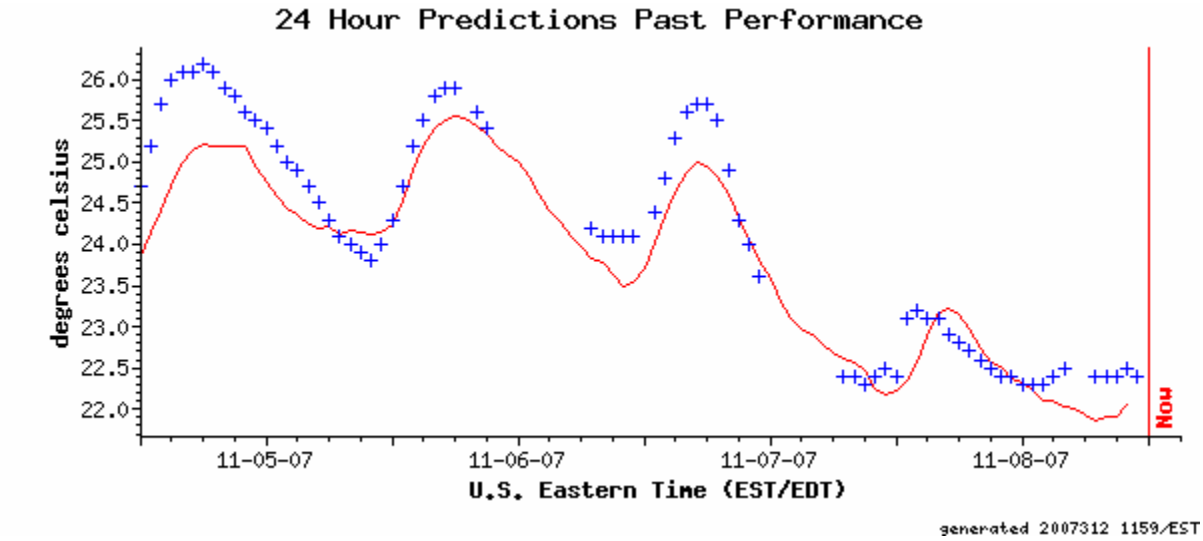

Figure 64. Web layout for the water temperature predictions performance for 24-hour predictions. The graph illustrates the model performance 2 ½ days after the predictions illustrated in Figure 62.

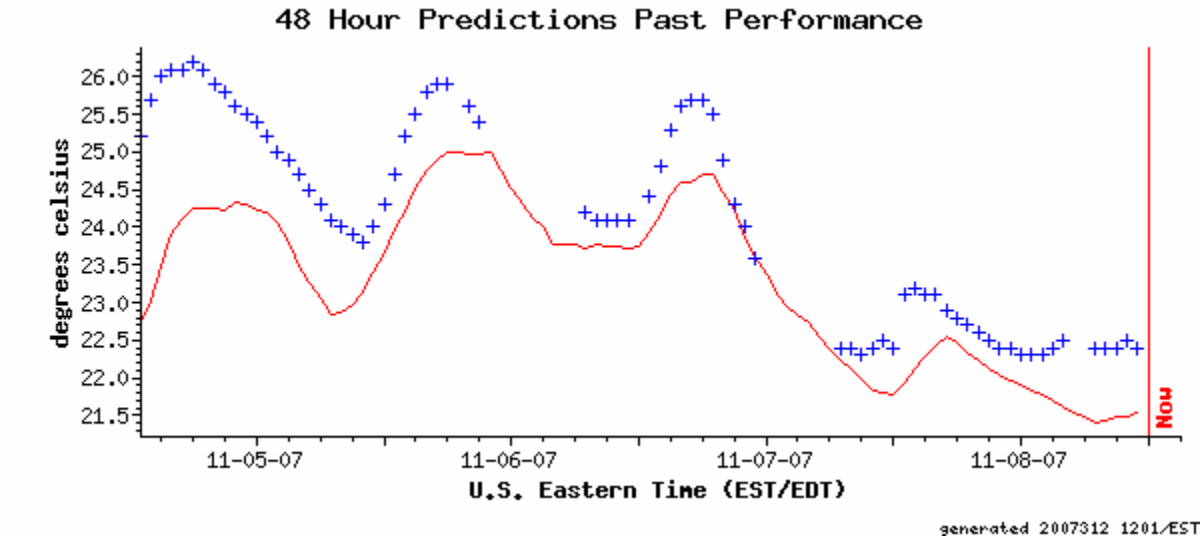

Figure 65. Web layout for the water temperature predictions performance for 24-hour predictions. The graph illustrates the model performance 2 ½ days after the predictions illustrated in Figure 62.

9. Conclusions and Recommendations

The main goals of the study were to both measure water temperature gradients in the Upper Laguna Madre and to design and test a water temperature predictive model. A particular emphasis was placed on cold water events because of their past impact on the local ecosystem. Temperature gradients were monitored hourly at the TCOON Rincon station and the former TCOON El Toro Island station at 3', 6', 9' and 12' within the water column starting respectively on February 27, 2006 and December 13, 2005. Several cold water events were monitored during the study including a January 2007 event with water temperatures decreasing from 22.5°C down to 4.6°C in 60 hours. Throughout the study period the water temperatures were found to be mostly homogenous, i.e. temperatures within a 0.5°C range throughout the water column. A small moderating effect at the bottom of the channel, i.e. for the 12' sensor, was observed during sharp temperature rises. Bottom temperatures during these events stayed cooler by 1°C to 2°C up to 5°C but the temperature gradients always rapidly disappeared at the most within 8 hours. This moderating effect at the bottom of the Laguna Madre was however not observed during the sharp temperature decreases associated with frontal passages. The results of this study indicate a homogeneous water column temperature wise during cold water events. Further monitoring could attempt to measure temperatures in the muddy bottom of the Laguna Madre to confirm that there is indeed no location within the water column where marine life may seek warmer temperatures during cold water events. Temperatures in shallow waters could also be monitored to investigate if significantly lower temperatures are reached at such locations. Comparing temperature records at both project stations and other stations in the Laguna Madre indicate a mostly homogeneous temperature distribution with some variability observed in the deeper waters of Corpus Christi Bay northward, the Brownsville ship channel southward, and at the Mansfield station which is linked to the Gulf of Mexico by a smaller ship channel. While the data quality was excellent at the Rincon station the Landcut station encountered problems. However as discussed in the report, these problems do not affect the above analysis in the opinions of the authors.

The predictive water temperature model was developed for the DNR/TCOON Bird Island station. A model based on Artificial Neural Networks was selected. Using the perfect prog approach performance was computed for several years with yearly average absolute error ranging from about 0.3°C for 3 hour predictions to about 0.7°C for 12 hour predictions, to about 1.0°C for 24 hour predictions and 1.7°C for 24 hour predictions. Year to year variability increased from up to 0.2°C for 3 hour predictions to up to 0.6°C, 0.14°C and 0.23°C for respectively 12 hour, 24 hour and 48 hour predictions. Cold water performance was analyzed for four events between 2003 and 2007 during which cold water temperature reached 8°C or below. The performance during these events was computed using past WRF-NAM predictions. During the cold events the mean average absolute error was lower than 1°C for all predictions increasing from 0.1°C for 3 hour predictions to 0.9°C for the longer prediction times. While the number of cold events with WFR-NAM predictions available is still small a mean average absolute error of 1°C is likely a good estimate of the average performance of the model for cold events. The cold event performance was homogeneous across the temperature range with variability and performance dominated by the accuracy of the WRF-NAM atmospheric predictions, i.e. the performance of the model will mostly depends on how well the atmospheric models capture the future dynamic of the cold fronts.

The performance of the model for cold water event was also evaluated based on its accuracy to detect an event. Based on the available data if a cold event is not predicted by the model, the chances of such event taking place are virtually nil. Once an event is predicted, the chances that the event will indeed take place varies depending on the extent of the forecast from 90% for 3 hour predictions to 85%, 83% and 64% for 12, 24 and 40 hour predictions. If an event is not observed the chances that one was predicted are virtually nil and if a cold water event takes place there is a 70% to 80% chance that the event was indeed predicted. The operational model was implemented as part of the DNR/TCOON website and is presently available at the website section.

The authors look forward to the use of the model and possible feedback from the users. Continuous monitoring of the water temperature gradients at the station locations is highly desirable particularly to capture more cold water events. Additional events, particularly colder events would be helpful to better define the performance of the model during these conditions and confirm the absence of a vertical temperature gradient for a broader range of conditions. Other recommendations include the addition of other locations south of the present locations, as well as measurements in shallower waters or in the muddy Laguna Madre bottom. Modeling wise additional work could be done to improve air temperature predictions for the Laguna Madre and consequently improve water temperature predictions as well following a. MOS approach based on the WFR-NAM predictions and the DNR/TCOON database of past measurements. The use of other machine learning based techniques such as random forest modeling could prove helpful in improving performance specifically during cold events.

10. Acknowledgments

The support of Texas Parks & Wildlife and the Coastal Conservation Association for this study is greatly acknowledged. Special thanks for the following individuals without whom the study would not have been possible, Dr. Larry McKinney, Kyle Spiller and Tony Oldfather from the Texas Parks & Wildlife Department, and David McKee from the Coastal Conservation Association.

11. References

Ball, R. Tissot, P.E., Zimmer, B., Adams J. and Sterba-Boatwright, B., 2007: ANN Predictive Water Temperature Modeling of Cold Water Events in a Shallow Lagoon. *5th Conference on the Applications of Artificial Intelligence to Environmental Science*, San Antonio, Texas, January 2006.

Britton, J.C. and Morton, B., 1989: Shore Ecology of the Gulf of Mexico. University of Texas Press.

Chen, P.Y., and Popovich, P.M., 2002. Correlation: Parametric and Nonparametric Measures. Sage University Papers Series on Quantitative Applications in the Social Sciences, 07-139. Sage.

Hagan, M.T., Demuth, H.B., and Beale, M., 1996. Neural Network Design. PWS Publishing Company.

The MathWorks, Inc., 2006: MATLAB r2006b. The MathWorks, Inc.

Mostella, A., J. S. Duff, and P. R. Michaud, 2002: Harmpred and Harman: Web-Based Software to Generate Tidal Constituents and Tidal Forecasts for the Texas Coast. Proc. of the 19th AMS Conf. on weather Analysis and Forecasting/15th AMS Conf. on Numerical Weather Prediction, 12-16 August 2002, San Antonio, Texas.

Rumelhart, D. E., Chauvin, Y., Eds., 1995: Backpropagation: Theory, Architectures, and Applications. Lawrence Erlbaum Associates.

Schureman, P., 1958: Manual of Harmonic Analysis and Prediction of Tides. U.S. Department of Commerce, Coast and Geodetic Survey, Special Publication 98. U.S. Government Printing Office.

Sutron, 2007. Sutron Corporation website url, last visited 11-7-2007: http://www.sutron.com/.

Texas Parks & WIldlife Department, 1997: TPWD News for February 3, 1997: Fish, Sea Turtles Dies on Coast During Recent Freeze. Texas Parks & Wildlife Department.

Tissot P.E., D.T. Cox, and P.R. Michaud, 2003: Optimization and Performance of a Neural Network Model Forecasting Water Levels for the Corpus Christi, Texas, Estuary. 3rd Conference on the Applications of Artificial Intelligence to Environmental Science, Long Beach, California, February 2003.

Wilks, D.S., 2006: Statistical Methods in the Atmospheric Sciences, 2nd Edition. Elsevier Academic Press.

YSI, 2007. Yellow Springs Instruments, Yellow Springs Colorado, website url, last visited 11-7-2007: http://www.ysihydrodata.com/ysi-yellow-springs-instruments.htm.